Dissertation zur Erlangung des Doktorgrades
der Fakultät für Chemie und Pharmazie
der Ludwig-Maximilians-Universität München

Studies on the Chemotaxis Network in *Halobacterium salinarum* and *Helicobacter pylori*

von

Andreas Schaer

aus Freiburg i. Br.

2002

Erklärung

Diese Dissertation wurde im Sinne von § 13 Abs 3 bzw. 4 der Promotionsordnung vom 29. Januar 1998 von Herrn Prof. Dr. Dieter Oesterhelt betreut.

Ehrenwörtliche Versicherung

Diese Dissertation wurde selbstständig, ohne unerlaubte Hilfe angefertigt. München, den 18. August 2002.

Dissertation eingereicht am: 30. August 2002
1. Berichterstatter: Hon.-Prof. Dr. D. Oesterhelt
2. Berichterstatter: Univ.-Prof. Dr. L.-O. Essen
Tag der mündlichen Prüfung: 12. Februar 2003

Danksagung

Die vorliegende Arbeit wurde am Max-Planck-Institut für Biochemie unter Anleitung von Prof. Dr. D. Oesterhelt angefertigt.

Mein besonderer Dank gilt Herrn Prof. Dr. D. Oesterhelt für die Überlassung des sehr interessanten Themas, für sein reges Interesse am Fortgang der Arbeit und sein stetes Bemühen, optimale Arbeitsbedingungen zu schaffen. Darüber hinaus weiß ich das in mich gesetzte Vertrauen, die mir gewährte große wissenschaftliche Freiheit und die Hilfe beim Erstellen vorliegender Arbeit sehr zu schätzen.

Ganz besonders möchte ich auch Herrn Prof. Dr. L.-O. Essen danken. Während der gesamten Promotionszeit stand er mir bei kleineren und größeren Problemen als Betreuer immer zur Seite. Ihm verdanke ich viele Anregungen, fruchtbare Diskussionen und Erläuterungen und die Einführung in viele biochemischen Arbeitsmethoden.

Danken möchte ich auch allen Laborkollegen und Mitgliedern der Abteilung Membranbiochemie für die fröhliche Arbeitsatmosphäre, die so manchen Fehlschlag zu verkraften half.

Mein herzlicher Dank gilt auch meinen Eltern sowie meinen Freunden, die nicht zuletzt durch ihre moralische Unterstützung wesentlich zum Gelingen dieser Arbeit beigetragen haben.

Für meine Eltern

1. Contents

1. Contents 1
2. Abbreviations 5
3. Introduction 7
3.1. The *E. coli* chemotaxis network 7
3.2. Novel chemotaxis proteins outside the *Enterobacteriaceae* 10
3.3. Halobacterium salinarum and *Helicobacter pylori* chemotaxis.....13
3.3.1. Chemotaxis network in *Halobacterium salinarum* 13
3.3.2. *Helicobacter pylori* - Chemotaxis of an important human pathogen.....16
4. Aims of this study 19
5. Results 21
5.1. Identification and expression of soluble MCP homologs from *H. salinarum* 21
5.2. Purification of Car and Htr15.....24
5.3. Characterization of Car by CD spectroscopy 26
5.4. Heat denaturation of Car.....32
5.5. Characterization of Car by ^{1}H-NMR.....33
5.6. Crystallization trials for Car.....35
5.7. Expression, purification and crystallization trials with Car fragments.....36
5.8. Expression of *H. salinarum* CheB and CheR in *E. coli* 37
5.9. Soluble receptor homologs in *C. jejuni* and *H. pylori*.....38
5.10. Crystallization of chemotaxis components Hp0599, Cj0448 and CheW.....42
5.11. The chemotaxis network in *H. pylori*.....46
5.11.1. Modulation of CheF autophosphoylation activity 46

5.11.2. Phosphotransfer reactions from CheF to response regulators....57
5.11.3. Phosphate group transfer through the Che protein network.....58
5.11.4. Autophosphorylation of CheF:D729K mutant.....60
5.11.5. Phosphotransfer reactions from CheF:D729K-P_i to response regulators.....62
5.11.6. Decay of CheY-phosphate 67
5.11.7. Reverse phosphotransfer from CheY to the kinase 69
5.11.8. Phosphorylation of response regulators by acetyl phosphate 72
5.12. Expression and purification of the motor switch protein FliM 74
5.13. Detection of *H. pylori* chemotaxis proteins by antisera 79
6. Discussion.....83
6.0. Soluble MCP homologues in two-component cascades 83
6.1. Recombinant production of halophilic signaling components in E. coli 84
6.2. The arginine receptor Car - a molten globule like receptor? 85
6.3. Role of eubacterial soluble receptors 87
6.4. Possible role of CheV proteins 94
6.5. The *H. pylori* motor and its switch 99
6.6. Adaptation in biological networks and chemotaxis in *H. pylori* 103
6.7. Gene regulation and adaptation in a stable environment 105
7. Materials and Methods 109
7.1. Bacterial strains and plasmids 109
7.2. General molecular biological techniques.....110
7.2.1. Culture of *E. coli* XL1 blue cells for plasmid growth 110
7.2.2. Purification of plasmid DNA from *E. coli* cells 110
7.2.3. General PCR protocol for DNA amplification 111
7.2.4. Purification of DNA after enzymatic reactions.....111
7.2.5. Preparation of vector DNA for ligation reactions 112
7.2.6. Preparation of PCR-derived DNA fragments for ligation reactions 112

7.2.7. Ligation of DNA molecules 113
7.2.8. Restriction analysis of plasmid DNA 113
7.2.9. Analysis of DNA by agarose gel electrophoresis 113
7.2.10. Sequencing of plasmid DNA 114
7.2.11. Preparation of short synthetic dsDNA linker 115
7.2.12. Construction of mutant genes by site-directed mutagenesis ... 115
7.2.13. Construction of mutant genes by PCR 116
7.2.14. Construction of chimeric FliM 116
7.2.15. Synthesis of *H. salinarum cheR* and *cheB* genes 117
7.2.16. Construction of N- and C-terminal fragments of Car 119
7.2.17. Preparation of electrocompetent *E. coli* cells 120
7.2.18. Transformation of *E. coli* cells 121
7.2.19. Primer design for PCR and sequencing reactions 121
7.3. Protein chemical methods 122
7.3.1. Test for pET28a(+) directed gene expression 122
7.3.2. Isolation of inclusion bodies from *E. coli* cells 123
7.3.3. Heterologous expression of proteins in *E. coli* 123
7.3.4. Purification of overexpressed proteins from *E. coli* 124
7.3.5. SDS-PAGE analysis of proteins 128
7.3.6. Detection of proteins after SDS-PAGE by Coomassie brilliant blue 129
7.3.7. Detection of proteins after SDS-PAGE by silver staining 129
7.3.8. Western transfer of proteins separated by SDS-PAGE to PVDF membrane 130
7.3.9. Immunodetection of proteins immobilized on PVDF membanes 131
7.3.10. Production of antisera against *H. pylori* chemotaxis proteins in rabbits 132
7.3.11. Protein concentration assay 133
7.4. Autophosphorylation and phosphotransfer reactions 133
7.4.1. Synthesis of [^{32}P] labeled dilithium acetyl phosphate 133

7.4.2. Acyl phosphate assay 134
7.4.3. Preparation of phosphorylated CheF:D729K..... 134
7.4.4. Phosphotransfer assay from phosphorylated CheF:D729K to response regulators 135
7.4.5. Phosphotransfer assay from phosphorylated response regulator CheY:K106R to CheF:D729K 136
7.4.6. CheF autophosphorylation and transphosphorylation activities using [γ^{32}P]-ATP. 136
7.4.7. Response regulator autophosphorylation by acetyl phosphate. . 137
7.4.8. Quantitation of radiolabel on CheF after SDS-PAGE by liquid scintillation counting 137
7.4.9. Quantitation of phosphotransfer reactions by "phosphoimaging" 138
7.5. ATPase assay..... 138
7.6. Circular dichroic measurements..... 136
7.7. ^{1}H-NMR spectroscopy with Car 139
7.8. Protein crystallography 140
8. References..... 143
Appendix A: Equipment 163
Appendix B: Primers 167
Appendix C: Gene sequences of synthetic genes 171
9. Summary..... 173

2. Abbreviations[1]

ADA	N-[2-acetamido]-2-iminodiacetic acid
ATP	adenosine triphosphate
BCIP	5-bromo-4-chloro-3-indolyl phosphate
bp	base pair
CD	circular dichroism
cp	centipoise
DEAE	diethylamino ethyl-
DMSO	dimethylsulfoxide
DNA	deoxyribonucleic acid
dNTP	deoxyribonucleotide triphosphate
dsDNA	double-stranded deoxyribonucleic acid
EDTA	ethylenediaminetetraacetate
IPTG	isopropyl-β-D-thiogalactoside
kb	kilobase
LB	Luria Bertani
LCR	ligase chain reaction
MCP	methyl-accepting chemotaxis-like protein
MES	2-[N-morpholino]ethanesulfonic acid
MPD	2-methyl-2,4-pentanediol
NADH	nicotinamide adenine dinucleotide, reduced form
NBT	nitroblue tetrazolium salt
NMR	nuclear magnetic resonance
OD	optical density
PAGE	polyacrylamide gel electrophoresis
PBS	phosphate buffered saline

[1] Throughout this work, the International System of Units is used as described in the IUPAC Manual of Symbols and Terminology for Physicochemical Quantities and Units (1979) without definition.

PCR	polymerase chain reaction
PEG	polyethylene glycol
pH	*potentia Hydrogenii*
pI	ionic strength
PMSF	phenylmethyl sulphonyl fluoride
PVDF	polyvinylidene fluoride
SDS	sodium dodecyl sulfate
UV	ultra violet

3. Introduction

Our world is populated by two different kinds of organisms: one is *Escherichia coli*, and the other is not. Since its first description by THEODOR ESCHERICH in 1885, *E. coli* serves as one of the best understood model organisms, and most of our knowledge in biochemistry and genetics originates from studies of this bacterium. Since the end of the 19th century it was known that *E. coli* cells migrate towards oxygen and organic nutrients, a behavior termed chemotaxis that is shared with many other organsims including animals and plants (ENGELMANN, 1882; PFEFFER, 1883; ENGELMANN, 1884; PFEFFER, 1887; for a review see WEIBULL, 1960). Based on the pioneering work of PFEFFER, the so called capillary assay was developed (SHERRIS *et al.*, 1957 and BARACCHINI & SHERRIS, 1959), where bacteria placed at the bottom of a capillary tube filled with nutrients entered the tube and formed clearly visible bands. In 1966, JULIUS ADLER was the first who studied *E. coli* motility in a simple chemically defined medium that allowed to determine which substances elicit chemotaxis. Today, the *E. coli* chemotaxis system is the best understood signal transduction network.

3.1. The *E. coli* chemotaxis network

E. coli comprises five membrane-bound chemoreceptor proteins[1] (MCPs from methyl-accepting chemotaxis-like proteins) to sense the presence of their respective ligands. With the exception of Aer, the oxygen sensor,

[1] In the present work, a protein is referred to as a 'receptor' when the protein directly perceives signals such as light or small molecular compounds. When a protein binds to a receptor to transmit information to downstream compnents, it is referred to as a 'transducer'. Since some receptors comprise transducer-like sequence signatures, the nomenclature is sometimes difficult to follow.

these receptors bind ligands at the periplasmic side of the cell membrane and communicate this information by a yet to be determined mechanism through the cell membrane into the cytoplasm, where the autophosphorylation activity of the histidine kinase CheA is modulated by the receptor occupancy (Fig. 1).

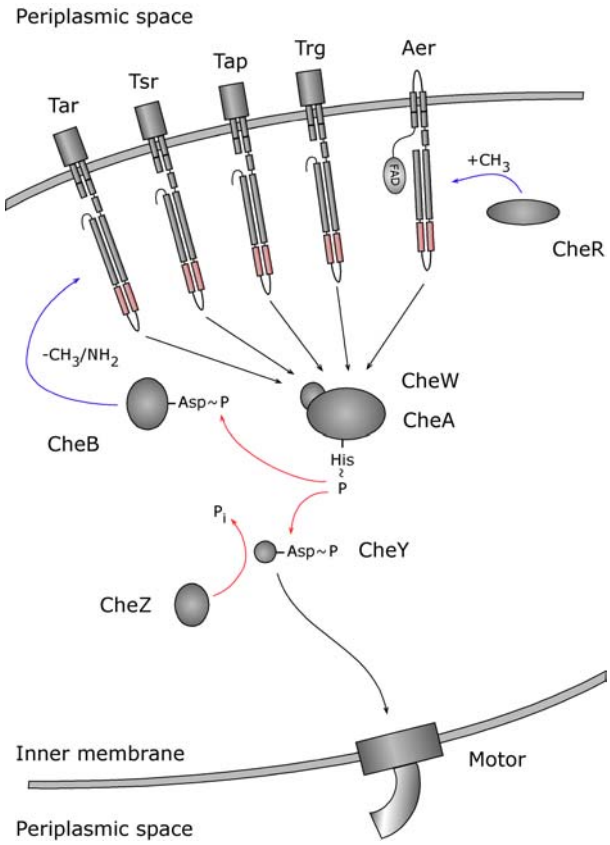

Fig. 1. The *Escherichia coli* chemotaxis network that controls cellular motility. Red arrows: phosphotransfer reactions, blue arrows: methylation/demethylation and deamidase reactions, black arrows: protein/protein interactions. For details see text. From LEVIT *et al.*, 1998, with modifications.

In contrast, Aer has a bound flavine adenine dinucleotide (FAD) cofactor in its cytosolic N-terminal PAS domain (ZHULIN *et al.*, 1997), while its overall domain organization resembles the structure of the other four chemoreceptors (HAZELBAUER, 1992; BIBIKOV *et al.*, 1997).

The protein kinase CheA binds to the signaling domains of the receptors (red) via the coupling protein CheW. The autophosphorylation activity of CheA depends on the signaling state of the receptors with attractant binding resulting in deactivation and *vice versa*). This kinase, together with the response regulator CheY, forms the archetypal two-component signal transduction system, in which the response regulator is phosphorylated by its cognate histidine kinase (HESS *et al.*, 1987; HESS *et al.*, 1988). Upon phosphorylation, CheY-phosphate affects the direction of rotation of the flagellar motor by binding to the switch complex of the motor (WELCH *et al.*, 1993; BREN & EISENBACH, 1998; BREN *et al.*, 1996). In *E. coli*, the CheY-phosphate signal is terminated through the spontaneous hydrolysis of CheY-phosphate as well as by CheZ, a response regulator phosphatase.

The methyl transferase CheR constitutively adds methyl groups derived from S-adenosyl-methionine to conserved glutamyl residues of the receptors. This modification shifts the signaling state of the receptors towards the unliganded state regardless of the occupancy with ligands (CheA activation). The receptor methylesterase/deamidase CheB is activated by phosphorylation through CheA. It removes the methyl groups that were added by CheR from ligand-bound receptors (CheA deactivation). Since its own activity depends on the CheA activity, and since CheR activity is independent of the CheA activity, this receptor methylation/demethylation creates a feedback loop that allows system adaptation (for reviews see FALKE *et al.*, 1997; STOCK *et al.*, 2000; AIZAWA *et al.*, 2000). Overall, this chemotaxis system enables the cell to migrate towards nutrients or away from repellents by sensing gradients of chemicals.

E. coli apparently evolved in an environment where sugars, amino acids and (di-)peptides served as energy sources, and therefore receptors to sense such substances are found in its inner membrane. Some ligands interact directly with the receptors, such as serine with Tsr or aspartate with Tar, while other chemicals first bind to binding proteins located within the periplasmic space. In these cases, ligand binding triggers a structural rearrangement of the binding protein that allows the subsequent interaction with the receptor. Maltose, for example, is sensed by Tar through interaction with the maltose binding protein. Although the information on the presence or absence of ligands is primarily communicated by the membrane-bound receptors to the Che protein network, these proteins are not the only means by which *E. coli* cells sense chemicals. CheA autophosphorylation activity is also controlled by the phosphoenolpyruvate-dependent phosphotransferase system that actively transports sugars across the cell membrane (reviewed in ALEXANDRE & ZHULIN, 2001). Whereas the structure of the isolated chemotaxis network components is largely known in atomic detail, their spatial arrangement in the signalling complex made of receptors, coupling protein CheW and CheA molecules as well as their exact stoichiometry remains to be determined.

3.2. Novel chemotaxis proteins outside the *Enterobacteriaceae*

Within the last few years, the entire genomes of many organisms have been sequenced, creating databases with thousands of predicted gene and protein sequence entries. Homology searches with *E. coli* chemotaxis proteins as search queries yields hundreds of predominantly bacterial proteins with homologous domains. The enteric system that once was considered to be the paradigm of an eubacterial chemotaxis network

appears nowadays as a rather exotic and simple signal transduction system. In other bacteria, systems with different sets of chemotaxis proteins are at work. However, many of these novel proteins consist of components homologous to *E. coli* Che proteins, but in different topological arrangements. Therefore, it appears that a process reminiscent of 'molecular lego' with protein domains created a plethora of novel proteins whose complex function can not be predicted from their simpler orthologs (Fig. 2)

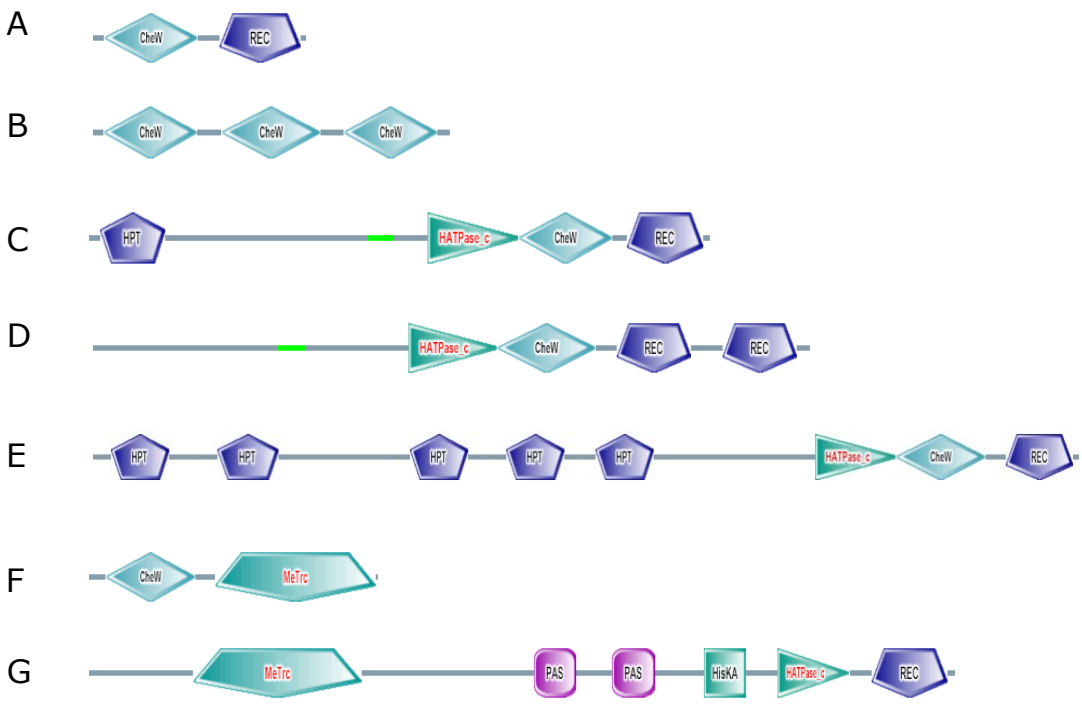

Fig. 2. Selection of 'novel' chemotaxis proteins from various organisms. Proteins are NCBI Protein Id A82180 (A), B82206 (B), BAA17198 (C), BAA10022 (D), AAC23932 (E), AAC67023 (F) and BAB78082 (G). CheW: two component signaling adaptor domain (turquoise diamonds), HATPase_c: histidine kinase-like ATPase domain (green triangles), HPT: histidine phosphotransfer domain (blue pentagons), HisKA: histidine kinase A (phospho-acceptor) domain (green rectangles), MeTrc: methyltransferase domain (large green pentagons), PAS: PAS domain (from **p**eriod circadian protein, **A**h-receptor nuclear translocator protein and **s**ingle-minded protein where this domain was first identified; pink rectangles), REC: CheY-homologous receiver domain (blue pentagons, upside down). For further details see http://smart.embl-heidelberg.de/smart/.

In many organisms like *Vibrio cholerae* or *Helicobacter pylori*, genes coding for proteins where a CheW domain is fused to a response regulator domain from the CheY superfamily were identified. The resulting fusion proteins were coined as CheV proteins (FREDRIK & HELMANN, 1994; ROSARIO *et al.*, 1994). Fig. 2A shows VC1602 from *Vibrio cholerae* as one example from a total of four CheV proteins in this organism. Another gene product in *Vibrio cholerae*, VC1402, is made up of three CheW domains (Fig. 2B). Whereas the archetypical histidine kinase CheA from *Escherichia coli* comprises a histidine phosphotransfer domain followed by a histidine kinase-like ATPase domain and a CheW-like domain, in *Synechocystis sp.* PCC 6803, an additional response regulator domain is fused to CheA, giving rise to a hybrid histidine kinase (Fig. 2C). Within the same organism, another hybrid kinase can be found where two CheY-like receiver domains follow the CheA domain (Fig. 2D). In *Pseudomonas aeruginosa*, a CheA ortholog is also fused to a response regulator domain as in *Synechocystis sp.* PCC 6803. This protein, however, contains five instead of one histidine phosphotransfer domains at its N-terminus (Fig. 2E). Whereas in *E. coli* CheR is a single protein, in *Treponema pallidum* and *Borrelia burgdorferi* proteins were identified where CheW-like domains were fused to a CheR methyltransferase domain (Fig. 2F), and in *Anabaena sp.* PCC 7120, a CheR domain is fused to a CheA histidine kinase and a CheY response regulator domain via two PAS domains (Fig. 2G).

The function of CheA, CheR, CheW and CheY in *E. coli* is well known, but the function of all of the proteins depicted in Fig. 2 remains currently enigmatic. It is well conceivable that the rearrangement of conserved domains allows the respective proteins to fulfill novel duties.

3.3. *Halobacterium salinarum* and *Helicobacter pylori* chemotaxis

H. salinarum and *H. pylori* share a certain fondness for unusual environments. Whereas the archaeon *H. salinarum* (WOESE *et al.*, 1990) inhabits environments with intense illumination and high salt concentrations as the Dead Sea or solar evaporation ponds (for an overview see OREN, 1994), *H. pylori* thrives in the mucous darkness of the highly acidic human stomach (for an overview see MONTECUCCO & RAPPUOLI, 2001). Both organisms contain orthologous proteins of the *E. coli* receptor and chemotaxis proteins, but the networking of their signaling pathways appear to be very different from the *E. coli* prototype according to their generic contents (TOMB *et al.*, 1997; NG *et al.*, 2000).

3.3.1. Chemotaxis network in *Halobacterium salinarum*

Halobacterium salinarum responds to external stimuli by altering the switching probability of its flagella in analogy to flagellated eubacteria. Whereas *E. coli* only responds to chemical ligands as for example amino acids or oxygen, *H. salinarum* also has the capability to respond to physical stimuli such as orange/UV light or blue light via the retinal proteins sensory rhodopsin I and II (SPUDICH, 1994; SPUDICH *et al.*, 2000). These two light perceiving proteins transmit the signal via two cognate transducer proteins HtrI and HtrII to the CheA/CheY two component chemotaxis network (RUDOLPH & OESTERHELT, 1995) thus enabling the cell to move towards ideal illumination conditions where the light driven proton pump bacteriorhodopsin converts light energy into chemical energy (HAUPTS *et al.*, 1999; TITTOR *et al.*, 2002). On the other hand, a phobic reaction with respect to an increase in blue light avoids regions of too intense illumination. Besides HtrI and HtrII, *H. salinarium* excels with a

set of 16 transducer proteins that can be assigned to several receptor families according to their architecture. All transducer proteins have different N-terminal domains followed by the highly conserved signaling domain important for signal transduction to the histidine kinase CheA (Fig. 3).

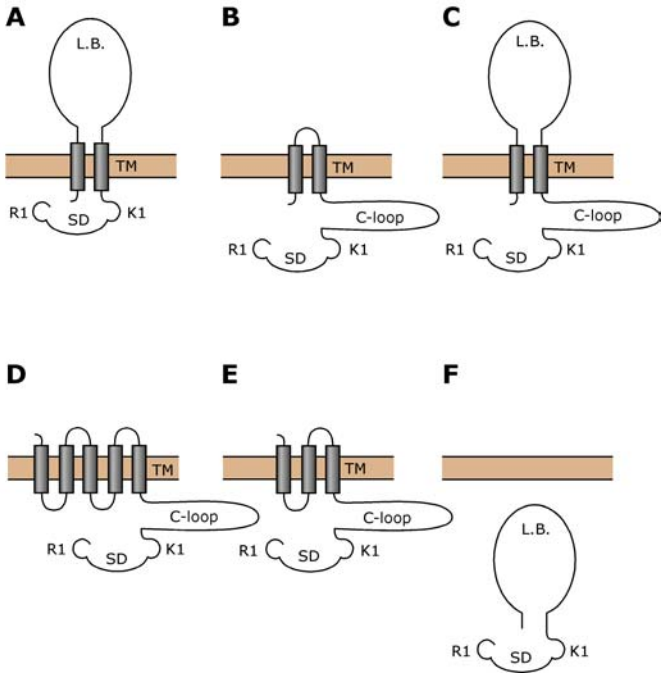

Fig. 3. Architecture of Tar compared to archaeal transducer proteins from *H. salinarum*. All these proteins are made up from several basic building blocks. **A.** Tar from *E. coli*, the archetypical enteric chemoreceptor, consists of a periplasmic ligand binding domain (LB) that is flanked by two transmembrane helices (TM). It is followed by the C-terminal signaling domain (SD). K1 and R1, the two regions where adaptive methylation takes place, enframe the signaling domain. **B.** Architecture of HtrI (AAG19913.1). **C.** Architecture of HtpIV and HtpVI (CAA64841.1 and AAD02052.1, respectively). **D.** Architecture of Htr8 (AAG19812.1). **E.** Architecture of HtpV and Htr17 (AAG19985.1 and AAG19968.1, respectively). **F.** Architecture of HtpIII (CAA64840.1) and Car (CAB38318.1). Receptors of this class do not contain transmembrane helices and therefore are soluble, cytosolic proteins. Since the nomenclature of the halobacterial transducers is ambiguous, the NCBI Protein Id is given in brackets for each protein. For a complete list of all halobacterial proteins see the Halolex database at http://www.halolex.biochem.mpg.de. From RUDOLPH *et al.*, 1996, adapted.

Despite the great diversity of transducer proteins, *H. salinarum* is equipped with the canonical set of Che proteins known from coliform bacteria, except that CheZ is absent like in all organisms outside the γ-proteobacteria (KIRBY *et al.*, 2001). In addition, the halobacterial genome codes for three non-enteric Che proteins: CheC1, CheC2 and CheJ (also named CheD; RUDOLPH & OESTERHELT, 1996) Table 1 gives an overview of the *H. salinarum* Che proteins.

Table 1. Chemotaxis proteins from *Halobacterium* sp. NRC-1[1)]

Protein	M_r (kDa)	NCBI Protein Id.	suggested function
CheA	71.9	AAG19393.1	histidine kinase
CheB	36.5	AAG19394.1	methyl esterase, adaptation
CheC1[2)]	21.0	AAG19392.1	Unclear, with no enzymatic activity[3)]
CheC2	20.4	AAG19871.1	Unclear, with no enzymatic activity[3)]
CheJ	11.0	AAG19390.1	Unclear, with no enzymatic activity[3)]
CheR	26.5	AAG19389.1	methyl transferase, adaptation
CheW1	19.2	AAG19396.1	coupling protein
CheW2	14.1	AAG19371.1	coupling protein
CheY	13.4	AAG19395.1	response regulator, motor switch factor

[1)]: *Halobacterium* sp. NRC-1 was chosen as reference since it is the only *Halobacterium* strain whose genome was sequenced and published in its entity to date. See DASSARMA *et al.*, 2000.

[2)]: This protein was also named CheD by some authors.

[3)]: for information on *Bacillus subtilis* orthologs see KIRBY *et al.*, 2001.

3.3.2. *Helicobacter pylori* - Chemotaxis of an important human pathogen

H. pylori was already present in the stomachs of humans when they left Africa to conquer the world more than 150,000 years ago (COVACCI *et al.*, 1999), and it is one of the most successful bacterial pathogens which colonizes more than half of the human population (PARSONNET, 1995). Most infected people are asymptomatic, but 15 to 20% of them develop severe gastroduodenal diseases during their lifetime, including gastric ulcers as first described by DONATI, 1586, adenocarcinomas, gastric lymphomas and tumors of the neuroendocrine system (FORMAN *et al.*, 1991; NOMURA *et al.*, 1991; PARSONNET *et al.*, 1991; GRAHAM *et al.*, 1992). To avoid discharge from the mucus to the lumen of the stomach, the mostly planktonic bacteria must swim perpetually back to the epithelial cell surface where they predominantly thrive on nutrient-rich exudates from the capillaries. Chemotaxis network-controlled motility is therefore an absolute prerequisite to establish a successful infection (LEE, 1996).

The *H. pylori* genome (TOMB *et al.*, 1997; ALM *et al.*, 1999) codes for only three membrane-bound chemotaxis transducer proteins, yet this organism has a remarkably unusual set of chemotaxis proteins (Fig. 4).

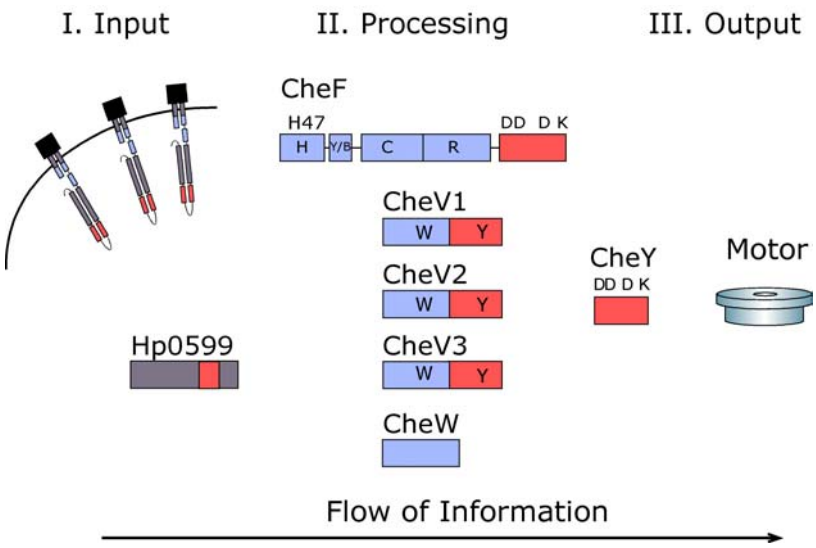

Fig. 4. Chemotaxis system in *H. pylori* (KELLY, 1998). Information from the external chemical world is communicated from the transducer proteins to the Che protein network where the output signal is computed. Domains in CheF are H: histidine box; Y/B: CheY/CheB binding domain; C: dimerization and kinase domain; R: regulatory domain (BILWES *et al.*, 1999). Domains in CheV proteins are W: CheW-like domain (blue); Y: CheY-like domain (red). Conserved residues important for this work are indicated above the respective proteins.

The three membrane-bound transducer homologs (Hp0083, Hp0099, and Hp0103) presumably sense the presence of their respective ligands in the periplasmic space and communicate this information to the Che protein network located in the cytoplasm. From the six Che proteins, only two orthologs, CheW and CheY, are found in *E. coli*. The hybrid histidine kinase CheF is a fusion protein of CheA and CheY, and the three CheV paralogs are CheW-CheY fusions. Receptor-modifying CheB and CheR orthologs are absent, as is the CheZ phosphatase. Whether receptor methylation occurs in *H. pylori* similarly as in *E. coli* or *H. salinarum* (SUNDBERG *et al.*, 1990; MARWAN *et al.*, 1995; STOCK *et al.*, 2000), and whether the chemotaxis network can adapt to changing ligand concentrations, is unknown. Likewise enigmatic is the role of the five response regulator domains, and which of these domains functions as

output signal that binds to the flagellar motor. A potential fourth receptor molecule, Hp0599, that was assigned as haemolysin secretion protein precursor HylB (TOMB *et al.*, 1997), lacks any detectable transmembrane spanning regions yet has the highly conserved signaling domain that is shared by all known bacterial transducer proteins. Table 6, p. 46 gives an overview on the exceptional set of *H. pylori* Che proteins.

4. Aims of this study

Since the discovery of the halobacterial chemotaxis transducer homologs it was known that some of them do not contain any predicted transmembrane helices (RUDOLPH *et al.*, 1996; ZHANG *et al.*, 1996). They should be soluble and reside within the cytosol of the bacterial cell. These proteins allow the unique opportunity to examine a bacterial chemotaxis system *in vitro* without the difficulties associated with transmembrane proteins. Furthermore, with the functional preparation of a soluble receptor, the *in vitro* reconstitution of the first archaeal signal transduction network (RUDOLPH *et al.*, 1995) could be completed to the extent where CheY phosphorylation is regulated by binding of ligand to the chemoreceptor, substantiating the assumption that soluble chemoreceptors exist and that halobacterial chemotaxis is related to the enteric paradigm. The availability of the proteins would also allow crystallization trials that might yield the first crystal structure of a complete receptor molecule.

During this work it became apparent that soluble proteins with high homologies to *E. coli* chemoreceptors are not limited to halophilic archaea. In *Helicobacter pylori*, as well as in *Campylobacter jejuni*, genes coding for soluble transducer proteins were identified. Their respective gene products would allow similar experiments as described above for the halophilic transducer homologues. Furthermore, until now, no details about the molecular interactions during chemotaxis in *H. pylori* are available. The expression and purification of the entire set of *H. pylori* Che proteins therefore permits an in-depth examination of the phosphotransfer reactions in this non-enteric chemotaxis network. Since motility is an absolute prerequisite to establish successful infections (LEE, 1996), a

deeper understanding of the signaling cascade that controls this motility might contribute to the fight against this important human pathogen.

The aims of this study were:

- to overexpress and purify the soluble transducer Car from *Halobacterium salinarum* for crystallization trials and to provide purified protein for *in vitro* reconstitution experiments of the signaling cascade by coworkers.
- to characterize purified Car and to examine various solvent compositions on the overall fold of Car by circular dichroic spectroscopy.
- to clone, overexpress and purify the putative transducer proteins Hp0599 and Cj0448 from *Helicobacter pylori* and *Campylobacter jejuni*, respectively, for crystallization trials.
- to verify the function of the putative transducer protein Hp0599 by establishing an in vitro assay where the receptor interacts with other components from the Che protein network.
- to clone, overexpress and purify the Che protein network from *Helicobacter pylori* to study its phosphotransfer reactions and its modulation by Hp0599.
- to obtain structural information on *Helicobacter pylori* CheW by X-ray crystallography.

5. Results

5.1. Identification and expression of soluble MCP homologs from *H. salinarum*

Previous studies have identified five structural genes in *H. salinarum* coding for soluble proteins with high homologies to the signaling domain of eubacterial receptor proteins (Table 2).

Table 2. Soluble receptor protein homologs from *H. salinarum*

Protein	M_r (kDa)	GenBank Acc No.	Protein Id.	Author
Car	49.1	AJ132321	CAB38318.1	STORCH *et al.*, 1999[1)]
HtpIII	50.8	X95588	CAA64840.1	RUDOLPH *et al.*, 1996[2)]
HtB	52.8	U75436	AAB17881.1	ZHANG *et al.*, 1996
Htr12	44.1	AE005061	AAG19751.1	NG *et al.*, 2000[3)]
Htr15	67.3	AE005032	AAG19381.1	NG *et al.*, 2000

A complete list of all halobacterial proteins including the receptor proteins and many additional informations can be explored under http://www.halolex.biochem.mpg.de.

[1)]: The structural gene for Car from *H. salinarum* strain S9 is absent in strain NRC-1 whose genome was sequenced by NG *et al.*, 2000. This protein is identical to HtH (GenBank Acc. No. U74668.1, Protein Id. AAC45264.1), BROOUN *et al.*, 1997.

[2)]: HtpIII was described simultaneously by RUDOLPH *et al.*, 1996 as HtpIII and by ZHANG *et al.*, 1996 as HtA (GenBank Acc. No. U75435; Protein Id. AAB17880.1). It is identical to Htr9 (GenBank Acc. No. AE005058; Protein Id. AAG19717.1; NG *et al.*, 2000)

[3)]: This protein was published previously as HtrXII (direct submission to GenBank by BROON *et al.*, 1997; GenBank Acc. No. AF036232, Protein Id. AAD02053.1)

All these proteins have the methyl-accepting chemotaxis-like domain at their C-terminal end, whereas it is assumed that ligand binding occurs at the N-terminal end of the protein (Fig. 5A, next page). Within the methyl-accepting (MA) domain, three conserved stretches of amino acids can be identified which are involved in the presumed function of this region: the signaling domain that interacts with other components of the chemotaxis

cascade and the K1 and R1 peptides which are important for adaptation (RUDOLPH *et al.*, 1996; Fig. 5B).

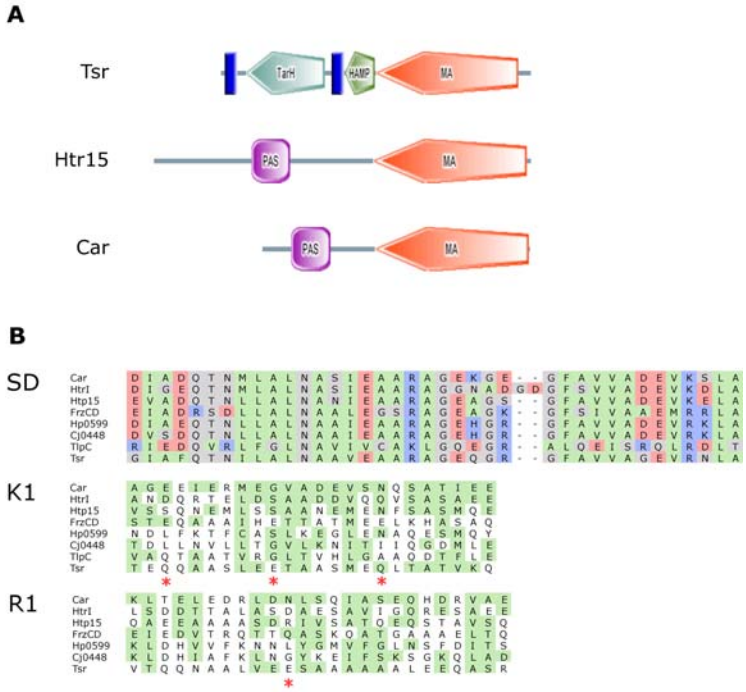

Fig. 5. Domain organization and homology of selected bacterial and archaeal transducer proteins. **A.** Domain organization of two soluble MCP homologs from *H. salinarum* in comparison with the *E. coli* membrane-bound chemoreceptor Tsr. The transmembrane helices of Tsr are indicated by blue rectangles. All three proteins share the conserved methyl-accepting chemotaxis-like domain (MA). TarH: ligand binding domain of Tar. HAMP: domain conserved in **h**istidine kinases, **a**denylyl cyclases, **m**ethyl binding proteins and **p**hosphatases. PAS: domain conserved in the **p**eriod circadian protein, the **A**h receptor nuclear translocator protein and the **s**ingle-minded protein. From http://smart.embl-heidelberg.de/smart **B.** Amino acid sequence homology of the signaling domain, the K1 and the R1 peptide of Tsr from *E. coli*, Car, Htp15 and HtrI from *H. salinarum*, TlpC from *Rhodobacter spheroides* and FrzCD from *Myxococcus xanthus* as well as Hp0599 from *Helicobacter pylori* and Cj0448 from *Campylobacter jejuni*, respectively. Color in B is red for acidic, blue for basic, green for non-polar and grey for uncharged polar amino acids, and red asterisks below the alignments in B indicate sites of receptor methylation in Tsr. Protein sequences were aligned using FASTA (PEARSON & LIPMAN, 1988).

Whereas membrane-bound receptors as Tsr from *E. coli* (included in Fig. 5. as reference) have two transmembrane helices in their ligand binding

domain, no such sequences were identified in the soluble counterparts. This prediction is in full agreement with the hydropathy profiles of the two proteins calculated following the method of KYTE & DOOLITTLE, 1982, (Fig. 6).

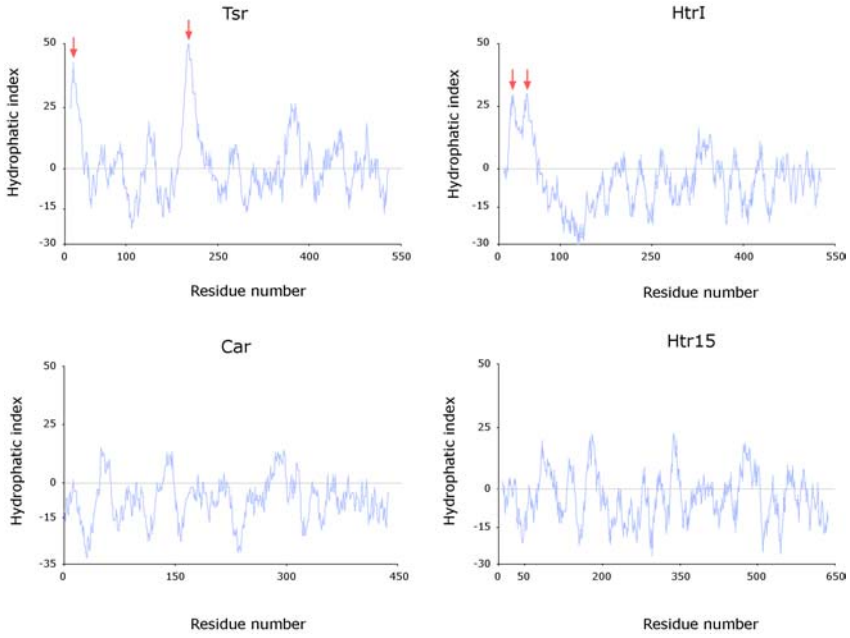

Fig. 6. Hydropathy profiles of proteins shown in Fig. 5 (Hp0599 and Cj0448 are shown in Fig. 15, p. 39, respectively). The algorithm of KYTE & DOOLITTLE, 1982, was used with a window size of 15. The two membrane spanning segments of Tsr and HtrI are clearly visible and indicated by red arrows. The other proteins lack transmembrane helices.

The genes coding for the MCP-like proteins Car HtpIII, HtB and Htr15 were amplified by PCR from genomic DNA of *H. salinarum* strain S9 and cloned into pT7-7 expression vectors using the NdeI and HindIII restriction endonuclease sites of the vector (the expression vector containing the *car* gene was a kind gift of F. STORCH). Two proteins, Car and Htr15, could be overexpressed in *E. coli* BL21(DE3)Gold, whereas the expression levels of HtB and HtpIII were too low to be detectable by SDS-PAGE of total cell extracts. The same result was obtained when HtB and

HtpIII expressed where in *E. coli* strain JM109(DE3). It was therefore not possible to reproduce the results from STORCH, 1999, who used this expression system for the heterologous expression of HtpIII. However, to further characterize Car and Htr15, purification schemes for the recombinant proteins were developed and Car as well as Htr15 could be purified from *E. coli* cytosol by standard FPLC techniques.

5.2. Purification of Car and Htr15

Car was first expressed as an N-terminal as well as a C-terminal His_6-tagged fusion protein that would facilitate its subsequent purification from *E. coli* cytosolic proteins by Ni-NTA chromatography. However, both His_6-tagged recombinant proteins failed to bind to Ni-NTA resin in appreciable amounts under all conditions tested including buffers with high amounts of denaturants such as urea or guanidinium chloride. The origin of this behavior is unclear, yet the halophilic proteins with their plethora of negatively charged surface residues might unfavorably interact with the positively charged histidine residues of the tag. Nevertheless, due to the amino acid composition of Car, the protein is highly soluble in saturated salt solutions even at high temperatures whereas *E. coli* proteins mostly precipitate under such conditions. As a first crude separation step, *E. coli* cytosol in 3 M potassium chloride was rapidly heated to first 52°C and then to 62°C. Most *E. coli* proteins were denatured and could be easily removed by centrifugation whereas Car remained in solution. Potassium chloride was then removed from the sample by dialysis, and Car was further purified on an anion-exchange resin utilizing again the markedly different amino acid composition of Car compared to the bulk of *E. coli* proteins. After a last chromatography step on hydroxyapatite, Car was at least 95% pure as judged by SDS-PAGE (Fig. 7). Since Car could be

purified without the use of the His_6-tag, all studies with Car used the un-tagged protein.

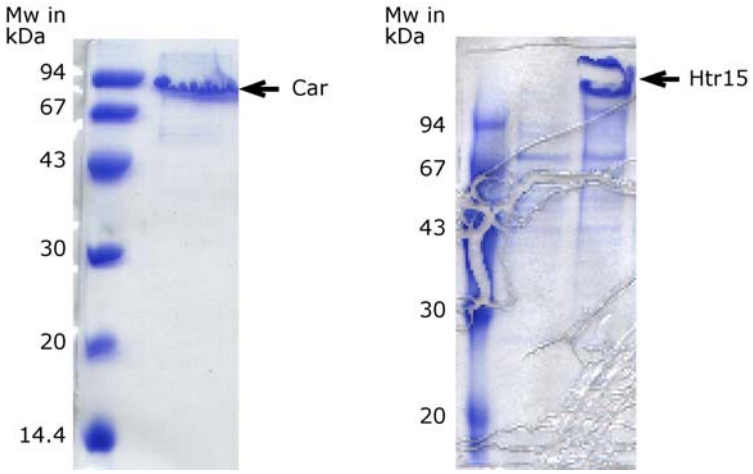

Fig. 7. Purified halobacterial receptor homologs Car and Htr15. Both proteins were heterologously expressed in *E. coli* and purified therefrom. The proteins with a molecular weight of 49.1 and 67.3 kDa, respectively, migrate at much higher apparent molecular weights than expected from the protein sequence indicating their extremely high content of acidic residues. Staining of the Htr15 band with Coomassie Brilliant Blue was always incomplete as can be seen by the white area in the middle of the band where no dye was bound by the protein.

In contrast to Car, the receptor homologe Htr15 was expressed as inclusion bodies in *E. coli*. The inclusion bodies could be dissolved in urea and the denaturant was removed by dialysis against a low salt buffer. Heat denaturation of contaminating *E. coli* proteins was not feasible as an additional purification step since Htr15 was not soluble in high salt buffer at elevated temperatures. This was surprising as both Car and Htr15 have a similar amino acid composition (27 and 23 % of acidic residues, calculated pI of 3.9 and 3.8). Besides this, the purification strategy - anion exchange chromatography and a purification step on hydroxyapatite - were nearly identical for both Car and Htr15. The purity of the Htr15 preparation was less than 80% as judged by SDS-PAGE analysis (Fig. 7).

Other chromatographic steps, for example size exclusion chromatography, hydrophobic interaction chromatography or cation exchange chromatography, were not possible since both proteins failed either to bind to the column or to elute from the columns under the conditions tested. This behavior is reflected by the minor impurities still present at the final stage of the purification scheme.

5.3. Characterization of Car by CD spectroscopy

Car was expressed in the low-salt environment of the *E. coli* cytosol, and the protein was exposed to low ionic strength buffers during its purification. Proteins from haloarchaeal bacteria are not only adapted to function in near-saturated salt solutions, but tend to unfold when salt is absent. In this study, CD spectroscopy with its high sensitivity towards protein secondary structural elements and ^{1}H-NMR (see 5.6.) were employed to examine whether purified Car adopted a defined three-dimensional structure or not. CD spectra of proteins almost exclusively composed of α-helices as myoglobin, for example, show a strong minimum both at 222 nm and at 208-210 nm and a pronounced maximum at 193 nm. In contrast, all-β proteins like plastocyanin have only one single minimum between 210 and 225 nm and a stronger positive maximum between 190 and 200 nm (VENYAMINOV & VASSILENKO, 1994). The intensity of these signals is therefore characteristic for the ratio and amount of α-helices and β-sheets present in a given protein. Fig. 8 shows the CD spectrum of Car in two different high salt buffers. The pronounced signals at 207 and 222 nm and the intensity of the signal at 207 nm compared to the signal at 222 nm clearly show the exclusive presence of α-helical secondary structural elements as expected from secondary structure prediction.

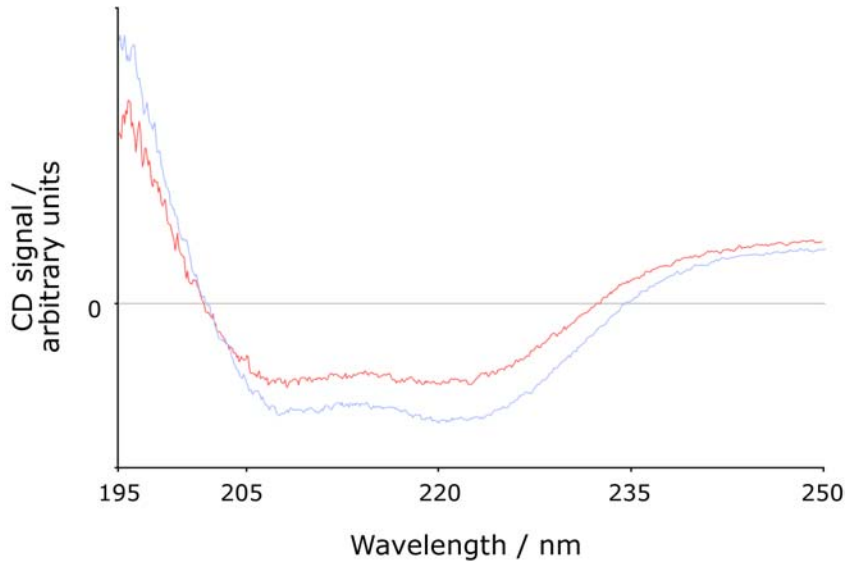

Fig. 8. Circular dichroic spectra of Car in aqueous high salt buffers. Car in 4 M sodium chloride, 20 mM potassium phosphate pH 8.0 at 20°C (blue curve) and Car in 3 M potassium chloride, 20 mM potassium phosphate pH 8.0 at 20°C (red curve). The CD signal is given in arbitrary units. Protein was diluted in the respective buffer to a concentration suited for CD spectroscopy. Data collection was at 20°C. Protein concentrations in both samples were different and therefore signal intensities can not be compared. For details see text.

H. salinarum maintains an internal level of salt (mainly potassium chloride) that is isotonic with the exterior (KUSHNER, 1988). The proteins of this organism are therefore adapted to potassium chloride concentrations approaching 5 M and usually require these high salt concentrations for stability and function. It is thought that under these conditions, the highly acidic proteins attract water molecules back to their surface in the form of a cooperative network of hydrated salt ions (FRANK & WEN, 1957; FRANK, 1958; DANSON & HOUGH, 1997) to avoid precipitation by their salting-out environment (TIMASHEFF, 1992). If the salt concentration is reduced, the negatively charged residues of the proteins are no longer shielded by the salt ions, and the proteins loose their tertiary structure due to charge repulsion.

Due to its ease, CD measurements were used to test the stability of Car under various solvent compositions. The change in signal intensities is thereby indicative for the rearrangement of structural elements in the protein. Car in storage buffer was diluted with assay buffer and CD spectra were taken from 190 to 250 nm. The strong α-helical signal at 222 nm disappeared gradually when Car was exposed to buffers with lower salt concentrations. Simultaneously, the signal ratio at 207 nm to 222 nm became >1, and the local minimum at 207 nm shifted towards shorter wavelengths indicating the loss of secondary structure and partial protein unfolding (Fig. 9, p. 29). This clearly shows that Car requires high concentrations of either sodium or potassium ions to maintain its fold. However, other salts as potassium or sodium chloride might also be able to maintain the native structure of the halophilic proteins. Especially calcium ions whose charge is twice the charge of sodium or potassium ions, but whose ionic radii are very close to the *radii* of the latter ions, stabilize halophilic protein (MADERN & ZACCAI, 1997). Due to their charge, their hydration shell is by far larger than compared to potassium, and a lower concentration is subsequently sufficient to promote water binding to the protein surface. As anticipated, calcium ions maintained the protein structure at much lower concentrations than potassium or sodium ions (Fig. 9C, p. 29). Whereas monovalent ions stabilized the structure of Car with increasing concentrations, calcium chloride had a denaturing effect on Car above a concentration of ca. 0.2 M.

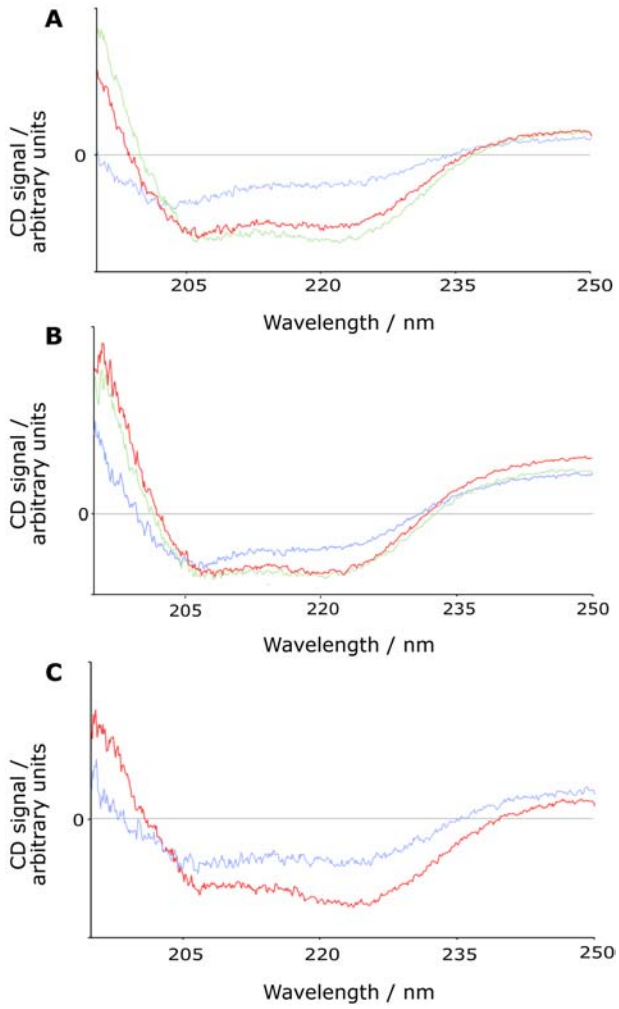

Fig. 9. Loss of secondary structure in Car when exposed to buffers with low ionic strength. **A.** Car in buffer A supplemented with sodium chloride. When the salt concentration was decreased, the CD signal became less pronounced and the spectrum changed. Sodium chloride concentrations were 4.0 M (green), 2.0 M (red) and 1.0 M (blue), respectively. Similar curves were obtained in buffers containing potassium **(B)** or calcium **(C)** instead of sodium ions. Potassium chloride concentrations in **B** were 3.0 M (green), 2.5 M (red) and 2.0 M (blue), and the calcium chloride concentrations in **C** were 0.5 M (red) and 0.3 M (blue), respectively. All measurements were taken at 20°C. Car was diluted in the respective buffer to a concentration range suitable for CD spectroscopy. Protein concentrations were constant but not measured in all test series to allow comparison of signal intensities.

Besides ionic strength, the solvent itself has a strong influence on the overall fold of Car: when water was substituted by deuterium oxide, the protein was stabilized in dilute salt solutions compared to water due to an

increase in the strength of hydrogen bonds (NÉMETHY & SCHERAGA, 1964; BONNETÉ *et al.*, 1994). The minimum (blue curve) indicates an optimal calcium concentration for Car (around 0.2 M). Going from this optimum towards higher salt concentrations, the salting-out effect of deuterium oxide does not compensate for the salting-in effect of the high calcium chloride concentrations, and Car unfolds due to the efflux of water from the hydration network around the protein (TIMASHEFF, 1992). In the presence of deuterium oxide, the curve is shifted to lower calcium chloride concentrations, indicating a stabilization of the protein structure (Fig. 10).

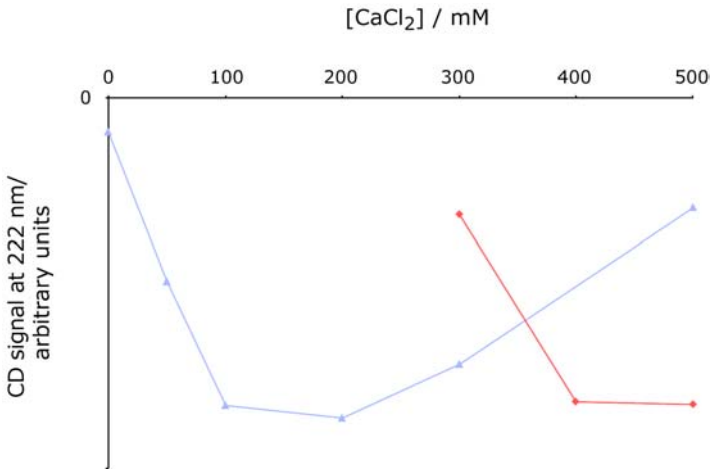

Fig. 10. Influence of calcium ions on the protein structure of Car in water (red) and deuterium oxide (blue) as solvents. CD spectra of Car were taken in the respective buffers at 20°C and the signal at 222 nm was plotted versus the calcium chloride concentration.

Proteins not only interact with salt or solvent molecules that surround them. Other compounds such as sugars (ARAKAWA & TIMASHEFF, 1982), polyols (GEKKO & TIMASHEFF, 1981), amino acids or methyl amines present in the solution also stabilize proteins (TIMASHEFF, 1991). Indeed, these molecules are used by a variety of organisms as stress-inducible osmolytes (SOMERO, 1986). It is well established that such compounds are

indeed present in *Halobacterium* (STORCH *et al.*, 1999), and therefore low molecular weight compounds such as polyethylene glycols or putrescin – albeit not physiological - were assayed for their influences on the fold of Car. Both compounds had a positive influence on protein stability (see Fig. 11).

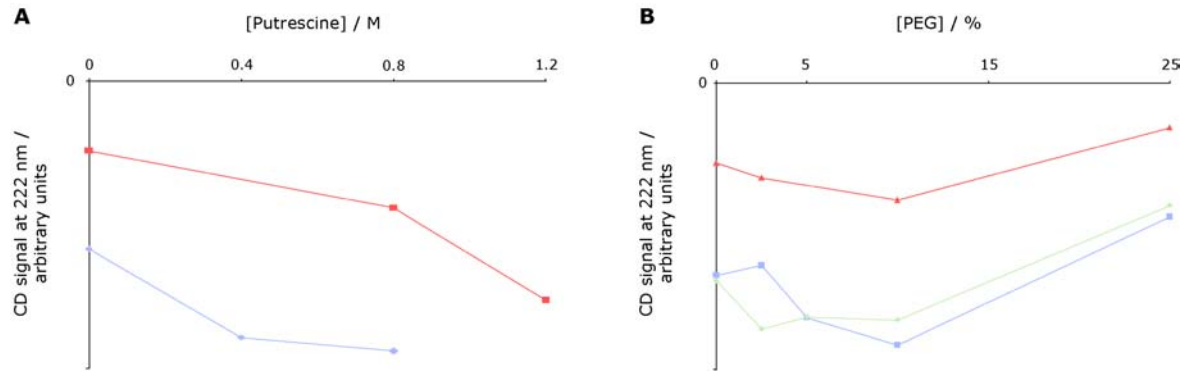

Fig. 11. Influence of small molecules on the secondary structure of Car when exposed to decreasing salt concentrations. **A.** Influence of putrescine on the secondary structure of Car in 2 M (blue) and 1 M (red) sodium chloride **B.** Influence of PEG 1000 (2 M sodium chloride, blue) and PEG 4000 (2 M sodium chloride, green; 1 M sodium chloride, red) on the secondary structure of Car. The curves were obtained by plotting the CD signal at 222 nm versus the additive concentration.

The experiments clearly showed that putrescine and polyethylene glycols do stabilize the secondary structural elements of Car. The α-helical content of the protein increases with an increasing additive concentration. As can be seen in Fig. 11B, the stabilizing effect of PEGs does not compensate the denaturing effect of a dramatically lowered salt concentration (signal intensities at 1 and 2 M salt concentration differ significantly). However, as in the case of calcium ions, PEGs denature the protein above an optimal concentration.

5.4. Heat denaturation of Car

The results from the CD spectroscopic measurement show that Car has a high α-helical content that is diminished by unfavorable solution conditions. These results, however, do not allow any conclusions to be drawn beyond the secondary structure of the protein. Native proteins not only possess α-helices or β-sheets, but their three-dimensional structure is almost uniform. Molten globules, in contrast, are also build from secondary structural elements yet do not have any distinguished tertiary fold. Both states might be distinguished by folding/unfolding experiments. It is well established that single-domain proteins fold and unfold with a high degree of cooperativity, whereas molten globules usually do not (LUO & BALDWIN, 1999; LAKSHMIKANTH *et al.*, 2001). Cooperative thermal unfolding of Car would therefore be indicative for the collapse of a previously existing defined tertiary protein structure.

When Car in high salt buffer was heated from 20°C to above 80°C, the CD signal at 222 nm became gradually weaker at a temperature of approximately 45 °C. At this temperature, the curve rose considerably steeper, whereas at even higher temperatures, the curve again rose only slowly (Fig. 12A). This sigmoidal slope was also apparent yet less pronounced when the protein was cooled down back to room temperature (data not shown). The CD spectra of Car before and after the heat denaturation did not differ significantly (Fig. 12B).

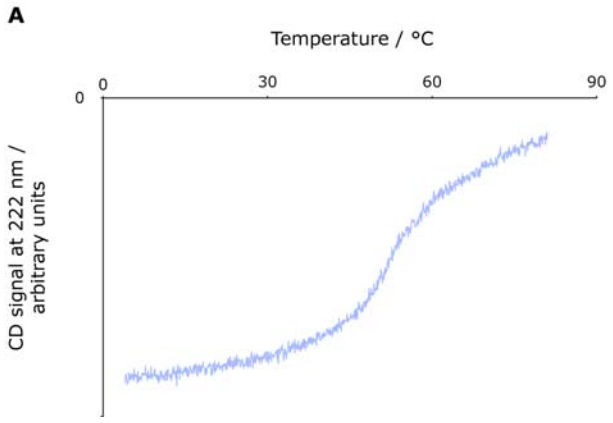

Fig. 12A. Heat denaturation of Car. The protein in high salt buffer was heated from room temperature to above 80°C at 1°C per min and the CD signal at 222 nm was recorded and plotted against the temperature.

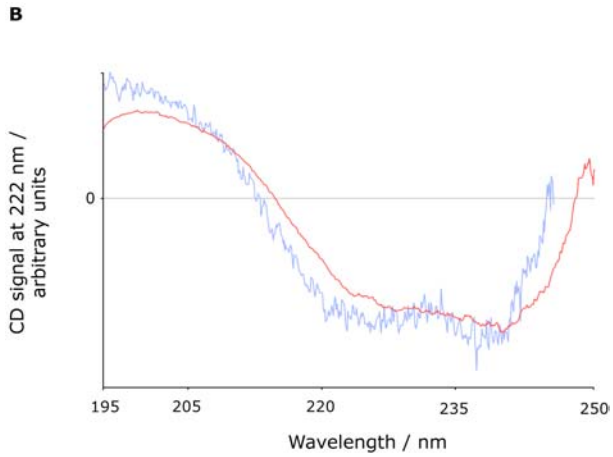

Fig. 12B. Heat denaturation and renaturation of Car. At the beginning (red curve) and at the end (blue curve) of the experiment, CD spectra were taken from 195 to 250 nm. The red curve is an average of four independent measurements. Data for the blue curve were discarded above 245 nm (out of range).

It is the sigmiodal slope of the heat denaturation curve that allows to conclude that Car unfolds in a cooperative mannor, indicating the presence of a well defined tertiary protein structure before the heat denaturation where this fold collapses. The fact that the CD spectra of Car

before and after the heat denaturation experiment are very similar (Fig. 12B) reveals a reversible thermally unfolding of the protein.

5.5. Characterization of Car by ^{1}H-NMR

NMR spectroscopic experiments of proteins require large amounts of pure proteins in very high concentration. When this is available, the method gives information on protein structure far beyond CD spectroscopy. Even simple ^{1}H-NMR spectra indicate whether the residues that gave rise to the respective signals all experience the same chemical environment or not. Broad, non-structured peaks emerge from residues in unstructured regions whose chemical environment is alike. However, the situation is more complex in cases of proteins with large molecular weights or with aggregated proteins. Due to quantum mechanical effects, the signals broaden and become indistinguishable from spectra of unfolded proteins.

In this study, purified Car was concentrated to 0.5 mM in high salt buffer and the viscous solution was subjected to ^{1}H-NMR measurements in a Bruker DRX600 NMR spectrometer. Fig. 13 shows a typical ^{1}H-NMR spectrum. The signals are not resolved but in distinct, large peaks, strongly suggesting the same chemical environment for all protons of the respective residues. Under the important assumption that Car does not aggregate, the signals clearly indicate that the protein had no defined tertiary structure. Combined with the data derived by CD spectroscopy it therefore must be concluded that Car obtained as described in this study adopts a molten globule-like structure composed mainly of α-helices. However, in the case that Car adopts a dimeric structure in solution and in the light that homologous proteins cluster *in vivo* as well as *in vitro* (see chapter 6), it is well conceivable that Car oligomers are simply too large to

yield well-resolved NMR spectra, and therefore the CD spectroscopic data might be more valid in reflecting the real folding state of Car.

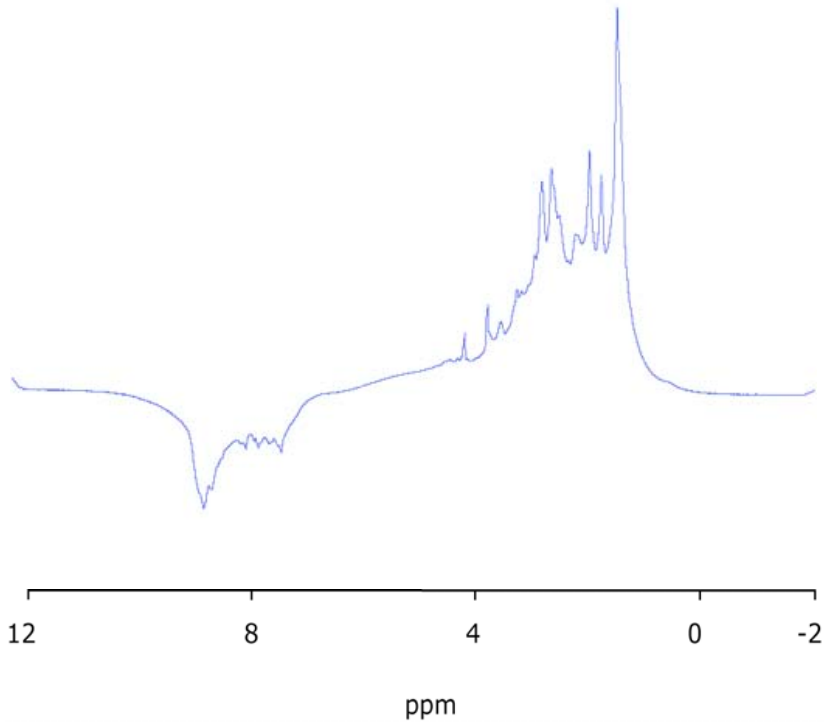

Fig. 13. ^{1}H-NMR spectrum of Car at a concentration of 0.5 mM as determined by the BRADFORD method. The signals of amid protons appear at 6 ppm, signals of aromatic protons and of protons at amino groups between 7 and 8 ppm, and Hα, Hβ and Hγ protons give rise to signals between 4 and 5, 2 and 3 and 1 and 2 ppm, respectively. The water signal is suppressed.

5.6. Crystallization trials for Car

None of the crystallization trials produced positive results in terms of protein crystals. Car was quickly denatured in the MPD/sodium chloride/water system (RICHARD *et al.*, 1995) under all conditions tested albeit pH values near neutral seemed to slow down protein precipitation. Phosphate also caused protein precipitation in the pH range below 6.0 and

above 7.0. Besides that, in many buffers from Hampton Research's Crystal Screen kit phase separation occurred after adding salt to a final concentration of 4 M, especially in solutions containing additives as organic solvents or polyethylene glycols.

5.7. Expression, purification and crystallization trials with Car fragments

Since full length Car did not yield protein crystals, an alternative strategy was chosen to further investigate the protein and possibly obtain structural data of at least parts of the transducer. Based on the idea that some regions of the protein might be unfolded while other parts could be more stable under the solvent conditions used to purify and crystallize the protein, six Car fragments were constructed. In doing so, information from the simple secondary structure prediction algorithm of the program DNASIS (Hitachi) was taken into consideration as well as the position of the previously identified domains and regions necessary for the proper function of the protein (Fig. 14). From all six N- and C- terminal domain constructs of Car, four could be overexpressed in *E. coli*: Dom2, Dom3, Dom4 and Dom6. The proteins were purified following the strategy initially developed for full length Car. One protein, Dom6, was used in crystallization trials with a modified Hampton Research Crystal Screen I kit in the presence of 4 M sodium chloride. As in the case with Car, the protein did either precipitate or stayed in solution for prolonged periods. All precipitates were dark brown and unstructured indicating denatured protein.

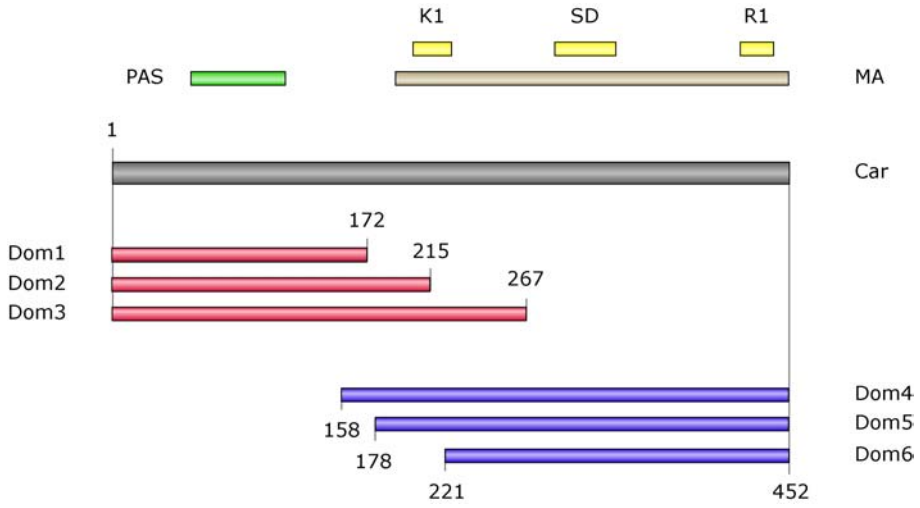

Fig. 14. Construction of the six Car fragments. The PAS domain (lime) and the methyl-accepting chemotaxis-like domain (MA, ochre) as well as the signaling domain (SD) and the K1 and R1 peptides (all in lemon) are depicted above the full length Car protein (gray) as calculated by the SMART algorithm (LETUNIC *et al.*, 2002). Below are the three N-terminal (ruby) and C-terminal (blue) fragments of Car (Dom1 through Dom6). Numbers indicate the amino acid positions in full length Car where the fragments start and end, respectively.

5.8. Expression of *H. salinarum* CheB and CheR in *E. coli*

The functionality of Car might be tested by various methods. In analogy to the *E. coli* chemotaxis network (NINFA *et al.*, 1991), an in-vitro assay where the receptor modulates the activity of the histidine kinase CheA would demonstrate its functionality. It was beyond the scope of this work to successfully establish such an assay. However, Car prepared during this study was examined without success by coworkers (Chie OTSUKA, personal communication) whether it influences CheA activity. The presence of receptor modifying enzymes CheB and CheR in *H. salinarum* allows an alternative strategy to be chosen: by the use of (S)-adenosyl-L-methionine, CheR should methylate conserved residues in the K1 and R1 regions of Car (see Fig. 5, p. 22), whereas CheB should remove the

methyl groups. To set up this assay, and to provide purified recombinant protein to coworkers, it was attempted to express the two halophilic proteins CheB and CheR from *H. salinarum* in *E. coli* BL21(DE3)Gold with the result that under all conditions tested, no detectable protein expression was achieved. To eliminate influences from *H. salinarum*'s non-*E. coli* codon usage preference, synthetic genes for the two proteins were designed using codons preferred by *E. coli*. In both cases, the ligase chain reaction produced the desired genes but none of it could be successfully expressed in *E. coli* BL21(DE3)Gold.

5.9. Soluble receptor homologs in *C. jejuni* and *H. pylori*

Database searches with the highly conserved signaling domains of Car and other receptors from *E. coli* identified one protein from *H. pylori*, Hp0599, that was erroneously annotated as a haemolysin secretion protein precursor (hylB; TOMB *et al*., 1997). Within the genome of the evolutionary closely related organism *C. jejuni*, three additional transducer-like proteins were identified (Table 3).

Table 3. Soluble receptor homologs from *C. jejuni* and *H. pylori*.

Protein	M_r (kDa)	GenBank Acc No.	Protein Id.	Author
Cj0246c	43.3	6967505	CAB72714.1	PARKHILL *et al.*, 2000
Cj0448c	40.5	6967817	CAB75086.1	PARKHILL *et al.*, 2000
Cj1110c	48.3	6968444	CAB73365.1	PARKHILL *et al.*, 2000
Hp0599	48.3	AE000573	AAD07662.1	TOMB *et al.*, 1997

One common feature of these proteins was their apparent lack of transmembrane spanning segments as predicted by hydropathy calculation algorithms. The KYTE-DOOLITTLE plot, for example, did not

indicate any regions of strong hydrophobicity in Hp0599 and Cj0448 (Fig. 15). Remarkably, the methyl-accepting chemotaxis-like domain is followed by a stretch of approximately 100 amino acids in length which is in contrast to the receptor proteins from *H. salinarum* or *E. coli*, where the polypeptide chain ends with the MA domain (see Fig. 5, p. 22). These stretches of amino acids are not homologous to any other protein sequences in public databases, yet there is a slight homology between Cj0448 and Hp0599 in this region (24% identity in 102 amino acids). Consequently, both proteins were chosen to investigate their properties.

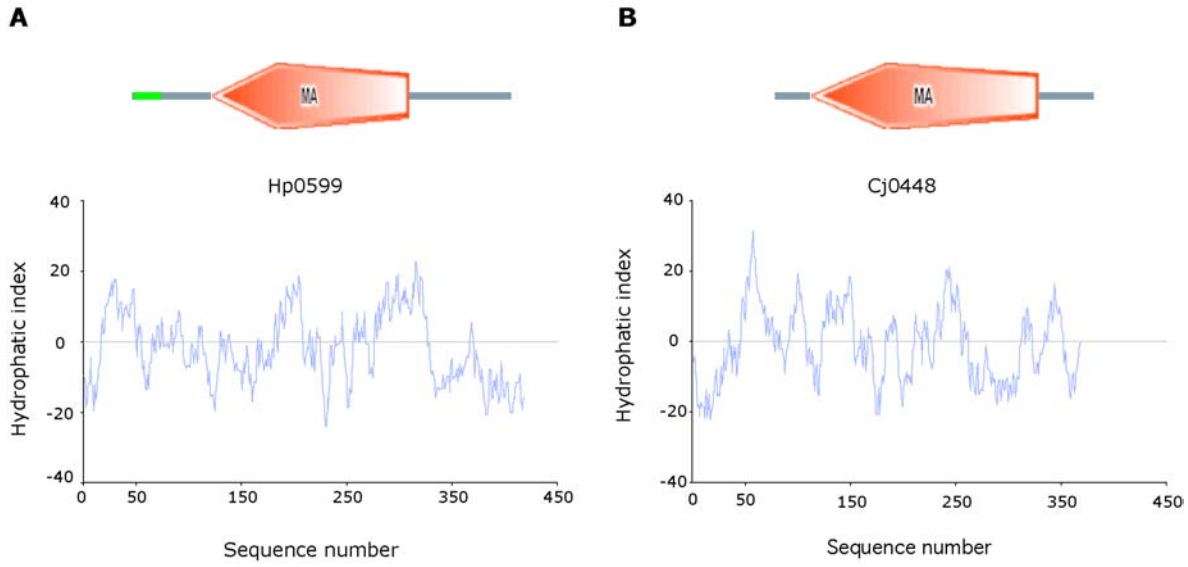

Fig. 15. Hydropathy profiles of the soluble receptors homologs Hp0599 from *H. pylori* (**A**) and Cj0448 from *C. jejuni* (**B**). The algorithm of KYTE & DOOLITTLE, 1982, was used with a window span of 15. Above the plot the domain architecture of the respective protein is depicted (for details see http://smart.embl-heidelberg.de/smart). MA: methyl-accepting chemotaxis-like domain; green stretch in Hp0599: predicted coiled coil region.

For this purpose, the genes for Hp0599 and Cj0448 were cloned into the pET28a(+) expression vector and expressed in *E. coli* BL21(DE3)Gold as N-terminal His_6-fusion proteins. The recombinant proteins could be

purified from the *E. coli* cytosol by affinity chromatography, ion exchange- and size exclusion chromatography, substantiating the assumption that they are soluble and not integral membrane proteins. After purification, both proteins were essentially pure (Fig. 16).

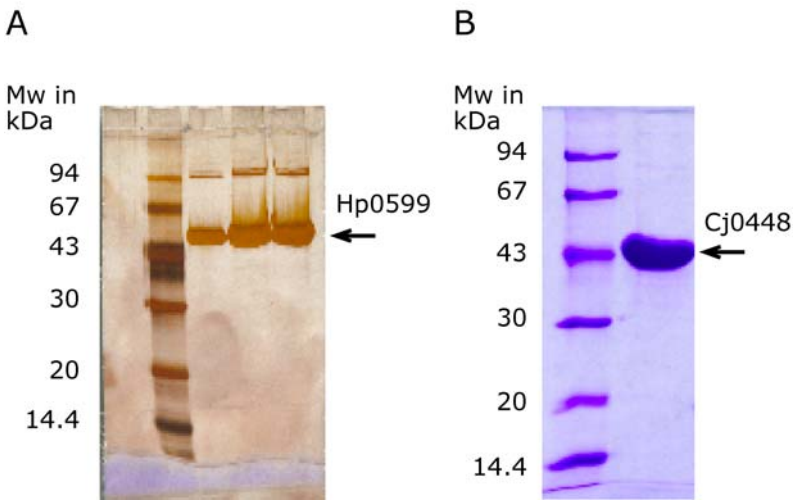

Fig. 16. Purified receptor homologs from *H. pylori* and *C. jejuni*. **A.** Silver stained SDS-PAGE showing Hp0599. **B.** Coomassie Brilliant blue stained SDS-PAGE showing purified Cj0448. The gels were run until the dye front reached the lower end of the gel, and recombinant proteins are indicated by arrows.

In the Hp0599 preparation, the band running at about 100 kDa is apparently dimeric Hp0599, since this band weakens when an excess of 2-mercaptoethanol was added to the sample, and it is the predominant band without 2-mercaptoethanol. This is consistent with the behavior of the protein in gel filtration experiments where it elutes as one single peak at an apparent molecular weight of 320 kDa (Fig. 17).

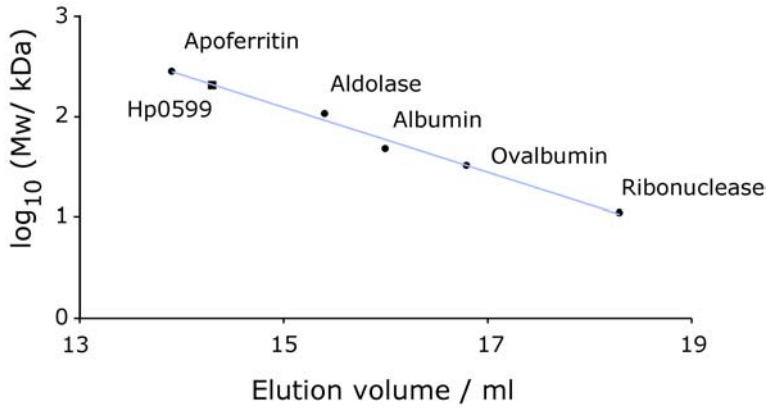

Fig. 17. Molecular weight determination of Hp0599 by size exclusion chromatography on a Superose 6 HR 10/30 column. The protein runs at approx. 320 kDa. The apparent molecular weight for ribonuclease A is 13.7 kDa, for ovalbumin 43.0 kDa, for bovine serum albumine 67.0 kDa, for aldolase 158 kDa, and for ferritin 440 kDa. The flow rate was 0.4 ml/ min of buffer (300 mM sodium chloride, 10 mM Tris-HCl pH 8.0 at 4°C), and the coefficient of correlation was 0.989 for the calibration line.

The calculated molecular weight according to its amino acid composition, however, is 48.3 kDa. Apparently, the protein is hexameric, a fact that is perfectly in accordance with the concept of clustered chemoreceptors in signaling arrays known from other bacterial species (GESTWICKI *et al.*, 2000). In the crystal structure of the cytoplasmic portion of Tsr from *E. coli*, the tails of three Tsr dimers come together into a trimeric structure (KIM *et al.*, 1999), and it is assumed that the same structure is present in cellular receptor clusters (SHIMIZU *et al.*, 2000). This hexameric structure might be the reason for the oligomerization state of Hp0599. In the receptor complexes, the conserved signaling domains of the receptors are at the tip of the structure, mediating the contact to CheA and CheW. It is worth noting that exactly this domain is highly conserved in all other proteins with an MA domain even outside the bacterial kingdom (Fig. 5, p. 22 and LE MOUAL & KOSHLAND, 1996).

5.10. Crystallization of chemotaxis components Hp0599, Cj0448 and CheW

As in the case of Car, the soluble transducer-like proteins from *H. pylori* and *C. jejuni* represent valuable targets for crystallization trials, and therefore it was attempted to produce protein crystals of high enough quality to gain structural information on these MCP-homologs. In experiments with Hampton Research's Crystal Screen I and II kits, for both proteins several buffer compositions were identified that produced protein crystals by vapor diffusion in 2 µl hanging drops. Table 4 summarizes the results.

Table 4. Initial crystallization conditions for *H. pylori* and *C. jejuni* receptor homologs

Protein[1)]	Precipitant	Buffer[2)]	Crystal shape
Cj0448	1.5 M Li_2SO_4	HEPES-Na pH 7.5	small, non-uniform spheroids
	1.4 M Na acetate	Na cacodylate pH 6.5	thin, hexagonal platelets
	0.8 M K- Na- tartrate	HEPES-Na pH 7.5	small, non-uniform spheroids
Hp0599	1.5 M Li_2SO_4	HEPES-Na pH 7.5	small, non-uniform spheroids
	8% PEG 8000	Tris-HCl pH 8.5	thin needles

[1)]: For crystallization, the His_6-tag of the protein was removed by thrombine as described in Materials & Methods, since the His_6-tagged protein did not crystallize under the conditions examined in this study.

[2)]: All buffers were 0.1 M final concentration.

To improve crystal quality, the buffer compositions of the initially identified conditions were systematically altered. The behavior of Hp0599 in a typical PEG screen is shown in Table 5.

Table 5. Typical PEG screen with Hp0599.

pH	% PEG 2000						% PEG 3350					
	4	5	6	7	8	9	4	5	6	7	8	9
7.0												
8.0				N					N	P		
9.0												
pH	% PEG 6000						% PEG 8000					
	4	5	6	7	8	9	4	5	6	7	8	9
7.0												
8.0			P	N	N	N			N		N	
9.0						N					P	N

One µl protein (10 mg/ml in 0.1 mM 2-mercaptoethanol, 0.5 mM EDTA, 10 mM Tris-HCl pH 8.0 at 20°C) was mixed with an equal amount of well solution. The plate was incubated at 18°C and protein crystals (N for needles, P for platelets) grew in a narrow zone between a region where the protein stayed in solution (white background) and a region where the protein precipitated (gray background).

The crystallization of Hp0599 is sensitive towards pH as well as PEG concentration. The tendency of the protein to precipitate increases with an increasing pH or PEG concentration, and only in a narrow range between the zone where the protein precipitates (gray areas in Table 5) and the region where it stays in solution (white areas) protein crystals were obtained. From the pH sensitivity of the protein it is apparent that charged residues are involved in protein/protein interactions that lead to crystal growth. Furthermore, the appearance of platelets where crystal growth occurred in two dimensions is limited to an even smaller region within or adjacent the area where needle-shaped protein crystals grew. Even though the pH differences in the experiments depicted in Table 5 where one pH unit from one row to the next and the differences in PEG concentration were one per cent, smaller parameter variations did only broaden the zone where crystallization occurred yet no three dimensional crystals appeared. Compounds with a known influence on crystal growth (Hampton Research Additive Screen I, II and III) were then added to the

initially identified buffer condition in the hope that this might lead to three-dimensional crystals without success.

The crystal structure of the cytosolic domain of Tsr (KIM *et al.*, 1999) shows that the conserved signaling domain that makes up a continuous stretch of 207 amino acids in Hp0599 (total length: 433 amino acids) is a more than 200 Å long coiled coil. It is therefore well conceivable that crystal growth occurs mainly in the plane orthogonal to the longitudinal axis of the coiled coils, and that growth in all three dimensions is slowed down by the lack of protein/protein contacts parallel to that axis. Furthermore, the Tsr fragment crystallized was a mutant fragment where all glutamate residues involved in receptor methylation were replaced by glutamine to 'mimic' the liganded state of the receptor. Without this modification, no crystals were obtained. However, the positions of the analogous residues in Hp0599 (see Fig. 5, p. 22) were not yet determined and it is questionable whether receptor methylation occurs in this organism at all due to the lack of genes homologous to *che*R and *che*B.

Hp0599 finally gave thin, often twinned quadratic platelets of approximately 100 µm in size (Fig. 18, p. 45). Analogous experiments as described for Hp0599 were also performed to improve Cj0448 crystal quality with comparable results. Cj0448 crystallized as thin hexagonal plates or, in the presence of 3% hexanediol, as snowflake-like objects. However, none of the protein crystals tested proved to be useful for X-ray structure determination due to poor X-ray diffraction. It is interesting to note that both receptor homologs failed in building three-dimensional crystals, substantiating the idea that crystal lattice formation might be hindered by the native coiled-coil structure of the proteins.

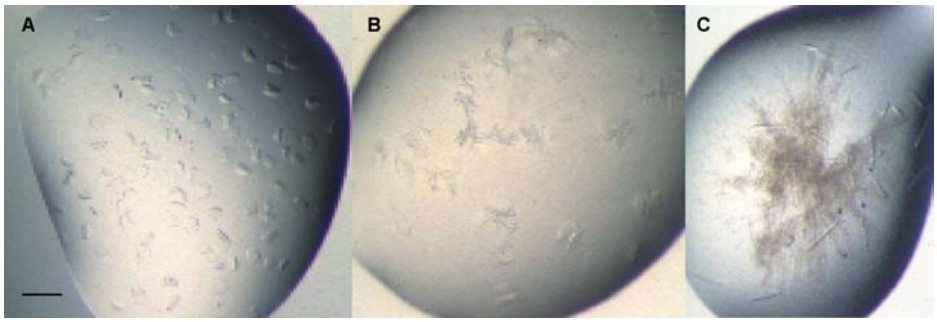

Fig. 18. Crystallization of soluble proteins Hp0599, Cj0448 and coupling protein CheW by vapor diffusion. **A.** Crystals of Hp0599 derived after several days at 18°C in hanging droplets of 1 µl protein (8 mg/ml in 0.1 mM 2-mercaptoethanol, 0.5 mM EDTA, 10 mM Tris-HCl pH 8.0 at 20°C) and 1 µl reservoir solution (6% PEG 6000, 100 mM Tris-HCl pH 8.0 at 20°C). **B.** Crystals of Cj0448 grown as in A with 1 µl of protein (10 mg/ml) and 1 µl reservoir solution (1.4 M sodium acetate, 10 mM Tris-HCl pH 7.5 at 20°C). The scale bar in A is approximately 250 µm in size. **C.** Crystals of *H. pylori* CheW grown at 18°C. One µl protein (6.5 mg/ml in 10 mM Tris-HCl pH 8.0 at 20°C, 300 mM sodium chloride, 10% glycerol) and 1 µl reservoir solution (1.4 M lithium sulfate, 10% glycerol, 10 mM Tris-HCl pH 7.5 at 20°C) were mixed as described.

The coupling protein CheW was also crystallized by vapor diffusion in 2 µl hanging drops (Fig. 18C) after removal of its His_6-tag. The protein has a pronounced tendency to precipitate at elevated concentrations (around 3 mg/ml) and it can not be shock frozen in liquid nitrogen even in dilute solutions due to the same reason. This tendency to aggregate is also reflected in the behavior of CheW after adding precipitant in crystallization experiments where it precipitates within a few hours (Fig. 18C). Thereafter, crystals appeared after days and seemed to grow from precipitated protein. After optimizing the crystallization conditions, CheW crystallized as long hexagonal columns with sharp edges and of considerably size. However, the resolution limit was only 4.6 Å as determined at beamline IDI43 at the European Synchrotron Radiation Facility, Grenoble. The space group was determined to be P6.

5.11. The chemotaxis network in *H. pylori*

The soluble receptor homologs from *H. pylori* and *C. jejuni* were successfully expressed in *E. coli*, purified therefrom and crystallized. Nevertheless, their function in chemotaxis - if any - remains questionable. From the orthologous membrane-bound proteins from enteric bacteria it is expected that the proteins directly interact with the Che protein cascade in the respective organisms. It was therefore necessary to show the functional interplay to assign a transducer-like function to Hp0599 and Cj0448.

5.11.1. Modulation of CheF autophosphorylation activity

Within the *H. pylori* genome, six genes were identified as putative structural genes coding for proteins involved in chemotaxis (TOMB *et al.*, 1997; Table 6).

Table 6. Chemotaxis proteins identified in *H. pylori* strain 26695 and strain J99.

Protein	M_r (kDa)	Strain 26695 Id.	Strain J99 Id.	ID. %	GenBank Acc. No.[1)]	Protein Id. [1)]
CheF[2)]	89.8	Hp0392	Jhp0989	95.0	AE000555	AAD07457.1
CheV1	36.6	Hp0019	Jhp0017	99.7	AE000524	AAD07087.1
CheV2	35.6	Hp0393	Jhp0988	97.4	AE000555	AAD07458.1
CheV3	35.6	Hp0616	Jhp0559	98.7	AE000576	AAD07681.1
CheW	19.0	Hp0391	Jhp0990	92.1	AE000555	AAD07456.1
CheY	14.1	Hp1067	Jhp0358	97.6	AE000555	AAD08113.1

[1)] GenBank accession numbers and protein IDs given refer to *H. pylori* strain 26695 genes and proteins. All proteins used in this work were derived from *H. pylori* 26695 genes.

[2)] Named after PITTMAN *et al.*, 1997.

To investigate their presumed function deduced from sequence homology to already characterized proteins, the respective genes were cloned into expression vectors, expressed in *E. coli* BL21(DE3) cells as His_6-tagged fusion proteins and purified therefrom as described in Materials & Methods.

Central to two-component chemotaxis networks is the histidine kinase that regulates the flux of phosphate groups through the whole system. In *H. pylori*, CheF is the respective kinase. Within its amino acid sequence, several residues can be identified homologous to conserved amino acids in other Che proteins (Fig. 19, next page). In the N-terminal CheA-like domain, the residue homologous to H47 becomes phosphorylated in CheA from the CheA kinase domain, whereas residues D729 and K781 in the C-terminal CheY-like domain are important for function in CheY (SILVERSMITH *et al.*, 1997). In this response regulator, the homologous aspartyl residue is phosphorylated by the cognate kinase, and the conserved lysine residue is important for CheY-phosphate autohydrolysis. CheF therefore appears to be a hybrid histidine kinase where a response regulator domain is fused C-terminally to a kinase domain. Che proteins with such an architecture were found previously in *Myxococcus xanthus* and other bacterial species as *Synechocystis* (MCCLEARY & ZUSMAN, 1990; KIMURA *et al.*, 2001), and hybrid histidine kinases from other signal transduction networks are ubiquitous in all three kingdoms of life.

Fig. 19. Domain analysis and sequence alignments of *H. pylori* CheF with paralogs from *H. pylori* and orthologs from other species. **A.** Schematic representation of CheF architecture. Domains in CheA-like N-terminal part (blue) are H: histidine box; Y/B: CheY/CheB binding domain; C: dimerization and kinase domain; R: regulatory domain (BILWES *et al.*, 1999). The CheY-like part is colored red. **B.** Amino acids 40 to 72 of CheF H box. Histidine residue 47 from CheF is highly conserved in all other histidine kinases (red arrow) **C** and **D.** Protein sequence alignment of CheF response regulator domain (amino acids 723 to 749 and 768 to 789, respectively), with other response regulators. Again, residues conserved in all proteins are marked by red arrows.

Fig. 20 shows a typical protein preparation of CheF after Ni-NTA chromatography followed by size exclusion chromatography.

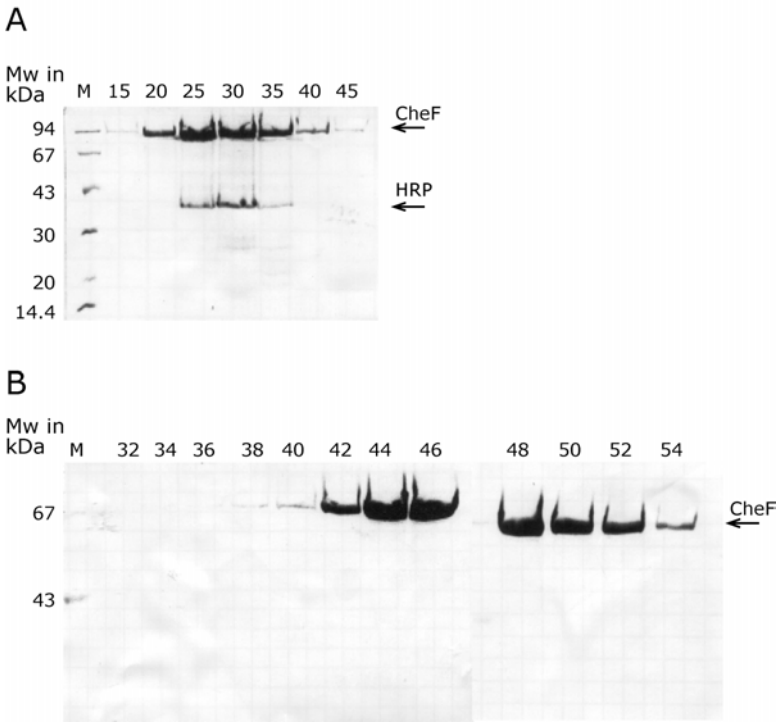

Fig. 20. Purification of CheF from *E. coli* cytosol. **A.** Eluent fractions from a 2.5x10 cm Ni-NTA column. Fraction size: 5 ml, gradient: 2.5 to 250 mM imidazole in 300 mM sodium chloride, 10 mM Tris HCl pH 8.0 at 4°C, 10 % glycerol in 300 min at a flow rate of 1 ml/min. **B.** Eluent fractions of a Sephacryl S300 HR column (1x60 cm). Probe volume: 1 ml (fractions 25 through 35 from A, pooled and concentrated), flow rate: 160 µl/min (300 mM sodium chloride, 10 mM Tris HCl pH 8.0 at 4°C, 20 % glycerol), fraction size: 7 min. Fraction numbers are indicated by numbers above the respective lanes. Probe volume was 15 µl of sample per lane. HRP: Histidine rich protein *from E. coli* as determined by N-terminal sequencing of the protein band.

The contaminating protein present after Ni-NTA chromatography is the histidine rich protein from *E. coli* that runs at a much higher apparent molecular weight as expected from its theoretical molecular weight (21 kDa). CheF could be purified from this protein by size exclusion chromatography. It is interesting to note that CheF does not elute from Superdex columns and therefore Sephacryl was chosen for gel filtration. Furthermore, in contrast to *E. coli* CheA, CheF does not bind Cibacron Blue coupled to Sepharose, an affinity resin that can be used to purify CheA

(HESS *et al.*, 1991) and that was successfully employed to do so in this study as a positive control (data not shown).

From the CheA-like domain in CheF, it can be expected that this protein autophosphorylates in analogy to CheA (HESS *et al.*, 1988). Furthermore, due to the response regulator domain additionally present in CheF, it can well be assumed that the phosphate group is passed to D729 from where it is ultimately transferred to water, resulting in the net-hydrolysis of ATP (Fig. 21).

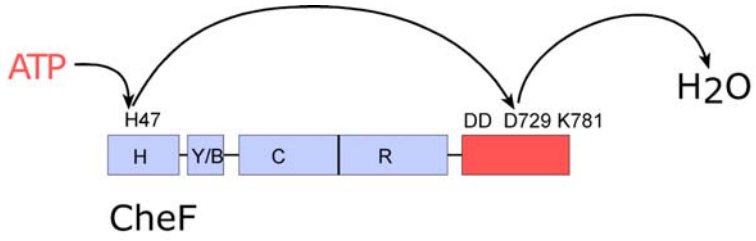

Fig. 21. Possible phosphotransfer reactions in CheF. The CheA domain in CheF is colored blue, whereas the CheY-like response regulator domain is red. Conserved residues are indicated above the protein. For the sake of simplicity, CheF is depicted as monomer and the phosphotransfer reaction is drawn in *cis*. However, whether such a transfer reaction occurs in *trans* or *cis* is unknown.

As anticipated, purified CheF autophosphorylates in the presence of ATP and Mg^{2+} ions, (Fig. 22).

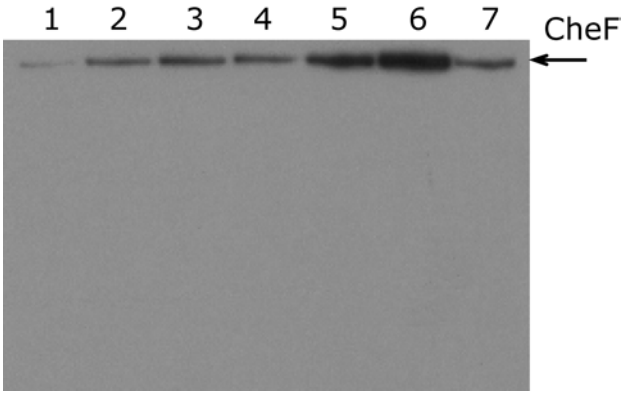

Fig. 22. Autophosphorylation activity of CheF. CheF (2 μM) was incubated in various buffers in the presence of 50 μM [γ-^{32}P]ATP (5000 Ci/mmol) for 20 min at room temperature. Thereafter, the reactions were stopped by the addition of 2x SDS buffer, proteins were separated by SDS-PAGE and transferred to a PVDF membrane. Exposure to X-ray film was 18 h. Assay buffer composition in lane 1 and 2: 5 mM $MgCl_2$, 5 mM $MnCl_2$, 1 mM DTE, 50 mM HEPES pH 7.5 at 20°C and in lane 3 through 7: 5 mM $MgCl_2$, 50 mM HEPES pH 7.5 at 20°C. CheF was dialyzed overnight at 4°C against 10 mM HEPES pH 7.5 at 20°C supplemented with 10 % glycerol (lanes 2 and 5), 300 mM sodium chloride (lane 4), 10 % glycerol and 300 mM sodium chloride (lane 6) and 5 mM 5 mM $MgCl_2$ in lane 7.

The protein phosphorylation level in the sample where the kinase was dialyzed overnight in the presence of sodium chloride and glycerol was higher compared to the samples without these additives. To investigate the function of the conserved residues in the response regulator domain of CheF, mutant proteins were constructed in the hope that this gives insight into the role of the CheY-like domain. Under the assumption that wild type CheF indeed hydrolyses ATP as depicted in Fig. 21, p. 50, it was expected that a slowdown of the phosphate group transfer reaction from the CheY-like domain to water would increase the CheF-phosphate concentration in the presence of ATP. In *E. coli* CheY, mutations of the conserved residue K109 increases the CheY-phosphate life-time by slowing down the phosphate bond hydrolyis (SILVERSMITH *et al.*, 1997). The analogous amino acid substitution in CheF lead to the CheF:K781R mutant. Under comparable conditions, this protein behaved considerably different as the

wild type: more label was present in CheF:K781R as in CheF (see Fig. 22). Furthermore, CheF:D729K was constructed where the aspartyl residue that is phosphorylated in CheY is substituted by a lysyl residue. It is also expected that this mutant retains more label as wild type CheF due to the lack of phosphate group efflux through the CheY-like domain (Fig. 23).

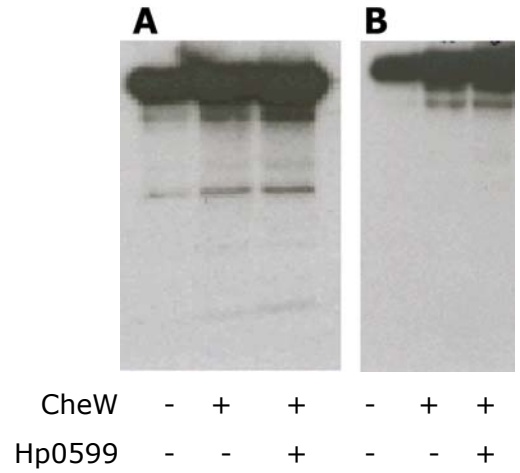

Fig. 23. Autophosphorylation behavior of mutant CheF proteins. CheF:H47G does not autophosphorylate in the presence of ATP (not shown), whereas both CheF:D729K **(A)** and CheF:K781R **(B)** autophosphorylate The addition of CheW and Hp0599 does increase the autophosphorylation level moderately (see below).

The *E. coli* CheA activity is modulated by the four chemoreceptors and the coupling protein CheW, and the response regulator CheY is phosphorylated by CheA. From the existence of homologous proteins in *H. pylori*, it is expected that CheF activity is regulated alike, and that the CheY ortholog is phosphorylated by CheF. To test this, CheW as well as the response regulator CheY from *H. pylori* were expressed in *E. coli* and purified therefrom as described in Materials & Methods (Fig. 24).

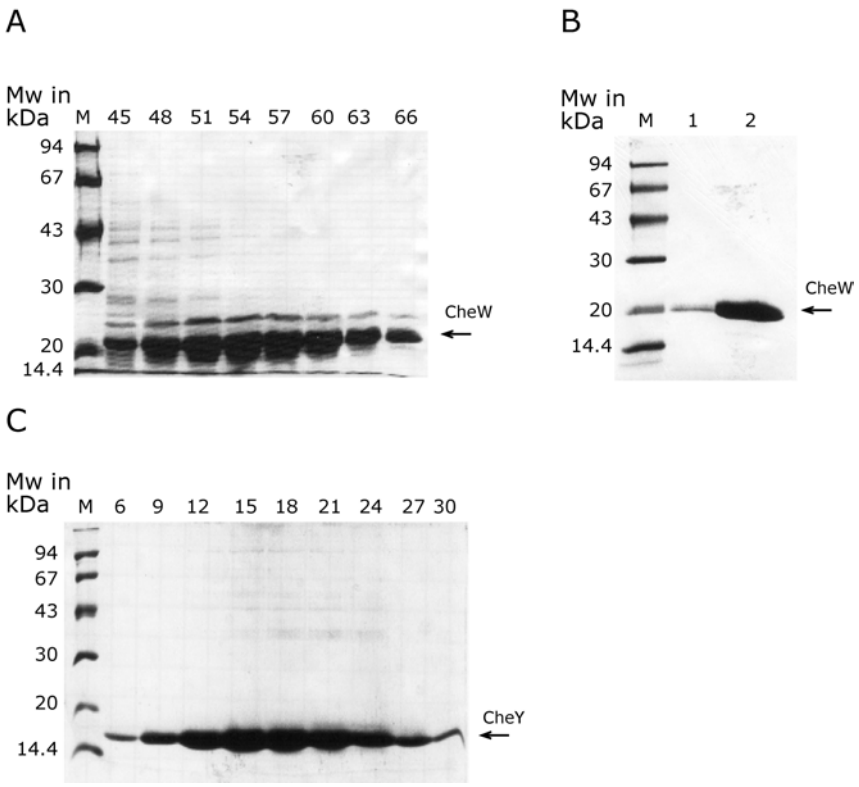

Fig. 24. Purification of heterologously expressed *H. pylori* CheW and CheY from *E. coli* cytosol. **A.** Eluent fractions of CheW from a 2.5x10 cm Ni-NTA column. Fraction size: 5 ml, gradient: 0 to 250 mM imidazole in 300 mM sodium chloride, 10 mM Tris-HCl pH 8.0 at 4°C, in 300 min at a flow rate of 1 ml/min. **B.** After removal of His6-tag, CheW was again bound to a Ni-NTA column and eluted with a step gradient of 10 mM imidazole in 300 mM sodium chloride, 10 mM Tris-HCl pH 8.0 at 4°C. Lane 1: column flow through during sample application. Lane 2: Eluted protein. **C.** Eluent fractions of CheY purified on an Ni-NTA column as described in A for CheW. Fraction numbers are indicated above the respective lanes. Sample volume was 15 μl sample per lane.

In this context it is important to note that CheW still binds to Ni-NTA resin even when its His6-tag is removed, presumably through the interaction of histidine residues present within the protein sequence. With the successful preparation of all of these proteins it was possible to attempt the reconstruction of the helicobacterial chemotaxis network *in vitro*. Fig. 25 shows that the autophosphorylation level of CheF is indeed influenced by the putative chemoreceptor Hp0599 and CheW.

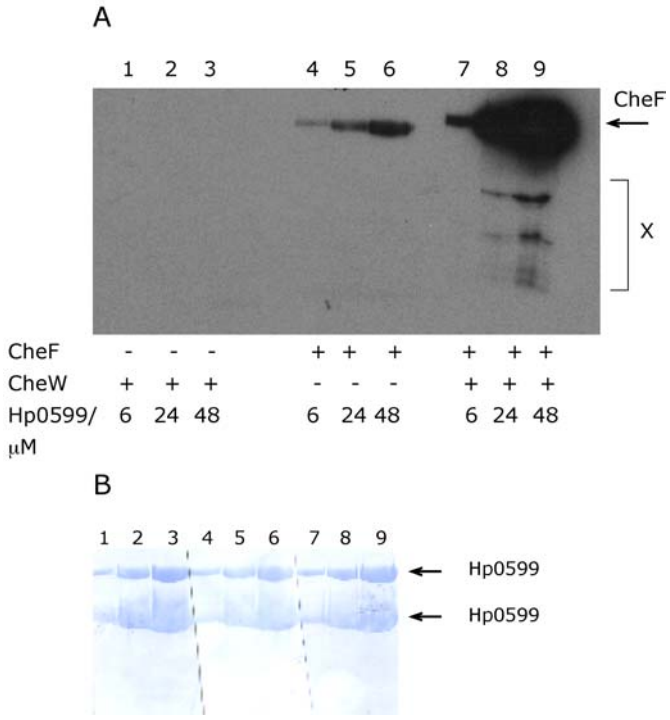

Fig. 25. Modulation of CheF autophosphorylation by CheW and Hp0599. **A.** Lanes 1 to 3: control reactions without CheF. Lanes 4 to 6: autophosphorylation of CheF in the presence Hp0599 without CheW. Lanes 7 to 9: autophosphorylation of CheF in the presence of both CheW and Hp0599. CheF and CheW concentrations were 0.5 μM when present as indicated by '+' below the autoradiograph. Hp0599 concentrations are given in μM. Phosphorylated CheF is indicated by an arrow. Contaminating proteins are marked by an X. The proteins were mixed and left at room temperature for five minutes. Thereafter, [γ-^{32}P]ATP (5000 Ci/mmol) was added to a final concentration of 0.1 mM. After 5 min, the reactions were stopped by the addition of 2x SDS buffer and proteins were separated by SDS-PAGE and transferred to a PVDF membrane. The membrane after autoradiography stained with Coomassie Brilliant Blue is shown in **B.** The membrane was cut into three pieces after protein transfer to allow preliminary detection of radioactivity bound to the membrane with an hand held counter.

Fig. 25 shows that (1) the kinase autophosphorylates and that neither of the other proteins present in the assay has an autophosphorylation activity in the absence of CheF, that (2) the CheF phosphorylation level is increased when the Hp0599 concentration is increased (compare lanes 4 to 6), that (3) CheW is important to further increase CheF phosphorylation level (compare lane 4 with lane 7 or lane 6 with lane 9, respectively), and

that (4) the CheF phosphorylation level is particularly dependent on the Hp0599 concentration (lanes 7 to 9). Interestingly, the kinase phosphorylation level is especially increased when Hp0599 is present in large molar excess. In contrast, only an equimolar ratio of CheW in respect to CheF appears to be sufficient for CheF phosphorylation to be increased dramatically by Hp0599. The weak bands visible in Fig. 25, lanes 8 and 9, presumably are fragments of CheF or contaminating proteins that become phosphorylated to a detectable level only when the CheF phosphorylation level is increased. Hereby, it is worth noting that the phosphorylation level of the kinase can not be increased further by an excess of CheW (Fig. 26).

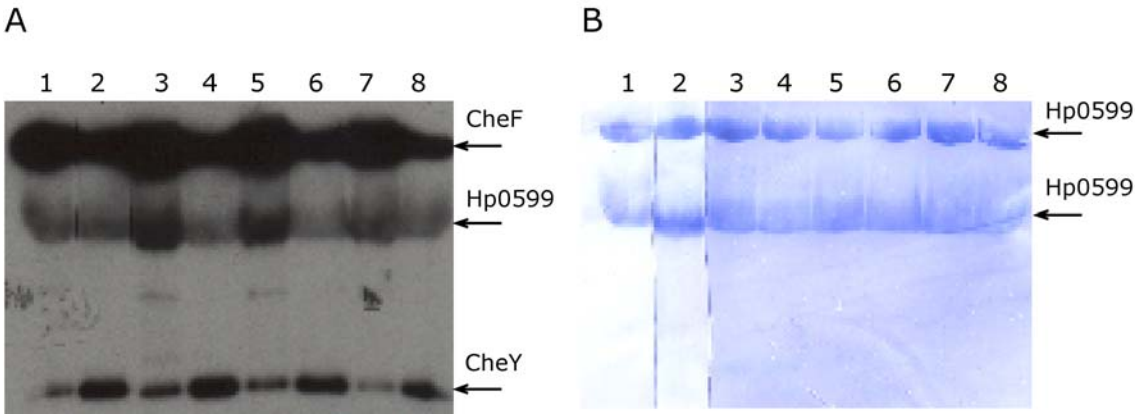

Fig. 26. CheF kinase autophosphorylation is independent of elevated CheW concentrations. CheF (0.1 μM), Hp0599 (85 μM) and CheW in various concentrations were mixed, [γ-^{32}P]ATP (5000 Ci/mmol) was added and the samples were incubated and analyzed as described in Fig. 25. In addition, CheY (0.8 μM) was included in four assays (lanes 2,4,6 and 8). CheW concentration was 0.3 μM (lanes 1 and 2), 3.0 μM (lanes 3 and 4), 1.5 μM (lanes 5 and 6) and 0.15 μM (lanes 7 and 8), respectively. The membrane after autoradiography stained with Coomassie Brilliant Blue is shown in **B.**

The CheF band intensity does not change significantly when the CheW concentration was increased more that 20-fold. On the autoradiograph shown in Fig. 26, Hp0599 appears also to be phosphorylated. This, however, is due to non-specific binding of label to the proteins that

occurred when the membrane was not thoroughly washed after the transfer of the proteins. The transfer of label to CheY (lanes 2,4,6 and 8 in Fig. 26) will be mentioned below.

As expected, CheW by itself does not activate CheF (Fig. 27).

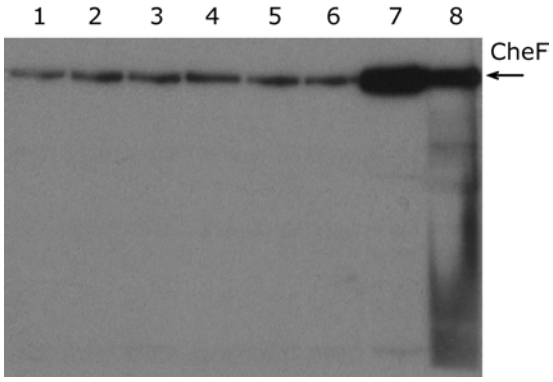

Fig. 27. CheW does not activate CheF. CheF (0.5 μM) and CheW in various concentrations (lane 1: no CheW; lane 2: 0.2 μM; lane 3: 0.5 μM; lane 4: 0.8 μM; lane 5: 1.5 μM; lane 6: 3 μM; lanes 7 and 8: 0.5 μM) were incubated as described in Fig. 25. In lanes 7 and 8, Hp0599 was added to a concentration of 8 and 4 μM, respectively.

Again, these findings match the data obtained from enteric signaling complexes where only a few CheA molecules are thought to bind an array of receptor molecules mediated through CheW (SHIMIZU *et al.*, 2000). Moreover, this shows for the first time that a soluble MCP homolog does increase the autophosphorylation level of a histidine kinase, again substantiating the assumption that these proteins are involved in chemotaxis.

5.11.2. Phosphotransfer reactions from CheF to response regulators

In analogy to the enteric system, CheF also transfers phosphate groups to *H. pylori* CheY (Fig. 28).

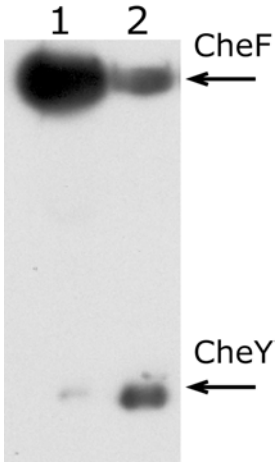

Fig. 28. Phosphotransfer reaction from CheF to CheY. CheF: 0.2 μM, CheW: 0.8 μM, Hp0599: 68 μM, CheY: 9 μM. Phosphorylated CheF and CheY are indicated by arrows. The proteins were mixed and left at room temperature for five minutes. Thereafter, [γ-^{32}P]ATP (5000 Ci/mmol) was added to a final concentration of 0.1 mM. After 5 min at room temperature, the reactions were stopped by the addition of 2x SDS buffer and proteins were separated by SDS-PAGE and transferred to a PVDF membrane.

Other response regulator proteins from *H. pylori* as for example CheV2 are also substrates of CheF and become phosphorylated by the kinase (see below, Fig. 33, p. 63). CheV2 was chosen in these experiments since the *cheV2* gene resides within one operon flanked by *cheW* and *cheF*. Whereas in this study it was directly shown for the first time that a CheV ortholog can be phosphorylated by its cognate histidine kinase, PITTMAN *et al.*, 2001 gained only indirect evidence through fluorescence quenching studies that upon the addition of acetyl phosphate, CheV3 autophosphorylates with a K_M value of 22 mM for acetyl phosphate.

5.11.3. Phosphate group transfer through the Che protein network

In the enteric signal transduction system, chemoreceptors and CheW activate the autophosphorylation activity of the histidine kinase, which in turn results in an increase in the CheA-phosphate concentration compared to the non-activated kinase. In addition, when the response regulator CheY is present, the phosphate group flux from the kinase to the response regulator depends on the CheA activity and is increased by CheW and a receptor (NINFA *et al.*, 1992). In *H. pylori*, the situation appears to be similar (increase in CheF-phosphate concentration upon addition of CheW and Hp0599) but is complicated by the fact that CheF is a hybrid histidine kinase with its own response regulator domain. Phosphate group flow therefore might branch in the presence of an additional response regulator after CheF autophosphorylation (Fig. 29).

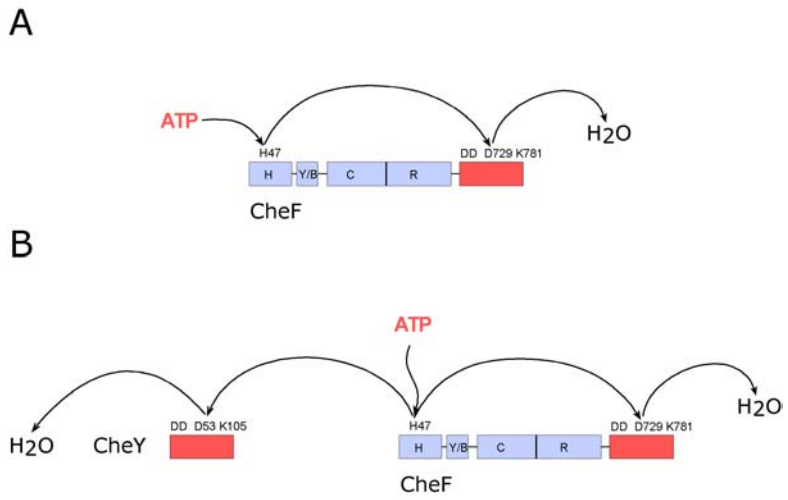

Fig. 29. Possible phosphotransfer reactions in the CheF/CheY system. **A.** In the absence of response regulators, CheF might still hydrolyze ATP via its own response regulator domain. In addition, this flux might change when receptor and CheW are present. **B.** When CheY is present, phosphate groups might be forwarded to either of the two domains, and again, the relative flux might be modulated by other components that interact with CheF.

To examine the flow of phosphate groups through a chemotaxis cascade, the so-called coupled assay where the consumption of ATP is linked to the oxidation of NADH was successfully employed by NINFA *et al.*, 1992, to measure CheA catalyzed ATP hydrolysis rates (Fig. 30).

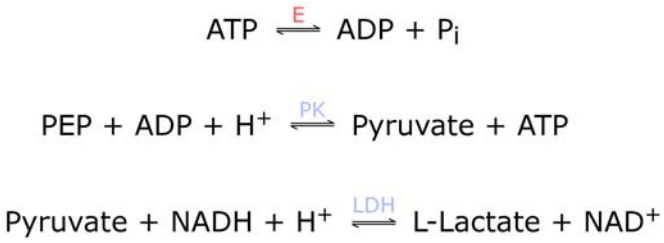

Fig. 30. Reaction scheme of the coupled assay. The ATP consumption of an enzyme E is coupled to the NADH oxidation activity of lactate dehydrogenase (LDH) via the pyruvate kinase (PK) reaction. ADP: adenosine triphosphate, PEP: phosphoenolpyruvate, NAD: nicotinamide adenine dinucleotide, oxidized form.

Adopted to the *H. pylori* system, this assay system would yield valuable insights into the function of the chemotaxis network. Especially the ratio of phosphate group flow from CheF to CheY *versus* the flow from CheF to its own response regulator domain could conveniently be measured. Furthermore, the question whether or not this flow is modulated by Hp0599 might be answered as well as its dependency upon addition of ligand to the receptor.

For the assay to produce reliable data, all components must be essentially free of contaminating proteins such as enzymes with NADH oxidation or ATP hydrolysing activities. In this study, CheF could not be purified to an extent where contaminating ATPases were no longer detectable. Furthermore, the ATPase activity varied considerably from day to day and from batch to batch. It was therefore impossible to obtain reproducible results that allowed the calculation of reliable ATPase activities even in

simple setups where CheF was activated by Hp0599, and where none or only one response regulator was present. However, the test was suited to show qualitatively that a mixture of CheF, CheW and Hp0599 consumed more ATP than the sum of the components (Fig. 31). In a control reaction with the mutant histidine kinase CheF:H47G that does not autophosphorylate in the presence of ATP, no increase in ATP consumption was observed upon the addition of CheW and Hp0599.

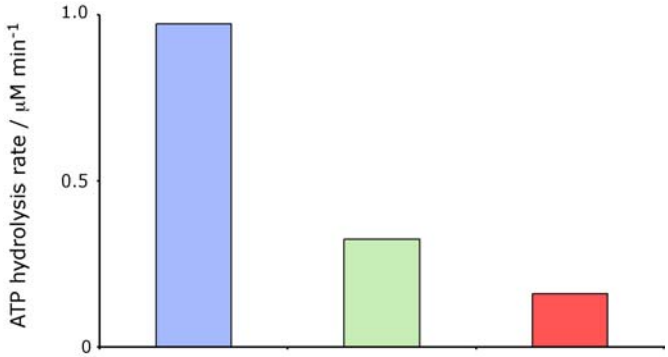

Fig. 31. Activation of CheF:D729K activity by CheW and Hp0599 in the presence of CheY. Hydrolysis of ATP by CheF/CheY was coupled to the pyruvate kinase and lactate dehydrogenase as described under 'Materials & Methods'. A mixture of all four proteins (blue) consumes more ATP than the sum of CheF:D729K alone (green) and (in a separate reaction) a mixture of CheW, Hp0599 and CheY (red). Chemotaxis proteins were present at the following concentrations: CheF, 0.6 μM; CheY, 5 μM; CheW, 2 μM; Hp0599, 84 μM.

5.11.4. Autophosphorylation of CheF:D279K mutant

In contrast to continuously monitor the ATP consumption of the Che protein network with the coupled assay, another strategy is to follow single phosphotransfer reactions with radiolabeled proteins. For example, the phosphorylation of CheY by CheF can be followed in analogy to the experiments of HESS *et al.*, 1988. To exclude any other phosphotransfer

reactions, and to be able to prepare stably phosphorylated CheF, the CheF:D729K mutant was used where an intra- or inter-CheF phosphotransfer can no longer occur. This protein was expressed and purified as wild type CheF. CheF:D729K autophosphorylates with an apparent first order rate constant of 0.2/min (Fig. 32). This rate constant is in the same order of magnitude as the respective rate constants of *E. coli* and *H. salinarum* CheA (HESS *et al.*, 1987; RUDOLPH *et al.*, 1995).

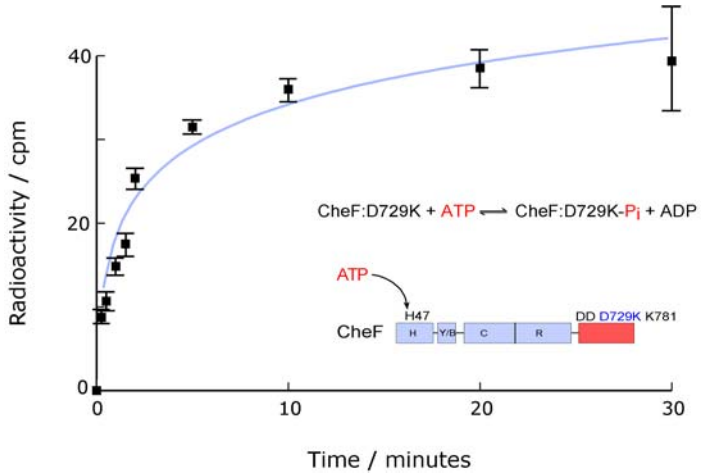

Fig. 32. Autophosphorylation kinetic of CheF:D729K. The protein was incubated at 25°C in the presence of 5 mM Mg^{2+} and [γ-^{32}P]ATP (0.2 mM, 5000 Ci/mmol). At the time intervals indicated, 20 µl samples were taken, immediately mixed with an equal volume of 2x SDS-buffer and frozen in liquid nitrogen. After thawing, the proteins were separated by SDS-PAGE and the protein bands were excised from the gel. Radioactivity bound to the protein was quantified by liquid scintillation counting. Each data point is the mean of two independent measurements, and the error bars were calculated using Microsoft Excel's STABWN function.

The phosphorylated protein can be purified from not incorporated label for further experiments by simply binding the His_6-tagged protein to a Ni-NTA column after the labeling reaction, followed by washing away not incorporated [γ-^{32}P]ATP and elution from the column. When preparing CheF:D729K-phosphate for subsequent phosphotransfer reactions, [γ-^{32}P]ATP with a specific activity of 30 Ci/mmol was used, and the specific

activity of the protein preparation was typically around 200 mCi/mmol as determined by liquid scintillation counting and protein concentration measurement by the BRADFORD method. The total level of phosphate incorporation was typically 0.7%, significantly lower than the level of phosphorylation observed with CheA from *E. coli* (100 %; HESS *et al.*, 1987), but in the same range as observed with CheA from *H. salinarum* (0.1 %; RUDOLPH *et al.*, 1995). A reason for this discrepancy might be the heterologous expression of the kinase in *E. coli*. Even so the kinase was expressed in the cytosol, the heterologous host might fail in folding the large, multi-domain CheF molecule. According to the literature, *E. coli* CheA is dimeric where dimerization is necessary for activity (SURETTE *et al.*, 1996). CheF might likewise require a correct oligomerizaton state to be functional. Whether this is a dimer as in the case of *E. coli* CheA or not remains to be investigated. However, the protein might not as readily oligomerize in *E. coli* as it would in its natural host. It is also conceivable that the response regulator domain in CheF exerts influence on the CheF autophosphorylation activity, or that the D729K mutant that was introduced into CheF might itself influence CheF function. Due to the excess of ATP and the fact that the labeling reaction exhibits a time-dependent saturation which can be fitted to a first order exponential, the low level of phosphorylation is more likely to be due to misfolded, inactive protein (RUDOLPH *et al.*, 1995).

5.11.5. Phosphotransfer reactions from CheF:D729K-P_i to response regulators

With the stably phosphorylated CheF mutant, the phosphotransfer reaction from the kinase to the response regulators can be explored (Fig. 33).

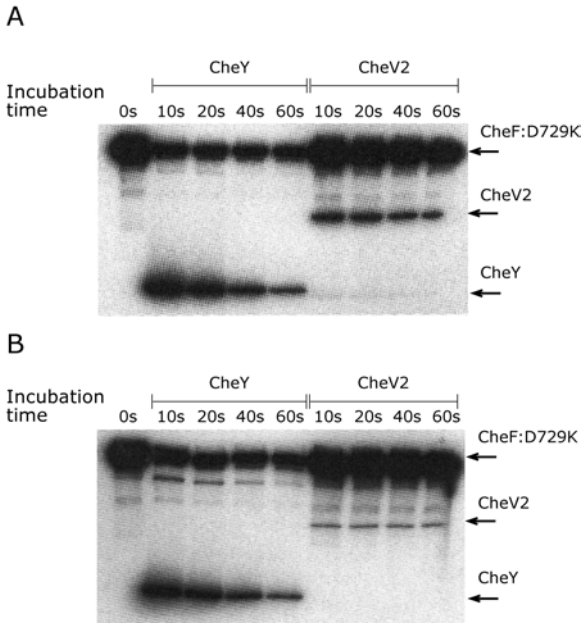

Fig. 33. Transfer of phosphate groups from CheF:D729K-phosphate to CheY and CheV2. **A.** CheF:D729K-P_i (2.9 μM) was incubated with an equal amount of either CheY or CheV2 in 5 mM $MgCl_2$, 50 mM potassium phosphate pH 7.5 at room temperature. Samples (20 µl) were taken from the reaction mixture, immediately mixed at the time points indicated (above autoradiograph) with an equal volume of 2x SDS-buffer and frozen in liquid nitrogen. After thawing, the proteins were separated by SDS-PAGE and transferred to a PVDF membrane. Exposure to X-ray film was overnight. **B.** The same experiment as described in A with the difference that the response regulator concentration was one tenth of the CheF:D729K-P_i concentration (0.3 and 2.9 μM, respectively). Phosphorylated proteins are indicated by arrows.

Phosphorylated CheF:D729K transfers its phosphate group very rapidly to the response regulator CheY (within the first ten sec of the experiment). Thereafter, the intensity of the CheF:D729K band does not change significantly, and residual label bound to the kinase is no longer transferred to the response regulator. This is in accordance with the time frame expected from data derived from the *E. coli* CheA to CheY phosphotransfer reaction (50 ms as measured in a stopped flow apparatus; STEWART, 1997), indicating a role for *H. pylori* CheY similar to the one of *E. coli*. In analogy to *E. coli* CheY, the life-time of *H. pylori* CheY-phosphate is short: the band intensity of CheY-phosphate is

decreased to approximately 50 % in lane 3 compared to lane 2 in Fig. 33, indicating an approximate life-time of CheY-phosphate of around 10 sec. Since CheF:D729K-P_i is stable without CheY (see 35, p. 66), the loss of phosphate groups must be due to CheY autodephosphorylation, and so it appears that CheY catalyzes its own dephosphorylation efficiently, since acyl phosphates have an expected half-life of several hours at neutral pH without catalysis (HESS *et al.*, 1988; STOCK *et al.*, 1995).

In contrast to CheY, CheV2 behaves very different. It also accepts phosphate groups from CheF:D729K-P_i, yet this reaction is slow. From the CheV2 band intensities it follows that the CheV2-phosphate concentration is always lower as the CheY-phosphate concentration in the analogous reaction. Furthermore, the reaction proceeds considerably longer as with CheY. Even 60 s after mixing the kinase with the response regulator, most of the label is still bound to the kinase, and the CheF:D729K-P_i band is not yet reduced to 50 % as compared to the band at 0 s. The transfer reaction that is completed within 50 ms in the case of *E. coli* CheA/CheY takes more than one minute with *H. pylori* CheV2. This might be due to a slow transfer of label from the kinase to the response regulator. Alternatively, CheV2 might not be phosphorylated to the same extent like CheY. In an extreme case, only a small fraction of the CheV2 proteins might accept phosphate groups from CheF (high portion of inactive CheV2 in the preparation, for example). The transfer reaction could than be still rapid, but the hydrolysis of CheV2-phosphate would become rate-limiting.

The CheV2-phosphate concentration appears to be constant during the first 60 s of the experiment (Fig. 33A), and therefore the half-life of CheV2-phosphate equals the half-life of CheF:D729K-P_i hydrolysis (hydrolysis of CheV2 becomes time dependent for the reaction). It might be estimated from Fig. 33 to be > 1 min. When the phosphorylated kinase

was used in a tenfold molar excess to the response regulators as in Fig. 33B, the differences in CheY and CheV2 behavior became again apparent: CheY rapidly accepts and hydrolyses all phosphate groups from CheF:D729K, whereas the reaction with CheV2 is considerably reduced. To quantify the amount of phosphate that is transferred from CheF:D729K-P_i to the respective response regulators, identical experiments as the one described in Fig. 33 where performed with the modification that the CheF bands were excised from the gel and the radioactivity bound to the protein was determined by liquid scintillation counting (Fig. 34).

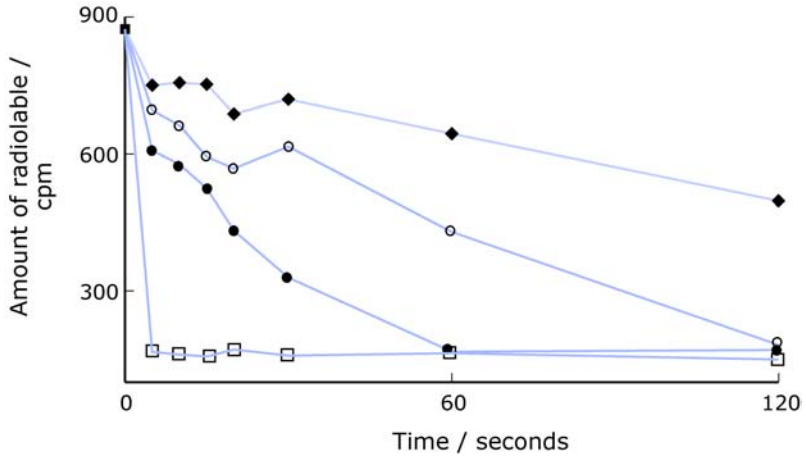

Fig. 34. Loss of label from CheF:D729K-P_i to CheY. Phosphorylated CheF:D729K (4 μM) was incubated at 25°C with various concentrations of the response regulators. At the time intervals indicated, 20 µl samples were taken, immediately mixed with an equal volume of 2x SDS-buffer and frozen in liquid nitrogen. After thawing, the proteins were separated by SDS-PAGE and the protein bands were excised from the gel. Radioactivity bound to CheF:D729K was quantified by liquid scintillation counting. The CheF:D729K-P_i to CheY ration was 1:1 (□), 5:1 (●), 10:1 (O) and 20:1 (◆). Each data point is the mean of two independent measurements.

Similar curves were obtained when CheV2 was present in the reaction mixture instead of CheY (Fig. 35).

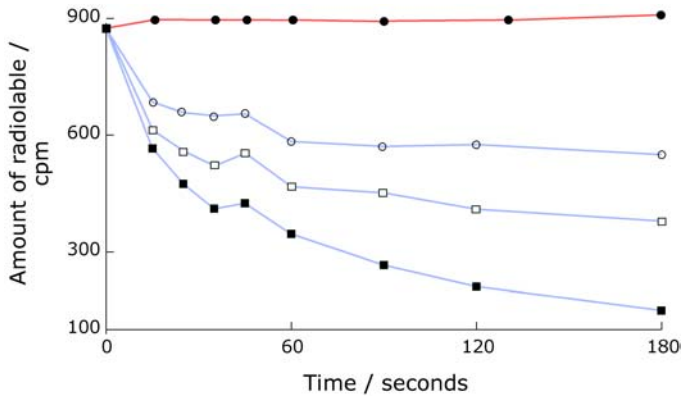

Fig. 35. Loss of label from CheF:D729K-P_i (2.8 μM) to CheV2. Reaction conditions as in Fig. 34. The CheF:D729K-P_i to CheV2 ration was 1:1 (■), 5:1 (□) and 10:1 (○). Red curve: radiolabel bound to kinase in absence of response regulator (under assay conditions). Each data point is the mean of two independent measurements. Data were normalized to data from Fig. 34 as basis.

Again, label was transferred to the response regulators, whereas in their absence, the label remained bound to the kinase (red curve in Fig. 35). Under the assumption that the dephosphorylation of the response regulator phosphates become rate-limiting for the dephosphorylation reaction of CheF:D729K-P_i, the CheY and CheV2 concentrations were successively lowered to ensure pseudo-first order conditions for the efflux of label from CheF:D729K-P_i. In the case of the reaction catalyzed by CheY, the life-time of CheY-phosphate can be determined from the linear parts of the curves (Fig. 34; 10 and 20 fold excess of CheF; 30 to 120 sec of experiment). This life-time is 14 ± 1 sec. As expected, the reaction proceeds considerably slower with CheV2 than with CheY. Even at equimolar concentrations of both proteins, the transfer of phosphate groups from the kinase to CheV2 takes more than 180 sec, and therefore the life-time of CheV2 phosphate can not be calculated from these data. Residual radioactivity remains bound to the kinase in both cases that is not transferred to the response regulators. Interestingly, between t≈20 and 30 sec, the curves apparently indicate a reverse flow of phosphate groups from the response regulator phosphates to the kinase.

5.11.6. Decay of CheY-phosphate

The life-time of CheY-phosphate might also determined by directly measuring the label bound to the protein. When CheY was mixed with an equimolar amount of from CheF:D729K-P_i, the transfer of phosphate groups is completed within the first few seconds of the experiment. Thereafter, the phosphoryl group flux from CheF to CheY is negligible, and the life-time of CheY-phosphate is reflected by the disappearance of label bound to CheY. It is difficult to excise the CheY band from gels after SDS-PAGE (faint band not visible without staining in contrast to prominent CheF), but the radioactivity may be measured by 'phosphoimaging' of the proteins after electroblotting to a membrane. Fig. 36 shows the hydrolysis of CheY-phosphate as measured by this method.

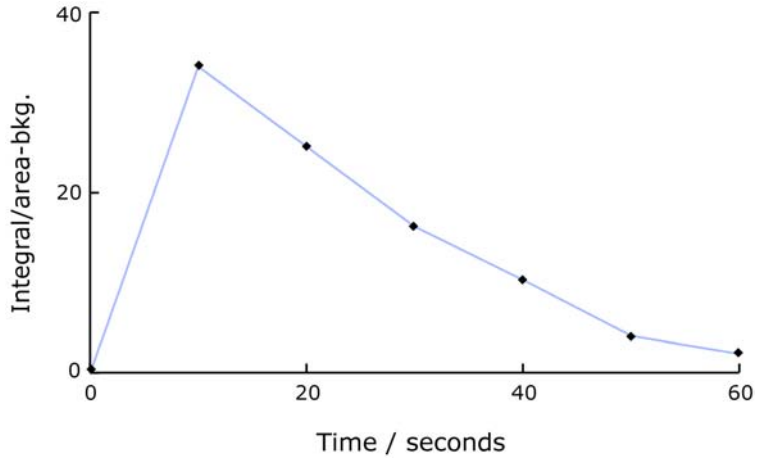

Fig. 36. Hydrolysis of CheY-phosphate. CheF:D729K-P_i was incubated with CheY in a ratio 1:1 and the reactions were stopped at the time intervals indicated. Proteins were separated by SDS-PAGE, transferred onto a PVDF membrane and the radioactivity was quantified by phospho-imaging. Each data point is the mean of two independent measurements.

From the curve in Fig. 36 the CheY-phosphate life-time can be calculated to be 19 sec, a number that resembles the determination of the life-time as described above. In the case of CheV2, this method is not suited for

the determination of the CheV2-phosphate half-live since the phosphotransfer reaction from the kinase to the response regulator is the rate-limiting step of the overall reaction in contrast to the phophotransfer reaction to CheY, where the hydrolysis of the response regulator phosphate becomes rate-limiting under these conditions (Fig. 37).

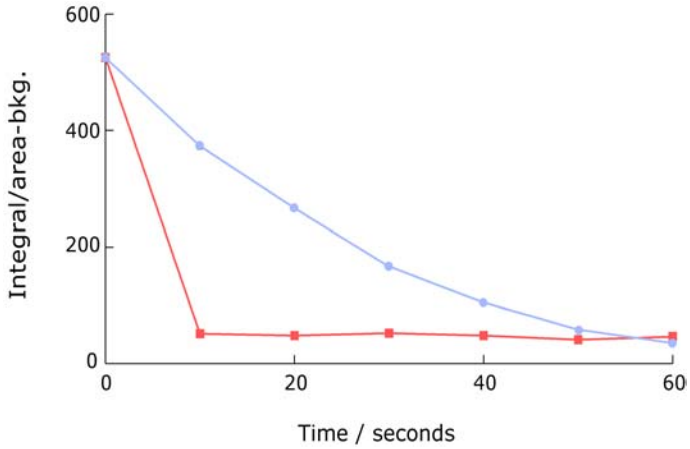

Fig. 37. Transfer of label from CheF:D729K-P_i to CheY (red curve) and CheV2 (blue curve) as measured by 'phosphoimaging'. Proteins were incubated and samples were taken as described in Fig. 34. CheF:D729K-P_i: 0.53 μM; CheY: 0.53 μM ; CheV2: 2.7 μM.

It is therefore not possible to simply determine the life-time of CheV2-phopshate from the decrease of the CheV2-phosphate concentration (see Fig. 36) due to the fact that the two phosphotransfer recations (from kinase to CheV2 and from CheV2 to water) proceed with similar rates.

5.11.7. Reverse phosphotransfer from CheY to the kinase

The so-called phosphate sink theory (SOUIRJIK & SCHMITT, 1996, 1998; ARMITAGE & SCHMITT, 1997) predicts a flow of phosphate groups from one response regulator back to the histidine kinase from where they are

supposed to be transferred to the phosphate sink for signal quenching. To examine this reverse phosphoryl-group transfer it was attempted to prepare and isolate phosphorylated CheY. Phosphorylated CheY free of ATP can be obtained by adding CheY to CheF:D729K-phosphate as described under 7.4.5. Due to its inherent instability, however, the protein hydrolyzes within seconds even in the absence of magnesium ions. When CheY is passed through a CheF:D729K-$^{32}P_i$ column (the phosphorylated protein bound to Ni-NTA resin by its His6-tag), most radioactivity is eluted from the column, but no CheY-$^{32}P_i$ can be detected in the effluent. To circumvent this problem, the CheY:K106R mutant was constructed that still accepts phosphate groups from CheF but is more stable towards hydrolysis (SILVERSMITH *et al.*, 1997). Fig. 38 shows an SDS-PAGE of the radioactive eluent fractions that where obtained by passing CheY:K106R through a CheF:D729K-$^{32}P_i$ column.

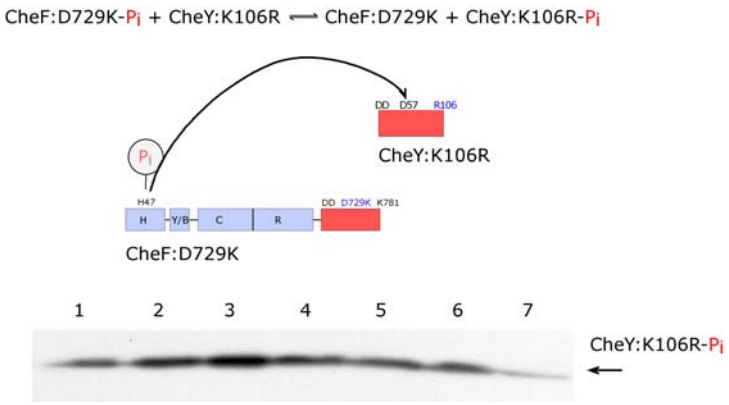

Fig. 38. Preparation of CheY:K106R-Pi. Radioactive fractions obtained by passing CheY:K106R through a 1 ml CheF:D729K-P_i Ni-NTA column as described under 7.4.5. were analyzed by SDS-PAGE followed by transfer of proteins to a PVDF membrane and exposure to an X-ray film for 2 d. Fraction numbers are indicated above the autoradiogramm. Fraction size was two drops (approximately 400 µl) at a flow rate of 1 ml/min. Phosphorylated CheY:K106R is indicated by an arrow.

The autoradiogramm in Fig. 38 clearly shows the presence of radiolabeled CheY:K106R as inorganic phosphate is not retained on a PVDF membrane when transferred by electroblotting. The protein hydrolyzes and eluent fraction stored on ice for more than 100 sec do no longer indicate the presence of CheY:K106R-P_i when analyzed as described above. Phosphorylated, ATP-free response regulator preparations allow the reverse transfer of labeled phosphate from the response regulator to the kinase (Fig. 39).

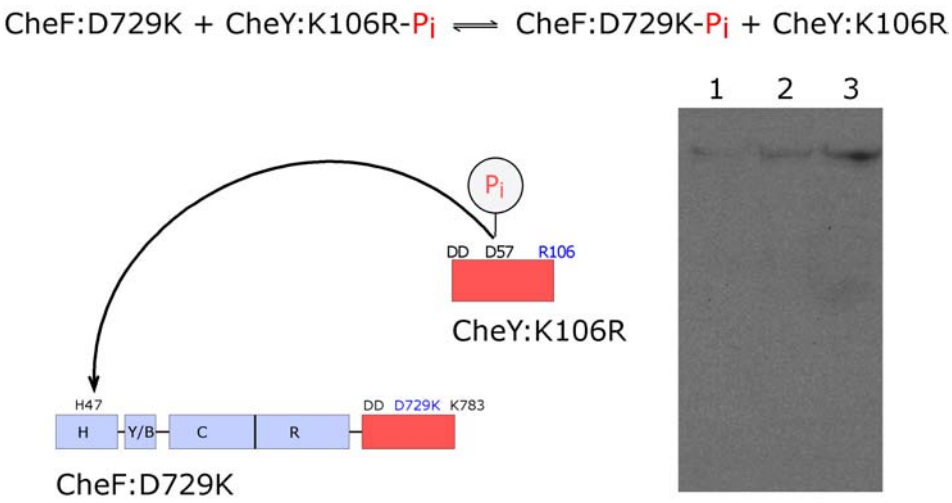

Fig. 39. Reverse phosphorylation of CheF:D729K by CheY:K106R-P_i. Aliquots of three different eluate fractions from the CheF:D729K-$^{32}P_i$ Ni-NTA column were separately mixed with three kinase aliquots (lanes 1 to 3). After incubation, the samples were separated by SDS-PAGE and radioactive proteins were detected as described. The bands correspond to CheF:D729K reverse phophorylated by CheY:K106R-P_i.

After analyzing the samples, the autoradiogramm shows the presence of phosphorylated CheF:D729K, and CheY:K106R-P_i can no longer be detected. The reactions that occur are more complex as the cartoon illustrates (see Fig. 39), and nascent CheF:D729K-P_i immediately disappears by CheY:K106R-catalyzed hydrolysis. This result shows that

CheY might reversely transfer its phosphate group to the kinase *in vivo*, an ability postulated by the phosphate think theory where the CheY signal is thought to be quenched by reverse phosphorelay to, for example, CheV2 or more likely, to the CheY domain of CheF.

5.11.8. Phosphorylation of response regulators by acetyl phosphate

Acetyl phosphate, a small molecule with a high energy phosphate group, is well-known as a substrate for response regulator autophosphorylation in *E. coli* (LUKAT *et al.*, 1992; MAYOVER *et al.*, 1999). This autophosphorylation ability was used by BREN & EISENBACH in an *in vitro* assay to produce CheY-phosphate *in situ*. CheY-phosphate bound to the motor switch factor FliM, whereas in control reactions, non-phosphorylated CheY did not bind FliM. It can be expected that one of the five *H. pylori* proteins with a CheY-like response regulator domain also binds to FliM in its phosphorylated state. It was therefore of interest whether acetyl phosphate can also be used to phosphorylate *H. pylori* Che proteins. To test whether acetyl phosphate serves as a substrate for response regulator phosphorylation in *H. pylori*, [^{32}P]-acetyl phosphate was synthesized from [^{32}P]-orthophosphoric acid and incubated with the respective proteins. CheY and the response regulator domain of CheF became clearly phosphorylated in the presence of acetyl phosphate (Fig. 40), indicating that both proteins catalyze their own phosphorylation (in CheF in addition to the autophosphorylation activity of the CheA-like domain) in analogy to other response regulators (ZAPH *et al.*, 1990; MCCLEARLY & STOCK, 1994; SILVERSMITH *et al.*, 1997). In contrast, phosphorylation of CheV2 and CheV3 by acetyl phosphate appears to be inefficient, because there are only comparably faint bands visible on the autoradiograph (lanes 1 and 2 in A) in the presence of 50 mM acetyl phosphate.

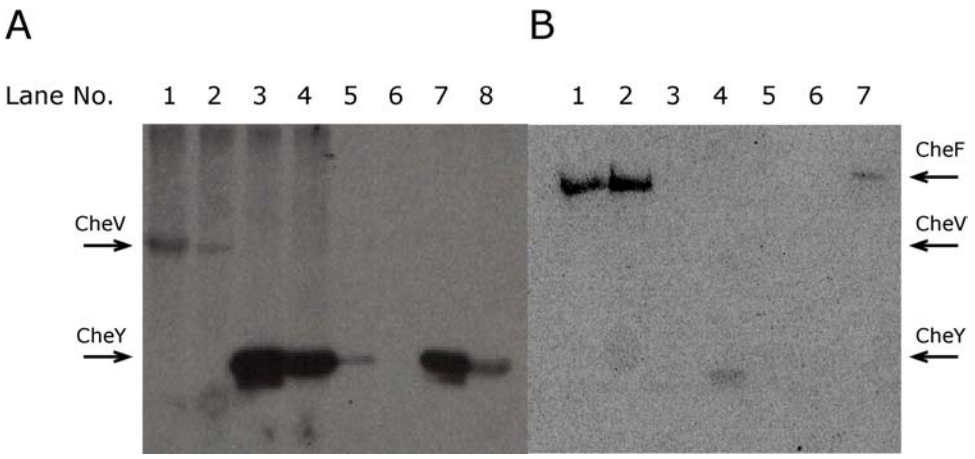

Fig. 40. Phosphorylation of response regulator domains by [^{32}P]-acetyl phosphate. To the respective proteins, acetyl phosphate was added to a final concentration of 5 mM (lanes 1 to 4 in A: 50 mM), and the mixture was incubated for 5 min at 30°C. Thereafter, the reactions were stopped by the addition of SDS sample buffer, the proteins were resolved by SDS-PAGE and transferred to a PVDF membrane. Exposure to X-ray film was 18 d in A and 5 d in B. **A.** Lane 1: CheV3, lane 2: CheV2, lane 3: CheY, lane 4: CheY:K106R, lanes 5 to 8 as lanes 1 to 4. **B.** Lane 1: CheF:H47G, lane 2: CheF:K783R, lane 3: CheF:D729K, lane 4: CheY, lane 5: CheV3, lane 6: CheV2, lane 7: CheF. Protein concentrations were 0.5 μM for the kinase and 2.5 μM for the response regulators. Buffer composition was 100 mM potassium phosphate pH 7.5 at 20°C supplemented with 5 mM $MgCl_2$.

The mutant protein CheF:H47G whose kinase domain no longer autophosphorylates in the presence of ATP but whose response regulator domain remained unaltered also autophosphorylates in the presence acetyl phosphate. Specific phosphorylation of D729 by acetyl phosphate is supported by the observation that the mutant D729K fails to accept phosphate from acetyl phosphate. The crosslinking assay to determine the FliM-binding capability of phosphorylated *H. pylori* response regulator proteins appears to be hence not suited for the CheV paralogs, but acetyl phosphate might be used to prepare the required CheF and CheY-phosphates *in vitro*.

5.12. Expression and purification of the motor switch protein FliM

In the chemotaxis networks of coliform bacteria, CheY is the response regulator that binds in its phosphorylated form to the motor switch factor FliM. Upon this event, the rotational bias of the flagellar motor is changed towards a higher counterclockwise to clockwise switching probability. The ability of CheY-phosphate to induce clockwise flagellar rotation is about 100 times the corresponding activity of unphosphorylated CheY (BARAK & EISENBACH, 1992). In other bacterial species with more than one CheY-like response regulator it is questionable which of these proteins is the actual switch factor. In this study, it was therefore attempted to examine the differences in CheY and CheV protein behavior beyond the findings that the two proteins are differentially phosphorylated by the histidine kinase. Binding to FliM of either of the proteins would further the understanding of the role of these proteins in chemotaxis.

It was first attempted to reproduce the results from BREN & EISENBACH, 1998, as a control reaction for possible interaction studies with *H. pylori* derived proteins. The genes coding for *E. coli* FliM and CheY were cloned into pET28a(+) expression vectors and expressed in *E. coli* BL21(DE3)Gold cells as N-terminal His_6-tagged fusion proteins. CheY was expressed in the cytosol, whereas FliM was refolded and purified following the protocol given by BREN & EISENBACH, 1998. Fig. 41 shows a typical preparation of the two proteins.

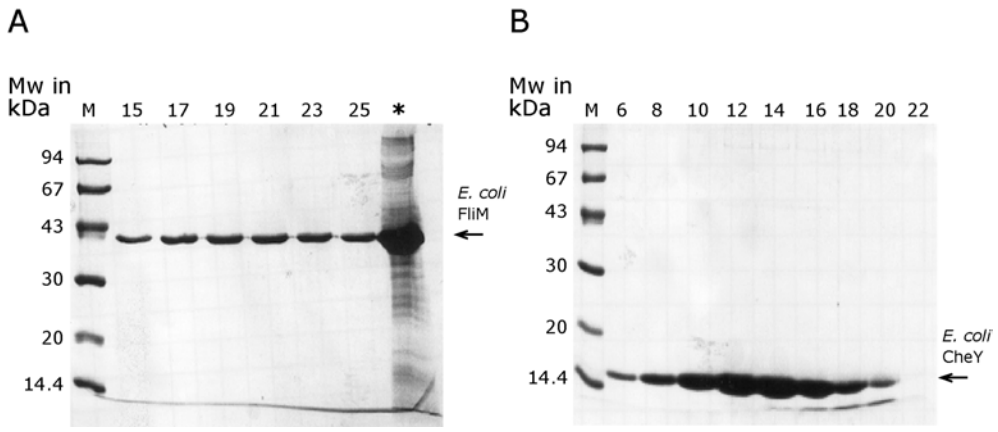

Fig. 41. Purification of *E.coli* FliM and CheY as described in Materials & Methods. **A.** Purification of FliM refolded from inclusion bodies. Eluent fractions from a 2.5x10 cm Ni-NTA column. Fraction size: 5 ml, gradient: 0 to 250 mM imidazole in 300 mM sodium chloride, 10 mM Tris HCl pH 8.0 at 4°C, 10 % glycerol in 300 min at a flow rate of 1 ml/min. Lane indicated by an asterisk: flow-through of column during sample application. **B.** Purification of CheY from *E. coli* cytosol performed as described under A except that no glycerol was included in the buffer. Fraction numbers are above the respective lanes, and the probe volume was 15 μl of sample per each lane.

The pronounced tendency to precipitate made it difficult to handle the purified FliM. The protein could not be stored either frozen or on ice, and it was necessary to prepare it fresh from inclusion bodies stored at –32°C. Furthermore, the concentration of FliM solutions was below 5 mg/ml, which made it difficult to use FliM in the CheY interaction assays. In spite of the purification of FliM being a difficult task, it was possible to show that *E. coli* CheY-P_i interacts with the motor switch factor (Fig. 42).

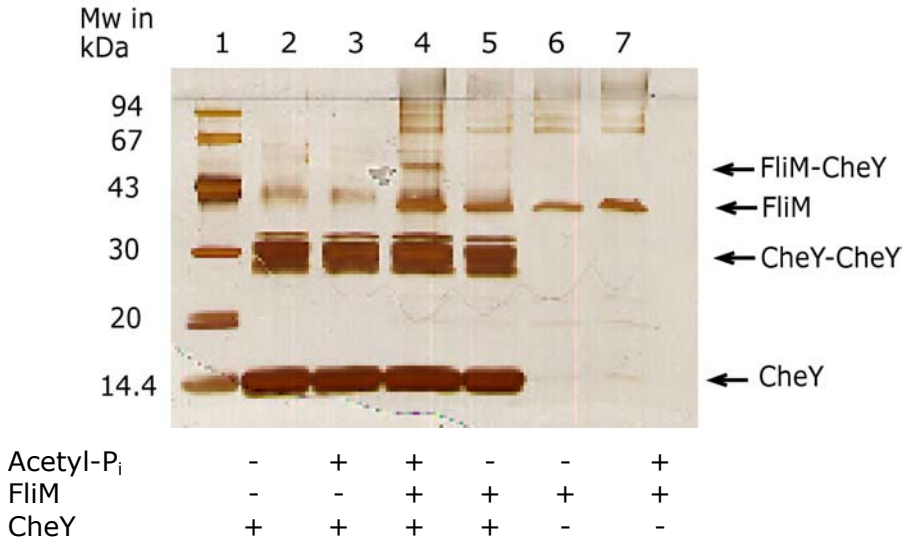

Fig. 42. Interaction of *E. coli* CheY-P_i with the *E. coli* motor switch protein FliM. After crosslinking, the proteins were separated by SDS-PAGE and silver-stained. All reactions contained 5 mM magnesium chloride and 1 mM *ortho*-phthaldialdehyde as crosslinking agent. Protein concentrations were CheY: 25 μM, FliM: 7.9 μM, and acetyl phosphate was 22 mM. Lane 1: marker protein. The faint bands in lanes 2 and 3 running at around 43 kDa and above are CheY trimers and higher crosslinking products. Similarly, FliM oligomers can be detected in reactions where FliM was present.

Only in the presence of acetyl phosphate (22 mM), CheY and FliM (25 and 7.9 μM, respectively), a protein band running at an appropriate molecular weight corresponding to crosslinked CheY-FliM heterodimers (51.9 kDa) appeared clearly visible before a background of CheY and FliM oligomers as was first shown by BREN & EISENBACH, 1998. In analogy to the experiments described above, it was attempted to heterologously overexpress *H. pylori* FliM in *E. coli*. Whereas the *E. coli* protein could easily be expressed as inclusion bodies, it was not possible to express *H. pylori* FliM. In the hope that *H. pylori* CheY might bind to the *E. coli* FliM protein that is homologous to the *H. pylori* ortholog, the crosslinking assay was performed with these two proteins, but no distinct band corresponding to a FliM-CheY dimer appeared (Fig. 43.)

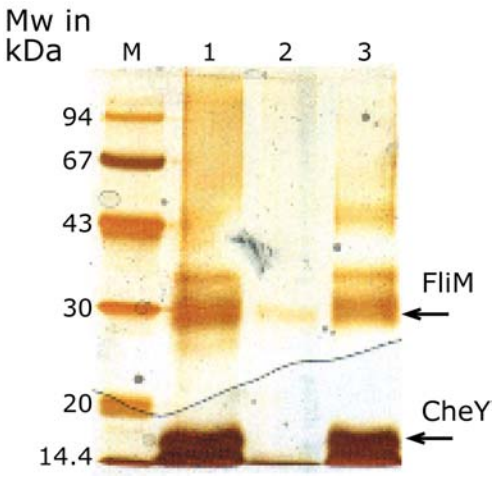

Fig. 43. Interaction assay with *H. pylori* CheY-P_i with the *E. coli* motor switch protein FliM. After crosslinking, the proteins were separated by SDS-PAGE and silver-stained. All reactions contained 5 mM magnesium chloride and 1 mM *ortho*-phthaldialdehyde as crosslinking agent. Lane 1: CheY, lane 2: FliM, lane 3: CheY and FliM, Lane M: marker proteins. Protein concentrations were CheY: 40 μM, FliM: 5 μM; and acetyl phosphate was 22 mM.

The amino acid sequence alignment of FliM from *E. coli*, *S. enterica* serovar Typhimurium and *H. pylori* reveals that despite the high homology of the three proteins, several residues conserved in the enteric proteins are different in *H. pylori* FliM. Fig. 44 gives an overview of the N-terminal sequence similarity of the two proteins from two enteric bacteria, *E. coli* and *S. enterica* serovar Typhimurium, respectively, and *H. pylori* FliM.

```
E. coli       M G D S I L S Q A E I D A L L - - - N G D S E V K D E P T A S V
S. enterica   M G D S I L S Q A E I D A L L - - - N G D S D T K D E P T P G I
H. pylori     M A D - I L S Q E E I D A L L E V V D E N V D I Q N V Q K K D I

E. coli       S G E S D I R P Y D P N T Q R R V V R E R L Q A L E I I N E R
S. enterica   A S D S D I R P Y D P N T Q R R V V R E R L Q A L E I I N E R
H. pylori     I P Q R S V T L Y D F K R P N R V S K E Q L R S F R S I H
```

Fig. 44. Protein sequence alignment of the N-terminal 60 amino acids of FliM from two enteric bacteria and *H. pylori*. In *E. coli and S. enterica* serovar Typhimurium, CheY-P_i binds to amino acids one to 16. The proteins show high sequence homologies but the differences might be sufficiently different to prevent *E. coli* CheY-P_i to bind to *H. pylori* FliM.

Some of these residues not present in *E. coli* FliM might be important for *H. pylori* CheY-phosphate binding to FliM. In the enteric chemotaxis system, the activated response regulator only binds to the 16 N-terminal amino acids of its target, and CheY-phosphate even binds to this region in the absence of the rest of FliM (LEE *et al.*, 2001b). It is conceivable that in *H. pylori*, binding to FliM occurs in a similarly defined region of the protein. To examine this, a chimeric FliM protein was constructed where the N-terminal 42 amino acids of *H. pylori* FliM were fused to the *E. coli* FliM C-terminal part (see Materials & Methods). This protein was expressed in *E. coli* and could successfully be purified from the cells following the method for wild type FliM (Fig. 45).

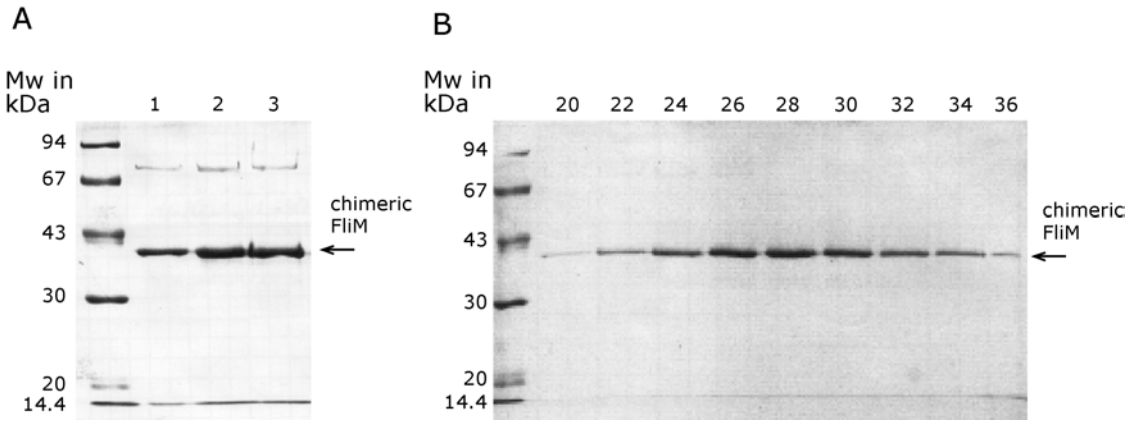

Fig. 45. Purification of chimeric FliM. **A.** FliM refolded from purified inclusion bodies. Lane 1: 10 µl sample, lane 2: 20 µl sample, lane 3: 30 µl sample. **B.** Eluent fractions from a 2.5x10 cm Ni-NTA column. Fraction size: 5 ml, gradient: 0 to 250 mM imidazole in 300 mM sodium chloride, 10 mM Tris HCl pH 8.0 at 4°C, 10 % glycerol in 300 min at a flow rate of 1 ml/min. Fraction numbers are indicated above the respective lanes. Probe volume was 15 µl of sample per lane.

When the crosslinking experiments were performed with the chimeric FliM protein, again no band corresponding to response regulator-FliM dimers appeared. The same holds true for experiments with the CheV2 protein

that were performed despite the knowledge that this protein autophosphorylates only weakly in the presence of acetyl phosphate.

5.13. Detection of *H. pylori* chemotaxis proteins by antisera

Gene expression in most organisms varies with the environmental conditions. It is therefore of interest which gene is expressed under what conditions. Furthermore, different bacterial strains might express different genes under the same conditions. The three CheV paralogs in *Helicobacter*, for example, might not be present at the same time, and even situations might exist where none of the *che* genes is expressed (SHAH *et al.*, 2000). Alternatively, the expression of a predicted open reading frame as Hp0599 is at least questionable. To gain information on the expression of the *H. pylori* che genes as well as Hp0599, polyclonal antisera against the respective proteins were raised in rabbits (Fig. 46).

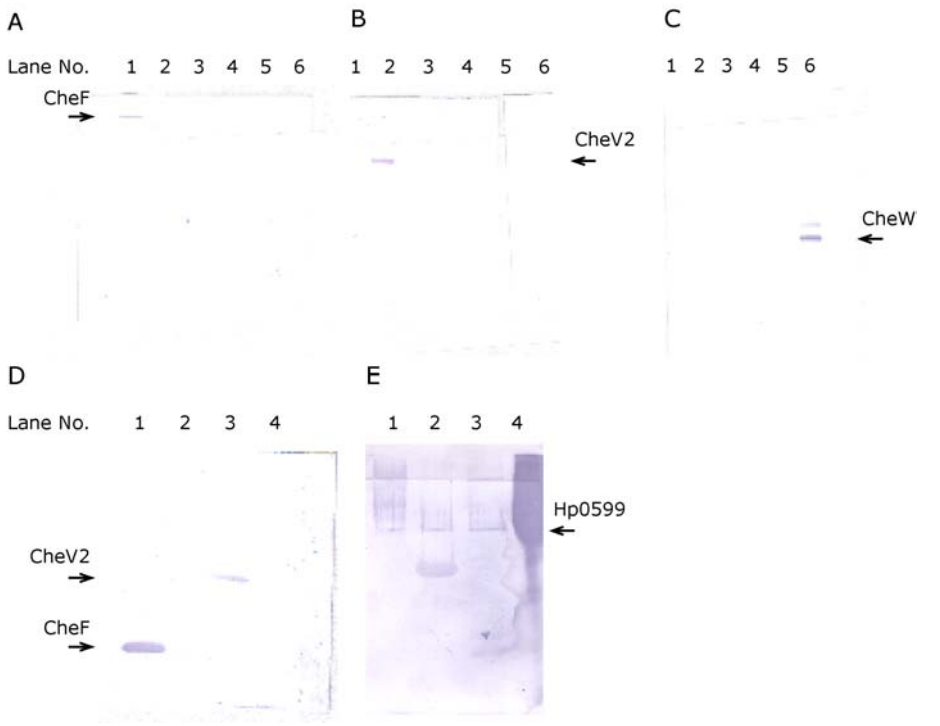

Fig. 46. Detection of purified chemotaxis proteins by antisera raised in rabbits. **A.** Anti-CheF antiserum. Lane 1, CheF; lane 2, *E. coli* CheY; lane 3, *H. pylori* CheY; lane 4, *E. coli* CheW; lane 5, CheV2; lane 6, *H. pylori* CheW; **B.** Anti-CheV2 antiserum. Lane 1, *H. pylori* CheW; lane 2, CheV2; lane 3, *E. coli* CheW; lane 4, *H. pylori* CheY; lane 5, *E. coli* CheY; lane 6, CheF. **C.** Anti-*H. pylori* CheW antiserum. Lanes 1 to 6 as in A. **D.** Anti-*H. pylori* CheY antiserum. Lane 1, *H. pylori* CheY; lane 2, *E. coli* CheY; lane 3, CheV2; lane 4, CheF. **E.** Anti-Hp0599 antiserum. Lane 1, CheF; lane 2, CheV2; lane 3, CheW; lane 4, Hp0599. The other bands in lanes 1 through 3 are due to unspecific binding of the antiserum to the other proteins present on the membrane and appear considerably weaker than the Hp0599 band (Hp0599 not well resolved on gel lead to smear in lane 4). The antisera were diluted 2500-fold in A through C, and 500-fold in D and E. All proteins were in a concentration range where they gave a clearly visible band on the PVDF membrane after staining with Ponceau S.

The antisera for CheF, CheV2, CheW and Hp0599 were specific and did not cross-react with any of the other Che proteins despite the presence of homologous domains. Orthologs from *E. coli* were also not detected, confirming the high specificity of the antisera. In contrast, the anti-CheY antiserum did recognize both CheY as well as

CheV2, presumably in its CheY-like domain. With these antisera, it should be possible to quantify the chemotaxis proteins in various *H. pylori* strains.

6. Discussion

6.0. Soluble MCP homologs in two-component cascades

The existence of soluble transducer molecules outside the kingdom of Archaea and their ubiquity was only realized and appreciated after their initial description in *Halobacterium salinarum* (RUDOLPH *et al.*, 1996; ZHANG *et al.*, 1996; STORCH *et al.*, 1999; NG *et al.*, 2000). Through various genome sequencing projects it became apparent that many bacterial and archaeal genomes code for transducer protein homologs that lack transmembrane spanning segments. Soluble MCP-homologs were found in diverse species like *Helicobacter pylori* (TOMB *et al.*, 1997), *Campylobacter jejuni* (PARKHILL *et al.*, 2000), *Pseudomonas aeruginosa* (STOVER *et al.*, 2000), *Sinorhizobium meliloti* (BARNETT *et al.*, 2001; CAPELA *et al.*, 2001; GALIBERT *et al.*, 2001), *Caulobacter crescendus* (NIERMAN *et al.*, 2001), *Rhodobacter sphaeroides* (WADHAMS *et al.*, 2000), *Vibrio cholerae* (HEIDELBERG *et al.*, 2000), *Bacillus halodurans* (TAKAMI *et al.*, 2000), *Borelia burgdorferi* (FRASER *et al.*, 1997), *Pyrococcus abysii* (http://www.Genoscope. cns.fr/Pab/), and others. In analogy to their membrane bound homologs, it is assumed that these proteins sense intracellular ligands and communicate this information via an archetypical two component system composed of a CheA histidine kinase and a CheY response regulator to the according target.

From this plethora of signal transduction circuits, the function from only one is known: Car, the cytoplasmic receptor from *H. salinarum* senses the intracellular arginine concentration (STROCH *et al.*, 1999). The ligands of all other soluble MCP-homologs are completely unknown. In chemotaxis systems with more than one histidine kinase and various response

regulator paralogs, the respective histidine kinase as well as the cognate response regulators also await their identification. Exceptions are only the soluble oxygen sensors like Aer from coliform bacteria (REBBAPRAGADA *et al.*, 1997) or HemAT from *H. salinarum* and *B. subtilis* (HOU *et al.*, 2000). At the beginning of this work it was therefore obvious that a successful *in vitro* reconstitution of a soluble chemical sensing signal transduction network would depend on the halobacterial Car/ CheA system.

6.1. Recombinant production of halophilic signaling components in *E. coli*

Compared to other expression systems, *E. coli* cells thrive well with appreciable growth rates, and expression levels of recombinant proteins using the T7 expression system (STUDIER & MOFFATT, 1986; ROSENBERG *et al.*, 1987) can reach up to 300 mg/l for proteins that are non-toxic to this organism (KUMAR *et al.*, 1994; GRIBENKO *et al.*, 1998; HAYASHI *et al.*, 1998). For the expression of halophilic proteins, however, the *E. coli* expression system apparently bears some disadvantages: for example, the low ionic strength of the *E. coli* cytosol might cause that proteins from halobacteria will not fold correctly *in vivo* and are therefore expressed under quasi-denaturing conditions. This problem could be avoided by overexpressing the halophilic protein of interest in organisms such as *H. salinarum* or *H. volcanii*. Both organisms can easily be transformed with appropriate expression vectors (FERRANDO-MAY *et al.*, 1993; SOHLEMANN *et al.*, 1997). However, these organisms grow considerably slower than *E. coli* (SRIVASTAVA *et al.*, 1987), and only a few separation techniques are available for protein purification in the presence of saturated salt concentrations. Taken together, the purification to homogeneity of a non-tagged halophilic protein from a complex background of other halophilic

proteins is rather tedious with techniques that have to be compatible with the high ionic strength requirements of the proteins. It therefore seemed more rewarding to overexpress Car in *E. coli* followed by a purification scheme that would allow the use of low salt buffers. Refolded Car could then be examined for correct folding by CD spectroscopy, ^{1}H-NMR or in a yet to be developed biological assay relying either on the presumed activation of CheA by Car or on its interaction with receptor modifying enzymes such as CheB and CheR, respectively. Indeed, such a strategy was already successfully employed for numerous other halophilic proteins (HECHT & JAENICKE, 1989; CONNARIS *et al.*, 1998; RICHARD *et al.*, 2000; WORBS & WAHL, 2000).

6.2. The arginine receptor Car - a molten globule-like receptor?

The proton one-dimensional solution NMR spectrum of Car lacks all chemical shift dispersions typical for native proteins and resembles spectra derived from denatured proteins. In the region between seven and eight ppm of the spectrum, the chemical shifts of the amide and aromatic protons do not deviate from those of a random coil (WÜTHRICH, 1986). In addition, the spectrum lacks signals upfield of 1 ppm (ring-shifted methyl protons) which are characteristic for native proteins (for an example of a NMR spectrum of a halophilic protein see MARG *et al.*, in press). Car expressed in *E. coli* as soluble protein and purified under low ionic strength conditions as described in this work therefore appears to lack a well-defined tertiary structure. Far-UV circular dichroic spectroscopy, however, clearly indicates the almost exclusive presence of α-helical secondary structure elements as well as a distinctive cooperative thermal unfolding transition in heat denaturing experiments. Other proteins previously described like α-lactalbumin display a similar behavior of being

intermediates between the folded and unfolded state. These so-called molten-globules are observed as short-lived intermediates during protein folding and can be stabilized by non-physiological solvent compositions (for details see SEELEY *et al.*, 1996, and references therein). It is therefore well conceivable that a molten globular-like state of Car is induced by the lack of specific protein-solvent interactions. This is also supported by the finding that small molecules like polyethylene glycols or polyamines exert a stabilizing influence on Car. A thorough investigation of the parameters affecting halophilic protein stability and folding at high salt concentrations might be helpful in understanding the structure of Car.

Interestingly, the cytoplasmic domains of enteric chemoreceptors that have high sequence homologies with the C-terminal domain of Car likewise display such a behavior typical for highly flexible, molten globule-like proteins (SEELEY *et al.*, 1996). Furthermore, the photoactive yellow protein that serves as a prototype for the PAS domain family (PELLEQUER *et al.*, 1998) shows a stimulus-induced transient unfolding behavior in solution where the protein retains most of its secondary structure but loses nearly all of its tertiary structure as determined by NMR and CD spectroscopic measurements (RUBINSTEIN *et al.*, 1998; LEE *et al.*, 2001). The signaling state of PYP is therefore thought to be a molten globule (LEE *et al.*, 2001). From this it can be expected that partial protein unfolding is also involved in other proteins containing PAS domains as for example in the N-terminal domain of Car. However, in the case of Car, it is not known whether the protein's global flexibility is due to being partially unstructured or characteristic of the functional receptor. The conformational plasticity may be important for interacting with other proteins of the signaling complex (with other Car molecules, with CheW, CheA, CheR and CheB; for details of a recent model of the signaling complex see SHIMIZU *et al.*, 2000) or it may accelerate binding of some of

these proteins (PONTIUS, 1993). Numerous other proteins, especially DNA- or RNA-binding proteins, and proteins involved in the regulation of the cell cycle and in membrane fusion events only function due to an intrinsic lack of tertiary structure in which changes in dynamics occur during function (reviewed in WRIGHT & DYSON, 1999). Similar changes might be involved in ligand binding to Car, or more likely, in the signal propagation to the CheW/CheA complex where alterations in protein conformation are needed to activate CheA phosphorylation (KIM, 1994).

It is also possible that the highly flexible state of Car is non-physiological. Other components of the signaling complex might be needed to stabilize a non-dynamic tertiary structure, and this structure would be the functional state of the receptor. From the literature it is known that bacterial chemoreceptors form stable complexes with CheA and CheW (GEGNER *et al.*, 1992) while CheB and CheR bind only loosely to these complexes. Consequently, the presence of these other proteins might be necessary for Car to adopt a defined tertiary structure.

6.3. Role of eubacterial soluble receptors

Most of our knowledge on chemotaxis transducers comes from the membrane-bound chemoreceptor proteins Tar, Tsr, Trg and Tap of *E. coli* and *S. enterica* serovar Typhimurium. The structure of Tar except its transmembrane helices is known in atomic detail, as the structures of the other chemotaxis components[2]. From biochemical and behavioral analysis comes a vast amount of additional data, yet the most fundamental questions on the chemotaxis network are still far from being solved (STOCK, 1999; BREN & EISENBACH, 2000). It is for example not known how

signals are transduced through the cell membrane or how the system realizes its sensitivity combined with an exceptional dynamic range (five orders of magnitude towards chemoattractant concentration in *E. coli* and seven in *R. shaeroides*; JASUJA *et al.*, 1999; AIZAWA *et al.*, 2000; PACKER & ARMITAGE, 2000; KIM *et al.*, 2001). In addition, minor receptors like Trg and Tap elicit a cellular response as strong as the much more abundant receptors Tsr and Tar (the latter receptors make up 98% of a cell's receptor repertoire). Finally, how the signals from various receptors sensing different ligands in a chemically diverse environment are integrated to compute the adequate output signal (change in phosphoryl group flux through the network to CheY) is yet unknown (SANDERS & KOSHLAND, 1988). The most elaborate theories as activity spread in receptor arrays (BRAY *et al.*, 1998; LEVIT *et al.*, 1998; DUKE & BRAY, 1999) describe the network's input system insufficient, and new experimental data showed that activity spread might indeed occur, but to a much lesser extend as previously anticipated (BORNHORST & FALKE, 2000).

It is known that the chemoreceptors in all bacteria investigated cluster predominantly at one cell pole (GESTWICKI *et al.*, 2000; SOURJIK and BERG, 2000; LYBARGER and MADDOCK 2000; ALLEY, 2001; LYBARGER and MADDOCK 2001). The same holds true for the soluble transducer protein TlpC from *Rhodobacter sphaeroides*, but the purpose of this clustering remains unclear. It is apparent that this receptor clustering must be important for the function of the whole network due to its conservation in various organisms. Moreover, the structure(s) that maintain these complexes must also be conserved and independent of the presence or absence of the cell membrane. Soluble transducers from *R. sphaeroides* not only cluster in *R. sphaeroides* cells, but also in the cytosol of *E. coli*. Whether the two transducer proteins from *C. jejuni* and *H. pylori* also cluster is

[2] The solution structure of *Thermotoga maritima* CheW was determined by F. W. DAHLQUIST *et al.*

unknown. However, similar studies as the ones from WADHAMS *et al.*, 1999, who could demonstrate the clustering of a soluble MCP orthologe from *R. sphaeroides* seem to be straightforward and readily applicable to the proteins from *H. pylori* and *C. jejuni*. A clustering in the cytosol would further substantiate our findings that the two proteins can play a transducer-like role in chemotaxis.

Cytosolic transducers as the ones examined in this study could therefore be valuable models in further investigations of the receptor function and the role of clustering and signal complex formation in chemotaxis. Their crystallization initiated in this work laid the ground for future experiments that might result in the first structure determination of an entire transducer. Furthermore, with soluble molecules, it might be feasible to co-crystallize the transducer proteins with other components of the chemotaxis cascade without the problems of handling integral membrane proteins. The structure of such a signaling complex would result in a much deeper insight into how the entire two-component system works.

It is tempting to speculate on the function of cytosolic signaling complexes. They might enable the cell to sense their inner metabolic state, whereas membrane bound chemoreceptors always sense signals from the periplasmic space. Such a metabolic signaling, however, would provide information on more general parameters as, for example, overall energy status or the availability of key metabolic intermediates or substrates. In one case from *H. salinarum*, the ligand of the soluble receptor Car, arginine, is known. In this organism, arginine is an important energy source during fermentation that can be transported across the cell membrane and metabolized by the arginine deiminase pathway (STORCH *et al.*, 1999). Here, arginine signaling might override

and still awaits its publication. For details, see SHIMIZU *et al.*, 2000; BOURRET, *et al.*, 2002.

signals perceived by other pathways. This integration of information would enable the cell to react to a parameter that is crucial for its survival under fermentation conditions. Halobacterial arginine taxis therefore equals energy taxis (Taylor & Zhulin, 1998).

What either of Cj0448 or Hp0599 senses is still unknown. The presumed ligand could be a molecule equally important for *H. pylori* metabolism as arginine for *H. salinarum* or a molecule generated in the metabolism *of H. pylori*. Capillary assays with living cells might identify chemoattractants as amino acids or sugars to which *H. pylori* responds, and the soluble receptors could be necessary for this behavior. MIZOTE *et al.*, 1997, and FOYNES *et al.*, 2000 have shown chemotactic behavior of *H. pylori* cells towards urea, urease inhibitors, sodium bicarbonate, chloride and hog gastric mucin, respectively. It is questionable whether the organism has a chloride or bicarbonate receptor, but urea might well be sensed by one of the four MCP homologs. In analogy to Car, urea or another compound might bind directly to the soluble receptors (Fig. 47C) which eventually could form signaling complexes similar to the membrane bound complexes known from *E. coli* (Fig. 47A).

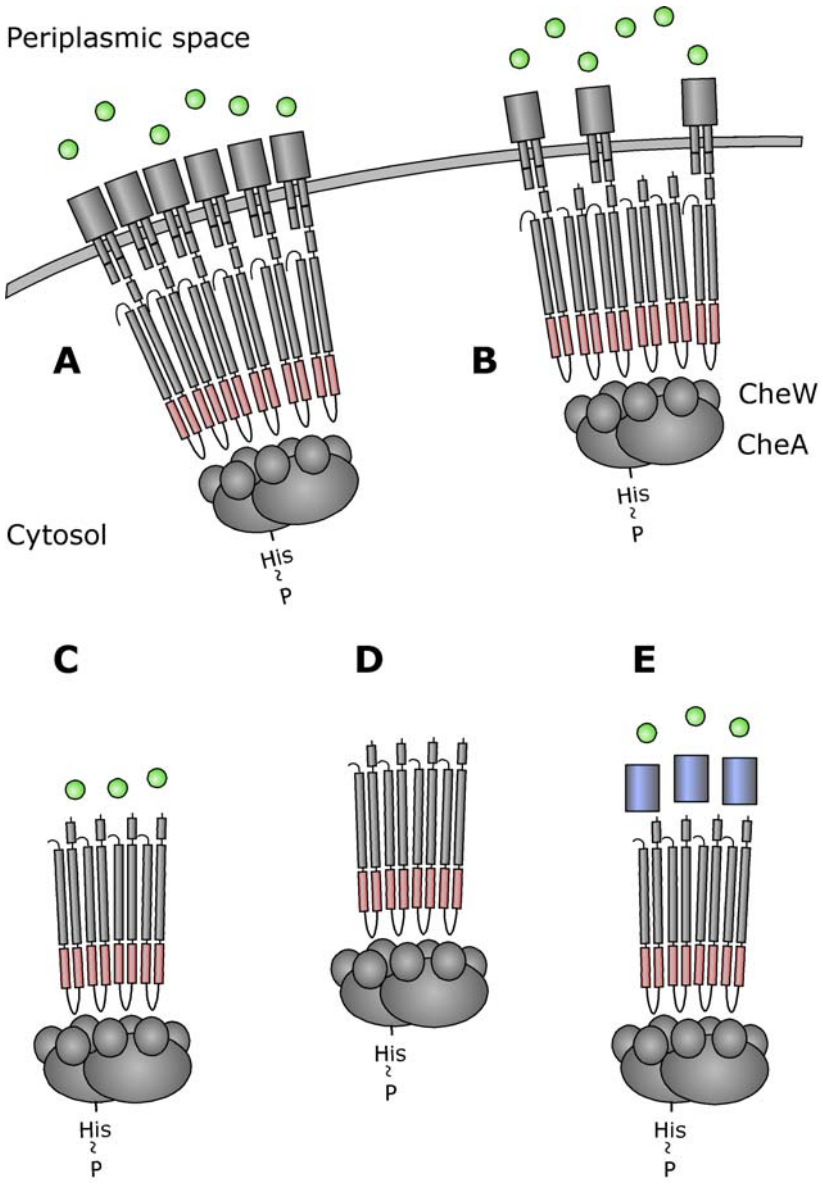

Fig. 47. Possible roles for soluble transducer or receptor proteins. Membrane-bound and soluble MCP homologues are depicted as long gray rods with the conserved signaling domains colored in red. The coupling protein CheW and the kinase CheA that together with the transducers build the so-called signaling complexes are depicted as gray spheres that cluster beneath the signaling domains of the MCP homologues. For the sake of simplicity, the stoichiometry of the signaling complexes was chosen arbitrarily. Ligand molecules are depicted as green spheres and putative receptor molecules that might interact with the soluble transducers are blue rectangles. For details see text.

Protein domain prediction algorithms, however, did not predict any known domains N-terminal to the signaling domains of Cj0448 and Hp0599. The location of such a domain is expected from the structural information of other transducers (for a complete list of known proteins containing the highly conserved signaling domain of bacterial transducers: http://smart.embl-heidelberg.de/smart/). Similarly, the small HAMP domain thought to be of importance for signaling in (trans-) membrane receptors (GALPERIN *et al.*, 2001) is also absent. In fact, the N-terminal part of both Cj0448 and Hp0599 is small, and predicted to be mainly unstructured. It is therefore questionable whether these stretches of amino acids are of sufficient length to form a ligand binding domain at all. This makes the existence of a protein possible that binds the actual ligand and, upon this event, in turn binds to the soluble transducers to elicit an adequate response (Fig. 47E). Such a scenario is known from other receptors like Tar (reviewed in FALKE *et al.*, 1997 or BOOS & SHUMAN, 1998) or the halobacterial transducers HtrI and HtrII (for details see SPUDICH, 1994; HOFF *et al.*, 1997; SASAKI & SPUDICH, 2000). Hp0599 and Cj0448 might also interact with a transport system whose occupancy in turn could be monitored. In these cases, any component that is either generated in the metabolism of *C. jejuni* or *H. pylori* or that is taken up by the two organisms could be the presumed ligand.

However, the soluble receptor homologs from *C. jejuni* and *H. pylori* might have totally different functions than being actively involved in signal transduction. Alternatively, soluble receptors might sequester the soluble components of the classical receptor complexes in a clustered state where they are not available for the chemotaxis cascade (Fig. 47D). The activation of the membrane-bound receptors could relocate CheW, CheF and other components to the membrane. In this scenario, soluble 'receptors' would affect receptor clustering and phosphoryl-flow to CheY

indirectly. Since it was shown in this work that Hp0599 and Cj0448 activate the histidine kinase CheF, cytosolic 'Che protein storage' by either of the two proteins would increase the basal phosphoryl group transfer through the chemotaxis network and thereby the response regulator phosphate concentration within the cell. On the other hand, cytosolic complexes of Che proteins on 'receptor scaffolds' could be involved in the modulation of flagellar rotation beyond the clockwise/counterclockwise level encountered by *E. coli*. The response regulator domains present in the putative soluble signaling complexes might interact with the motors to control the rotational bias in a sophisticated manner. Soluble receptor homologs could also cluster together with membrane-bound receptors to form mixed signaling complexes associated to the plasma membrane (Fig. 47B). In the case that they do not actively sense any signals (no signalling domain present in these proteins), their presence in these 'mixed' complexes would nevertheless influence the response regulator phosphate concentration: addition of ligand would only affect the 'real' sensor molecules, and the activity of the truncated, soluble MCP homologs would remain unaltered. In this scenario, the CheF kinase activity after adding the respective ligands would be higher in the mixed complexes compared to classical complexes. Such a mechanism might eventually realize a novel form of adaptation to various ligand concentrations presumed that the presence of the 'blind' receptors in the signaling arrays finally depends on the response regulator activity. Such roles in sequestering chemotaxis components as described here are fully compatible with the observation that Hp0599 is a cytosolic highly abundant protein as shown by two dimensionally gel electrophoresis of the entire *H. pylori* strain 26695 proteome (Max-Planck-Institute for Infection Biology; for details see http://www.mpiib-berlin.mpg.de/2D-PAGE/).

In general, soluble MCP homologs seem to be ubiquitous, and again as in the case of its unusual set of chemotaxis proteins, an organism as *E. coli* appears to be the exception. Even in *C. jejuni*, two more genes within the genome are predicted to code for soluble transducer-like proteins (see table 3, p. 38).

6.4. Possible role of CheV proteins

CheW-CheY fusion proteins ('CheV proteins'; FREDRICK & HELMANN, 1994; DOIG *et al.*, 1999) were found in the genomes of various organisms such as *Bacillus subtilis*, *Staphylococcus aureus*, *Vibrio cholerae*, *Pseudomonas aeruginosa*, *Campylobacter jejuni*, *H. pylori* and others (for a complete list, see http://smart.embl-heidelberg.de/smart/). From *E. coli* and other (coliform) organisms it is known that the response regulator CheY is the motor switch factor, and CheW is an adaptor protein that connects the transducer proteins with the histidine kinase (the CheW domain of CheA has regulatory functions; see BILWES *et al.*, 1999; SHIMIZU *et al.*, 2000). The role of the CheV proteins in the chemotaxis system, however, remains enigmatic. It was therefore of great interest to assess the function of the three CheV paralogs of *H. pylori* to understand their interplay with the other components of the chemotaxis network.

In the present study, it was shown that CheV proteins (CheV2 and CheV3 from *H. pylori*), in addition to CheY, are targets for the phosphoryl group transfer from CheA. Phosphorylation of the protein presumably occurs in the C-terminal response regulator-like domain on a conserved aspartyl residue as deduced from sequence homology to *E. coli* CheY in this region of the CheV protein. Whereas the phosphotransfer reaction between CheF-phosphate and CheY proceeds very rapidly, the transfer to CheV2 is slow.

This is in accordance with the recent findings of KARATAN *et al.*, 2001, in the homologous *Bacillus subtilis* chemotaxis system. The authors also find that CheV-phosphate is very stable compared to CheY- or CheB-phosphate from both *E. coli* and *B. subtilis.* Their results with wild type and mutant *B. subtilis* cells in the tethered-cell assay suggest that CheV plays a crucial role in adaptation to the attractant asparagine sensed by McpB. The prolonged lifetime of CheV-phosphate, as well as the slow phosphorylation kinetics of CheV might be necessary to allow enough time for the excitatory signal to cause a sufficient period of smooth swimming (KARATAN *et al.*, 2001). In *H. pylori*, a similar mechanism might be at work where the CheA activity is modulated by the presence of CheV. Unfortunately, no comparable experimental data are available for *H. pylori*. PITTMAN *et al.*, 2001, have shown the importance of CheV1 for helicobacterial chemotaxis. A deletion strain of *cheV1* was no longer chemotactic, whereas strains deleted in *cheV2*, *cheV3*, or both showed no phenotype under the conditions tested. Furthermore, neither *cheV2* nor *cheV3* could complement isogenic *E. coli cheW* or *cheY* mutants, yet the expression of both genes in *E. coli* abolished chemotaxis. These results are difficult to interpret, especially in the light that the chemotaxis networks in *B. subtilis* and *H. pylori* differ significantly.

For the *H. pylori* chemotaxis network with its apparent lack of receptor modifying enzymes, adaptation through the CheV proteins could be the only means by which the chemotaxis network might adapt. Their CheY domain allows protein phosphorylation (shown for CheV2 and CheV3 in this work), thus providing a possible feedback loop from the output of the chemotaxis network. If CheV proteins are involved in system adaptation, this adaptation mechanism must follow the theoretical constraints of asymptotic tracking which can not be relaxed without loosing exact adaptation (see chapter 6.6.). One prediction would be that the CheV

proteins not only bind to the receptors, but their affinity to the receptors must also change with their phosphorylation state. Moreover, there should be a difference in the receptor complex activity upon binding of CheV to this complex, as well as a different binding affinity of CheV towards receptors with and without bound ligands. The underlying theory that favors this scenario is that the phosphorylation of the CheY domain could trigger structural changes within the adjacent adaptor domain. Alternatively, the oligomerization state of CheV could be altered in a way that would lead to the exposure of the CheW domain. The CheV proteins might therefore play a regulatory function in non-enteric chemotaxis systems. Of special interest in this context is the absence of an obvious regulatory feedback loop, e.g. by receptor methylation, in *Helicobacter* that enables the enteric chemotaxis system to adapt.

From the presence of the response regulator domain in CheV, on the other hand, one might conclude that the proteins shuttle between the receptor complex and the flagellar motors as already well known from *E. coli* CheY. Another possibility is that the CheY domain in CheV serves as a phosphate sink in a similar fashion as the one that was postulated for CheY orthologs in *Rhodobacter* or *Sinorhizobium* (SOURJIK and SCHMITT, 1996; ARMITAGE & SCHMITT, 1997; SOURJIK and SCHMITT, 1998; PITTMAN *et al.*, 2001*)*. From the kinetic data presented in this work regarding the CheF to CheV phospho-relay it follows that the transfer of phosphate groups to CheV is considerably slower than the one to CheY. A similar situation can be found in *R. sphaeroides* where several CheA proteins only phosphorylate their cognate CheYs efficiently (SHAH *et al.*, 2000; MARTIN *et al.*, 2001). This might rule out a role of the CheV proteins as a phosphate sink, but we do not know if this transfer rate changes under conditions where a cognate ligand binds to the receptor complex. A better candidate for the phosphate sink, therefore, would be CheY, since CheY is rapidly phosphorylated by

CheF and CheY-phosphate is highly unstable as was shown both in this study. This, nevertheless, immediately raises the question which of the response regulators in *H. pylori* is the motor switch factor (see below).

However, the phosphate-sink theory from *Rhodobacter* and *Sinorhizobium* has some general problems. It was never shown in an *in-vivo* or *in-vitro* system that the flow of phosphate groups from CheA to the flagellar motor switch factor reverses when ligand is added to a mixture containing all components of the respective chemotaxis system (Fig. 48).

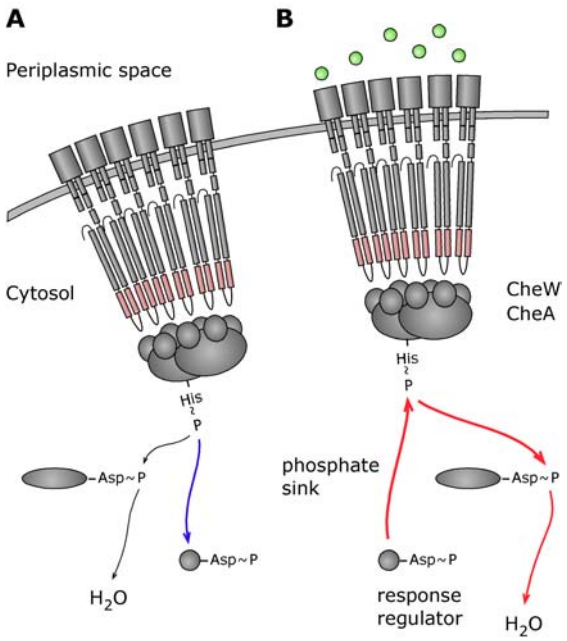

Fig. 48. Expected phosphoryl group transfer in the hypothetical phosphate sink theory in a chemotaxis system as in *E. coli* where addition of ligand decreases CheA histidine kinase activity. Under equilibrium conditions where no ligand is present (**A**), the phosphate groups are transferred mainly to the response regulator to generate the output signal (blue arrow). When ligand (green spheres) is added (**B**), the histidine kinase autophosphorylation activity is reduced and the response regulator phosphate signal is rapidly quenched by passing the phosphate groups to the hypothetical phosphate acceptor molecule via the histidine kinase (red arrows). The signaling complex is depicted as described in Fig. 47, p. 91.

Furthermore, the phosphate groups coming in to the kinase must then be 'forwarded' to the 'phosphate sink' to quench the output signal (the phosphorylated kinase is stable towards hydrolysis on the time scale of the transphosphorylation events and a response regulator domain must be present in the system for signal termination). In *E. coli*, the response regulator phosphatase CheZ decreases the lifetime of CheY phosphate tenfold (SEGALL *et al.*, 1985; BREN *et al.*, 1996; SCHARF *et al.*, 1998), and it is generally assumed that signal termination occurs almost exclusively by this mechanism. Other bacteria might employ other mechanisms to quench the chemotaxis signal, since the presence of CheZ seems to be restricted to the *Enterobacteriaceae* and *Pseudomonaceae* groups. The underlying logic for such a rather complex signal termination mechanism as a 'phosphate sink', in principle, remains elusive since a shortened lifetime of the response regulator would be a sufficient means in all cases where the signaling complex can still produce a high enough concentration of response regulator phosphate under equilibrium conditions. The quest for the phosphate sink that would allow the fast signal decay could therefore be misleading.

Finally, in *Helicobacter*, the situation is even further aggravated by the presence of the CheY-like domain in CheF. The repertoire of five response regulator domains is unusual in the light of the simple enteric chemotactic system. Any of the five CheY domains might bind to the motor's switch complex or might be involved in signal quenching.

6.5. The *H. pylori* motor and its switch

H. pylori has five to seven sheathed flagella on one cell pole. The bacterium is highly motile and moves with appreciable velocities. In a

solution of 10 cp, *H. pylori* moves at up to 80 μm/s, whereas *E. coli* reaches only 30 μm/s (YOSHIYAMA *et al.*, 1999). *H. pylori* can still move in a viscous environment of up to 200 cp, whereas *E. coli* is immobilized at 20 cp. Orthologs of all proteins necessary to build the flagellar motor in *E. coli* are present in *H. pylori*. However, the helicobacterial motors and flagella contain additional building blocks. One is the minor flagellin FlaB (SUERBAUM *et al.*, 1993; JOSENHANS *et al.*, 1995; SUERBAUM, 1995), another is spirillin[3], and other yet uncharacterized proteins might also participate. In analogy to the *E. coli* motors, the *H. pylori* motor switch presumably is composed of three proteins, FliG, FliM and FliN, that together form the cytosolic MS ring. Upon binding of the switch factor (CheY-phosphate in *E. coli*; CLUZEL *et al.*, 2000), the proteins in the MS ring undergo structural rearrangements that result in an increased CCW to CW switching probability. Most of our knowledge on these events comes from coliform bacteria (BERG, 2000), and helicobacterial motors are not yet characterized.

In *E. coli*, CheY-phosphate binds to the N-terminal 16 amino acids of FliM as shown by molecular crosslinking experiments with purified proteins in the presence of acetyl phosphate to generate CheY phosphate (BREN & EISENBACH, 1998, and this work, Fig. 42, p. 75). Similar experiments with components of the *H. pylori* chemotaxis system could not be performed since *H. pylori* FliM could not be overexpressed in *E. coli*. Consequently, a chimeric FliM was constructed assuming that the homologous proteins might interact. However, *H. pylori* CheY could not be crosslinked to *E. coli* FliM, presumably because other residues only present in *H. pylori* FliM specifically mediate this interaction. Hereby, the N-terminal amino acid residues not present in *E. coli* FliM might be of importance. Likewise, a

[3] This protein seems to be restricted to the *Campylobacter* and *Helicobacter* groups of the ε-proteobacteria. A homologous protein from *Wolinella succinogenes* was first described by BERENDES, 1998.

chimeric FliM protein that was constructed by fusing the *H. pylori* FliM N-terminal 42 amino acids to the C-terminal *E. coli* FliM also failed to show any interactions with CheY of *Helicobacter*. Apart from the difficult solubility characteristics of *H. pylori* FliM, it has a pronounced tendency to aggregate at high concentrations, and it might be questionable whether *H. pylori* CheY-phosphate binds to FliM at all due to the presence of overall five CheY-like response regulator domains in this chemotaxis system (Fig. 49).

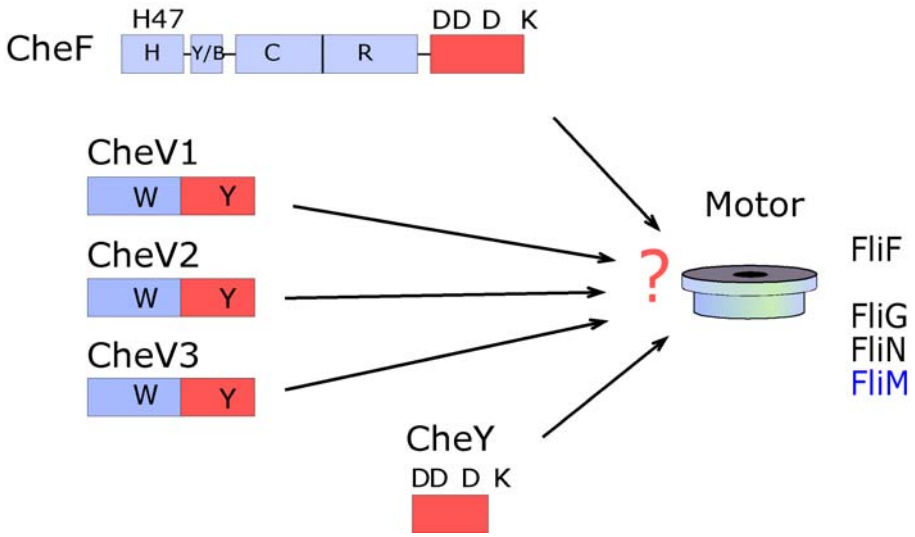

Fig. 49. *H. pylori* Che proteins with CheY-like response regulator domains. In *E. coli*, CheY phosphate is the output signal of the chemotaxis network that binds to FliM located in the switch complex beneath the membrane bound FliF disc. In *H. pylori*, five proteins eventually could bind to FliM and induce motor switching.

FOYNES *et al.*, 2000 showed that *H. pylori* cells deficient in CheF, in both CheF and CheY, and in the CheY domain of CheF exhibited a smooth swimming phenotype that reminds to the phenotype of *E. coli* cells lacking CheY. The authors concluded that not CheY but CheF with its CheY domain

is the flagellar motor switch factor. The authors also mentioned the presence of the soluble transducer protein Hp0599 and its apparent capability to form soluble signaling complexes. The smooth swimming phenotype, however, might only be the result of a 'malfunctioning', complex chemotaxis network that was deprived of some of its important components. Under the assumption that CheF is indeed the switch factor, one is faced with several other problems: does CheF build receptor complexes as known from the homologous proteins of all other bacteria investigated? And if so, how can such a complex with a molecular weight of several megadaltons bind to FliM? Furthermore, in *E. coli*, it is not the binding of one CheY phosphate molecule that induces motor switching, but the binding of several such response regulators. If this holds true for *Helicobacter*, the motor would need to bind either several such large complexes or many CheF molecules from one complex need to bind to the MS ring. The role of membrane-bound transducer molecules in such a scene remains enigmatic, since membrane bound signaling complexes should not be able to bind to the cytosolic MS ring at all. To clarify these questions will be difficult with the techniques used to gain insight into the homologus enteric model: as it was shown in this study, *H. pylori* FliM was not expressed in *E. coli* and is therefore not as easily available as *E. coli* FliM. The use of chimeric FliM might overcome this problem, but it is unclear whether the switch factor will bind to this protein. Furthermore, the CheV proteins autophosphorylate only to a very limited extend in the presence of acetyl phosphate, and response regulator to FliM crosslinking experiments that rely on response regulator autophosphorylation are hence not suited for the CheV proteins. The preparation of phosphono-CheV (and CheY, if necessary; see HALIKDES *et al.*, 1998; HALIKDES *et al.*, 2000) might circumvent this problem and was initiated in the present work (construction and expression of the CheV2 double mutant CheV2:D241C/C274S for derivatization) yet is behind the scope of this

work. In the case that CheF binds to the motor switch factor, the feasibility of protein-protein interaction assays (CheF or whole signaling complexes with FliM) will be limited by the mere size of the interacting components and again by the preparation of CheF phosphorylated in its response regulator domain. *In vivo* experiments with fluorescence labeled fusion proteins to localize *H. pylori* chemotaxis components (SOURJIK & BERG, 2000) might be more suited as the *in vitro* assays conducted in the present work.

Arguments in favor of CheF being the motor switch factor come from a computational analysis of several prokaryotic genomes that claims that the chemotaxis operon in *H. pylori* is highly expressed (KARLIN & MRÁZEK, 2000). This might be necessary if CheF would be the switch factor. Similarly, Hp0599 forms a prominent spot on a two-dimensional SDS-PAGE derived from a total *H. pylori* cell extract indicating a high concentration of this protein in the cell (see http://www.mpiib-berlin.mpg.de/2D-PAGE/ for details). The availability of specific antisera directed to CheF, Hp0599 and other chemotaxis network components will allow to exactly measure the expression levels of these proteins in further experiments.

6.6. Adaptation in biological networks and chemotaxis in *H. pylori*

Complex networks like metabolic pathways, food webs or man-made structures must be able to counteract perturbations to ensure proper function (BHALLA & IYENGAR, 1999; STROGATZ, 2001; for a historic overview see BENNETT, 1993). For example, the availability of glucose, *E. coli*'s favorite carbon source, represses the expression of enzymes for the catabolism of other sugars even in their presence, and the depletion of

glucose in the medium induces a change in the cell's enzyme repertoire. The chemotaxis system of coliform bacteria that senses temporal gradients of chemicals is one of the best understood biological networks and the way how its components interact to build a simple yet robust signal transduction system whose steady-state output is independent of the input signal becomes more and more apparent (for recent review see SHIMIZU *et al.*, 2000 and FOUSSARD *et al.*, 2001). Following the model of BARKAI and LAIBLER and using techniques from control and dynamical systems theory (ISIDORI & BYRNES, 1990), YI *et al.*, 2000 have shown that this asymptotic tracking behavior originates in the specific structure of the system that creates this property inherently. It does not lie in a fine-tuning of system parameters. In this model, the covalent modification of the receptor complex by CheB and CheR generates a closed loop system in which the system error is fed back into the system (integral feedback control; Fig. 50). In fact, integral control is not only sufficient, but necessary for robust perfect adaptation.

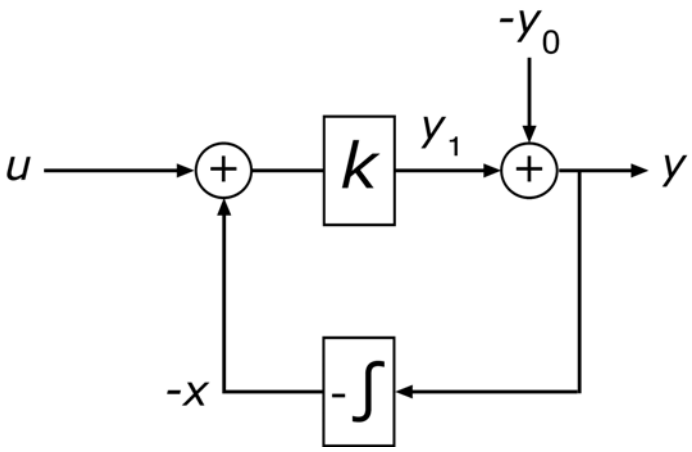

Fig. 50. Block diagram of integral feedback control in the BARKAI-LEIBLER model of chemotaxis in *E. coli*. The ligand concentration u is the input variable, and receptor activity is the output of the chemotaxis system with the gain *k*. For the system to adapt, $y(t) = (y_1) - (y_0)$, the output error of the system, must become zero for $t \rightarrow \infty$. In the case of the chemotaxis network, this equals that receptor array activity (y_1) reaches its basal activity (y_0) after a sufficiently long period of time at all ligand concentrations. This is realized by the feedback loop in which the time integral of the output error *y* (receptor array deactivated through ligand binding compared to its basal activity when ligand is absent, for example) is fed back into the system. The result is $y = k(u-x)-y_0$ becomes zero at stady-state for all u. In the chemotaxis network, $-x$ equals the receptor methylation level. Adapted from YI *et al.*, 2000.

The evolutionary advantage of such a chemotaxis system for *E. coli* is obvious: its robustness permits a large parameter space in which the system can evolve and adjust to environmental changes, and its properties are preserved even if the network components are modified or produced in varying quantities (BARKAI & LAIBLER, 1997). However, the *H. pylori* chemotaxis system lacks receptor modifying enzymes and therefore it remains enigmatic whether the network adapts, and if so, how. One possibility is the presence of up to now unknown proteins with functional homology to CheB and CheR. In fact, within the *H. pylori* genome, 42% of all ORFs are of unknown function, 55% of which are specific to this

organism. However, the system could also achieve asymptotic tracking by means other than receptor methylation. The feedback loop that is necessary for adaptation could be realized by any other mechanism whatsoever, as long as it provides the system with information on the time integral of the output error. Therefore it is tempting to speculate on the role of the three CheV paralogs in the *Helicobacter pylori* chemotaxis system proteins (see chapter 6.7.).

Another possibility is that *H. pylori* has a chemotaxis system that lacks a feedback loop analogous to the one known from enteric bacteria. Such a system would not be able to adapt to changing ligand concentrations, its steady-state output value would always depend on the system input and on the concentration of the network components. Apparently, such a chemotaxis system is of only limited value to the cell. It is difficult to imagine such a simple system especially in the light of its importance to *H. pylori*: non-chemotactic bacteria are not virulent, they do not establish infections in humans or in the gnotobiotic piglet model (for an overview see FALK *et al.*, 1998). Furthermore, the non-adherent *Helicobacter* population that makes up 90% of all *Helicobacters* in the stomach perpetually needs to relocate from the mucus to the cell surface in order to avoid their discharge into the digestive tracks. Chemotaxis as the means of control over motility is crucial for this ability.

6.7. Gene regulation and adaptation in a stable environment

The environment in which *H. pylori* thrives, the surface mucous cell type layer (SLOMIANY *et al.*, 1987; OTA *et al.*, 1992; SHIMIZU *et al.*, 1996), appears to be of remarkable stability and uniformity over time. The number and complexity of regulatory circuits in any given organism

positively correlates with the number and complexity of external environmental forces acting on the organism (see STOVER *et al.*, 2000, and references therein). Within the genomes of free-living bacteria, more proteins involved in regulatory functions can be identified than in genomes of endosymbionts, and free-living bacteria with a highly diverse lifestyle like *Pseudomonas* or *Sinorhizibium* possess more signal transduction networks than less flexible species (STOVER *et al.*, 2000; FINAN *et al.*, 2001; BARNETT *et al.*, 2001; CAPELA *et al.*, 2001;). As far as *H. pylori* is concerned, one striking feature of the organism is the low abundance of known regulatory proteins as exemplified by the existence of only three sigma factors involved in transcriptional regulation and four two-component systems of largely unknown function (two of the sigma factors are exclusively involved in flagellin gene expression; TOMB *et al.*, 1997; BEIER & FRANK, 2000, BJÖRKHOLM *et al.*, 2001). Another factor that might have driven the loss of regulatory networks during *H. pylori* evolution besides the environmental stability is the lack of competition by other microorganisms. However, the parameter space in which the bacterium operates might be narrow enough to permit a reduction in both the number of signal processing circuits as well as their dynamic range. This could account for the possible lack of genes coding for the receptor-modifying proteins CheR and CheB in the *H. pylori* genome. Rather sophisticated adaptation mechanisms like receptor methylation might just not be a necessity for this organism since the environmental conditions it experiences never change to an extend that would render such an apparatus useful. Somehow contradictory to that is the fact that the chemotaxis system in *H. pylori*, as well as in other members from the ε-subgroup of proteobacteria, is at least as complex as the one that can be found in coliform bacteria. It is not the diversity in transducer proteins, but it is rather the unusual set of chemotaxis proteins that make up this complexity. However, further experiments not only with isolated

chemotaxis components but also with living cells are clearly needed to investigate the importance of adaptation in *H. pylori* chemotaxis.

7. Materials and Methods

Solutions and labware for bacterial cell cultures and molecular biological techniques were autoclaved or sterile filtered. All enzymes were purchased from New England Biolabs (Beverly, USA) and all chemicals were from Sigma-Aldrich (Deisenhofen) unless otherwise indicated (see Appendix A). Radiochemicals were purchased from Amersham Pharmacia (Freiburg). Chemicals used for crystallization trials were of the highest purity available, and solutions were sterile filtered before use. All numbers given in *per cent* refer either to weight per volume or, in cases of liquids, to volume per volume. All experiments involving standard techniques were performed following the manufacturer's protocols and recommendations when available if not otherwise explicitly indicated.

7.1. Bacterial strains and plasmids

Unless otherwise indicated, *Escherichia coli* strain XL1 blue (BULLOCK *et al.*, 1987) was used for plasmid growth and maintenance, and strain BL21(DE3) (STUDIER *et al.*, 1990) was used for high-level expression of recombinant proteins directed by either plasmid pT7-7 (GALLAGHER, 1992; for halophilic proteins), plasmid pET28a(+) and pET36b(+) (Novagen; see Appendix B) derived vectors harboring the gene of interest under the control of the T7 promotor (STUDIER & MOFFATT, 1986; ROSENBERG *et al.*, 1987). All expression plasmids were constructed by ligating appropriately digested PCR products into the plasmid DNA. The resulting vectors were sequenced to ensure no mutation was introduced into the gene sequence during the amplification reactions.

7.2. General molecular biological techniques

Kanamycin (pET based vectors) and ampicillin (pT7-7 based vectors) were the selection markers, and all media or agar plates to grow transformed bacteria were supplemented with either of the two antibiotics (kanamycin at a concentration of 30 µg/ml, ampicillin at a concentration of 100 µg/ml). The media (LB broth, terrific broth and SOC agar plates) for bacterial growth were prepared following the instructions given by GALLAGHER, 1992; the agar plates contained 1.5% agar-agar.

7.2.1. Culture of *E. coli* XL1 blue cells for plasmid growth

A 100 ml Erlenmayer flask containing 50 ml of LB broth with an appropriate antibiotic was inoculated with a single colony of *E. coli* XL1 blue harboring the plasmid of interest. The flask was incubated overnight on a platform shaker at 37°C and 250 rpm. From this cell culture the plasmid DNA was purified as described under 7.2.2.

7.2.2. Purification of plasmid DNA from *E. coli* cells

All plasmids used throughout this work were purified from an overnight *E. coli* XL1 blue cell culture using the QIAprep procedure as recommended by the manufacturer. Plasmid DNA was always eluted from the spin columns with 50 µl elution buffer.

7.2.3. General PCR protocol for DNA amplification

For DNA amplification reactions, an appropriate amount of template DNA was added to a mixture of 10 µl of each primer at a concentration of 2 µM, 20 µl 10 mM dNTPs (2.5 mM each; TaKaRa), 10 µl 25 mM magnesium chloride, 10 µl 10x TaKaRa LR Taq reaction buffer, 2 µl DMSO and 5 units TaKARa LA Taq in a total volume of 100 µl. After an initial denaturation step of 94°C for 3 min, all reactions were cycled (denaturation, annealing and extension) for 30 cycles of 94°C for 45 sec, 45°C for 45 sec and 63°C for 1 min for each kb of DNA to be synthesized. Thereafter, an aliquot of the reaction mixture was run on an agarose gel to visualize the amplification products. The remaining DNA was purified from the other components of the reaction mixture using the QIAquick procedure as described under 7.2.4.

7.2.4. Purification of DNA after enzymatic reactions

For the purification of DNA after enzymatic reactions the QIAquick procedure was used essentially as recommended by the manufacturer, except that the column was washed twice with washing buffer and that the purified DNA was eluted from the spin columns with 120 µl of elution buffer in the cases where the DNA was further processed in enzymatic reactions except ligations. In all other cases the DNA was eluted with 30 µl elution buffer to ensure a high DNA concentration.

7.2.5. Preparation of vector DNA for ligation reactions

Vector DNA was prepared as described under 7.2.2. For restriction of vector DNA, 120 µl DNA solution was digested with 100 units each of the appropriate restriction endonucleases in a total volume of 150 µl supplemented with reaction buffer as recommended by the endonuclease's manufacturer. After 30 min at 37°C, the DNA was purified from the reaction mixture as described under 7.2.4. Subsequently the 5´-phosphate groups were removed from the linearized DNA molecule by shrimp alkaline phosphatase (USB) treatment as follows: 15 µl reaction buffer and 3 units shrimp alkaline phosphatase were added to the DNA solution according to the supplier's instructions in a total volume of 140 µl. Again, after 30 min at 37°C, the vector DNA was purified from the reaction mixture as described and stored at -32°C until further use.

7.2.6. Preparation of PCR-derived DNA fragments for ligation reactions

DNA fragments to be ligated into expression vectors were digested by appropriate restriction endonucleases which cut at cleavage sites that were introduced by the PCR-primers. To 120 µl DNA preparation, 20 µl of the restriction endonuclease reaction buffer and 100 units each of the restriction endonucleases were mixed in a total volume of 150 µl. The reaction was allowed to proceed for 30 min at 37°C. Thereafter, the DNA was purified from the other components of the reaction mixture as described under 7.2.4.

7.2.7. Ligation of DNA molecules

Linearized vector DNA was prepared as described under 7.2.5., and PCR-derived DNA fragments to be ligated to the vector backbone were prepared as described under 7.2.6. All ligations were prepared by adding 4 µl 5x ligation buffer (Gibco BRL), 2 µl insert DNA, 1 µl vector DNA, 1 µl 10 mM ATP and 2 µl T4 DNA ligase (Gibco BRL) to 10 µl water. The reaction mixture was carefully mixed, and after an initial step of 24°C for 15 min, all reactions were cycled for 99 cycles of 24°C for 2 min, 18°C for 2 min and 12°C for 2 min followed by 1 h at 12°C.

7.2.8. Restriction analysis of plasmid DNA

From cell cultures of bacterial colonies obtained after transforming bacterial cells with ligation reactions, plasmid DNA was isolated as described under 7.2.2. Plasmid DNA was digested with the restriction endonuclease(s) used to construct the desired plasmid by mixing 5 µl plasmid preparation, 10 units each restriction endonuclease in a total volume of 10 µl of 1x reaction buffer supplied with the restriction endonuclease. After incubation at 37°C for 30 min the DNA was resolved on an agarose gel as described under 7.2.9.

7.2.9. Analysis of DNA by agarose gel electrophoresis

Agarose gel electrophoresis of DNA was performed in commercially available submarine gel tanks of appropriate size following the method of McDONELL *et al.*, 1977 and SOUTHERN, 1979 as described in GALLAGHER, 1992. All agarose gels used throughout this study were run in TBE buffer

(44.5 mM Tris base, 44.5 mM boric acid, 1 mM EDTA in water) and were prepared by dissolving 0.7 % agarose and 0.5 µg/ml ethidium bromide in TBE buffer. Samples containing an appropriate amount of DNA were mixed with 6x loading buffer (0.1% bromophenol blue, 15% Ficoll type 400 in water) prior to sample application, and the gel was run at 4 V/cm until optimal separation was achieved. Thereafter, the DNA was visualized by illumination with UV light. As size marker, Gibco BRL's 1 kb DNA size marker was used.

7.2.10. Sequencing of plasmid DNA

All sequencing reactions were carried out following the chain termination method originally developed by SANGER *et al.*, 1977, with the modifications by TABOR & RICHARDSON, 1987, using Perkin Elmer's ABI Prism BigDye Terminator Cycle Sequencing Ready Reaction kit as recommended by the manufacturer. In short, 2.5 µl plasmid DNA, 7.5 µl water, 1 µl DMSO, 5 µl sequencing primer at a concentration of 10 µM and 4 µl BigDye reagent were mixed in a PCR tube, and the reaction was cycled (denaturation, annealing and extension) after an initial denaturation step of 94°C for 3 min for 30 cycles of 94°C for 45 sec, 43°C for 45 sec and 60°C for 5 min. Thereafter, 10 µl of water were added to the reaction mixture, and the newly synthesized DNA was purified from other components of the reaction mixture by size exclusion chromatography on Sephadex G-50 columns as follows: the DNA solution was applied to either an AutoSeq G-50 disposable spin column (Amersham Pharmacia Biotech) or, in the case of many probes, to a Millipore MultiScreen-HV 96 well plate. Subsequently, the DNA was eluted from the columns as recommended by the respective manufacturer, dried in a speed vac and resuspended in 3 µl denaturation buffer (100 mg dextran blue, 1 ml 25 mM EDTA in 7 ml

deionized water). The DNA probes were denatured for 2 min at 96°C and the amplification products were resolved on an ABI Prism 377 DNA sequencer.

7.2.11. Preparation of short synthetic dsDNA linker

Short synthetic dsDNA fragments with protruding ends for ligations were prepared from appropriately designed oligonucleotide pairs by mixing 50 µl of each oligonucleotide at a concentration of 5 µM in a microcentrifuge tube. The mixture was incubated at 96°C for 5 min and was thereafter allowed to cool down to room temperature. The solvent was removed in a speed vac and the DNA was dissolved in 100 µl of 10 mM Tris-HCl pH 8.5 at room temperature. Subsequently, the DNA was phosphorylated in a final volume of 120 µl containing 3 units polynucleotide kinase (USB), 1 mM ATP and 1x polynucleotide kinase buffer as recommended by the manufacturer. The reaction was allowed to proceed for 45 min at 37°C. Thereafter, the DNA was purified from the other components of the reaction mixture using the QIAquick procedure as described under 7.2.4.

7.2.12. Construction of mutant genes by site-directed mutagenesis

To introduce point mutations into cloned genes the QuickChange site-directed mutagenesis kit (Stratagene) was used essentially as recommended by the manufacturer.

7.2.13. Construction of mutant genes by PCR

In all cases where the DNA sequence to be altered was near (< 120 bp) the 5´- or 3´- end of the gene, the novel gene sequence was introduced by PCR with an oligonucleotide bearing the mutation. The oligonucleotide was designed to cover the sequence beginning at least 20 bp down- or upstream of the desired mutation going all the way to either the 5´- or 3´-end of the gene including flanking sequences recognized by restriction endonucleases for the generation of overlapping ends. Subsequently, the resulting PCR fragment was cloned into an expression vector as described under 7.2.7.

7.2.14. Construction of chimeric FliM

To construct a chimeric FliM protein where the N-terminal 42 amino acids of the *H. pylori* FliM protein were fused to the C-terminal 45 to 334 amino acids of the *E. coli* FliM protein, a PCR primer was designed whose 3´- end was directed to the *H. pylori fliM* gene sequence (bp 111 to 141) and whose 5´- end was directed to the *E. coli fliM* gene (bp 135 to 170; see Fig. 51, p. 91). PCR with this primer and a primer directed to the 5´-end of the *H. pylori fliM* gene in a PCR with a plasmid harboring the *H. pylori fliM* gene as template gave a PCR product whose 3´- end was homologous to the *E. coli fliM*. Subsequently, this PCR product was used as a primer in a second PCR to amplify the full length chimeric gene from a plasmid containing the *E. coli fliM* gene. This chimeric gene was cloned into an expression vector as described under 7.2.7.

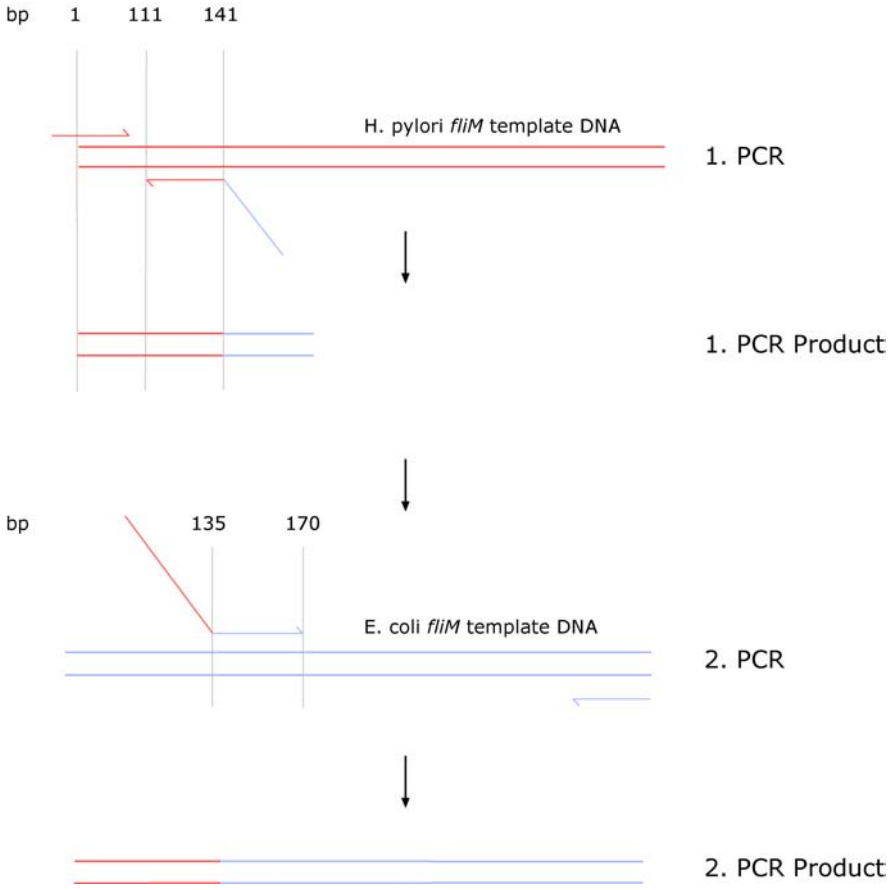

Fig. 51. Synthesis of the chimeric *H. pylori* - *E. coli fliM* gene. In the first PCR, a PCR primer was used whose 3'-end is complimentary to the *H. pylori fliM* gene (red part of reverse primer) and whose 5'-end is complementary to the *E. coli fliM* gene (blue part of reverse primer). The resulting first PCR product was used as primer in the second PCR. The resulting second PCR product is the desired chimeric gene.

7.2.15. Synthesis of *H. salinarum cheR* and *cheB* genes

The protein sequence of *H. salinarum* CheR and *H. salinarum* CheB was reverse-translated to the according DNA sequence using the *E. coli* codon usage table. From this novel gene sequence, oligonucleotides for the LCR (LANDEGREN, 1988) were designed as follows: beginning at the 5´-end of the coding strand, the gene sequence was divided into one 35 bp long oligonucleotide, followed by 75 bp long oligonucleotide all the way to the

3´-end of the gene (see Fig. 52, p. 93). The missing bases of the template strand (in any case, < 75) were omitted. For the non-coding strand, oligonucleotides were designed in the very same way as described for the coding strand so that the 5´-end of the first oligonucleotide was the complement of the 3´-end of the coding strand. From all oligonucleotides, the solvent (20% acetonitrile in water) was removed in a speed vac, the oligonucleotides were dissolved in water and the concentration was adjusted to 10 µM. Thereafter, all oligonucleotides (18 in the case of *cheR*, 26 in the case of *cheB*) except the ones at the 3´-end of each strand to be synthesized were phosphorylated using polynucleotide kinase as described in 7.2.11. except that the oligonucleotides were not purified after the reaction. The LCR was performed in a total volume of 100 µl with 100 nM of each oligonucleotide and 4 units of *Pyrococcus furiosus* DNA ligase (Stratagene) in 1x reaction buffer as supplied by the manufacturer. The LCR reaction was cycled (denaturation and annealing/ligation) for 30 cycles of 94 °C for 30 sec and 76 °C for 40 sec after an initial denaturation period of 1 min at 94°C. Ten µl of the reaction mixture were loaded on an 0.7% agarose gel in TBE (44.5 mM Tris base, 44.5 mM boric acid, 1 mM EDTA in water), and the band corresponding to the synthetic gene was excised and washed twice in 500 µl sterile water for 5 min. Thereafter, the agarose was minced in a microcentrifuge tube with a small Teflon pestle. DNA was extracted from this slurry by adding an appropriate amount of 10 mM Tris-HCl pH 8.5 at 20°C followed by vortex mixing for one min. From this DNA solution, one µl was used as a template in a PCR reaction with appropriate primers to amplify the full-length synthetic gene (see Fig. 52). The nucleotide sequence of both synthetic genes is given in Appendix C.

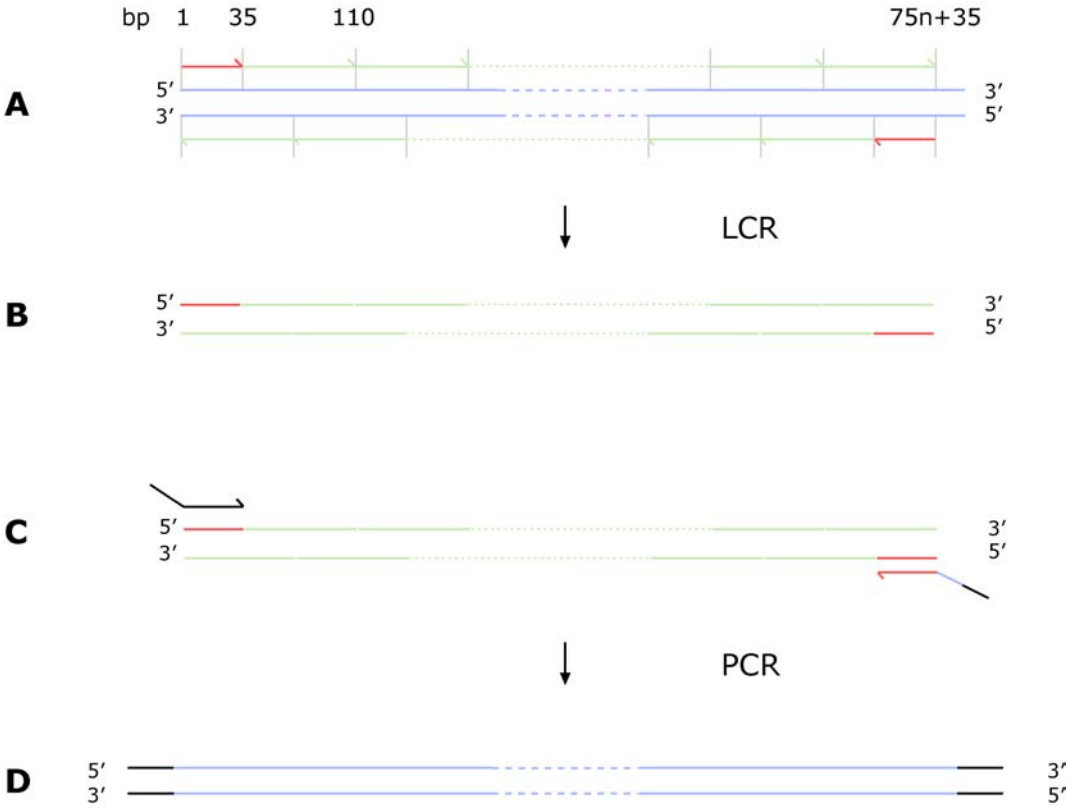

Fig. 52. Construction and synthesis of artificial genes by the Ligase Chain Reaction. Based on the DNA sequence to be synthesized (blue double strand in A), short oligonucleotides were designed for both strands as described in the text. From these primers, the dsDNA was synthesised during the LCR (B). After its separation from other products formed during the LCR by agarose gel electrophoresis, the synthetic gene was PCR amplified. The forward primer also introduces the necessary restriction endonuclease recognition sites for subsequent ligation of the PCR product (black arrow in C). The appropriately designed reverse primer not only introduces these sites at the gene's 3´-end but also the remaining bp (bp beyond 35+75n; blue and black part of the arrow symbolising the reverse primer in C, respectively). The resulting PCR product (D) is the desired synthetic gene that can be cloned into an expression vector as described in 7.2.3. through 7.2.7.

7.2.16. Construction of N- and C-terminal fragments of Car

Starting from the amino acid sequence of Car, the protein's secondary structure was computed using the program DNASIS (Hitachi). From these

calculations, the N- and C- terminal domains of Car were predicted and six different gene fragments coding for three N- and three C- terminal domains were constructed by PCR as described above.

7.2.17. Preparation of electrocompetent *E. coli* cells

From a frozen glycerol culture of the desired *E. coli* strain stored at -80°C a small amount of the frozen cell suspension was removed by a sterile platinum loop. The cells were streaked out on a SOC agar plate and the plate was incubated overnight at 37°C. At the following day, 50 ml LB broth was inoculated with a single bacterial colony and the flask was incubated overnight on a platform shaker at 37°C, 250 rpm. This starter cell culture was thereafter diluted 100-fold in LB broth, and the cells were further incubated on a platform shaker at 250 rpm, 37°C. Typically, one liter LB broth in a two liter Erlenmeyer flask was used to grow the bacteria, and the following quantities refer to one liter of cell culture. When the bacterial culture reached an OD_{595} of 0.8, the flask was removed from the shaker and cooled down to 0°C in an ice water bath. After 20 min, the bacteria were harvested by centrifugation in 450 ml centrifuge tubes at 4°C for 10 min at 2500xg_{max}. The cell pellet was washed with 450 ml ice cold water and the cells were recovered by centrifugation as described above. This washing step was repeated twice with first water followed by an ice cold solution of 10% glycerol. Thereafter, the cells were resuspended in 2.5 ml of ice cold 10% glycerol, divided into 50 µl aliquots, shock frozen in liquid nitrogen and stored for further use in microcentrifuge tubes at -80°C.

7.2.18. Transformation of *E. coli* cells

Electrocompetent *E. coli* cells were thawed on ice, and in all cases where DNA from plasmid preparations was to be transferred into the appropriate *E. coli* strain, 25 μl of electrocompetent *E. coli* cells were mixed with 100 nl of plasmid DNA solution obtained as described under 7.2.2. If plasmid DNA obtained in ligation reactions was to be transformed to *E. coli* cells, 2 μl ligation reaction was mixed with 50 μl electrocompetent *E. coli* cells. Then the DNA cell suspension was transferred to ice cold electroporation cuvettes (0.2 mm gap width) and the electroporation was performed using Biorad's Gene Pulser System (settings were 1.5 kV, 800 Ω, 25 μF). The transformed cells were resuspended in 1 ml LB broth, transferred to 10 ml plastic cell culture tubes, and incubated for phenotypical gene expression in a shaker at 37°C for 45 min. Thereafter, the bacteria were plated out (50 µl in all cases where plasmid DNA preparations were to be transformed, and 300 µl in all other cases) on SOC agar plates containing the appropriate antibiotic and the plates were left upside down in an incubator at 37°C overnight.

7.2.19. Primer design for PCR and sequencing reactions

Most primers to amplify DNA by PCR were designed as shown in Fig. 53 (for a complete list see Appendix B). Primers to be used in sequencing reactions were designed by OLIGO (Version 4.04, National Biosciences Inc.) with a primer length of 20 bp.

Fig. 53. PCR primer design. The DNA sequence to be amplified is depicted as red double strand. The part of the PCR primer complementary to the DNA strand was always 30 bp in length (red part of primer) followed by a restriction endonuclease recognition site (green) and 6 bp overhangs to allow restriction endonuclease binding (blue).

7.3. Protein chemical methods

7.3.1. Test for recombinant protein expression

An overnight *E. coli* cell culture in 50 ml LB broth was diluted 100-fold in a 5 liter Erlenmeyer flask with terrific broth containing the appropriate antibiotic. This expression culture was then incubated on a platform shaker at 24°C and 130 rpm until the cells reached an OD of 0.8 at 595 nm. Expression of protein was induced by the addition of IPTG (Gerbu) to a final concentration of 1 mM. After 2, 4 and 6 hours, a 1 ml aliquot was taken from the culture and the bacteria were collected by centrifugation in a microcentrifuge tube. The cells were lysed by the addition of 100 µl 2x SDS sample buffer. Total cell proteins were analyzed by SDS-PAGE and visualized as described under 7.3.5. A prominent protein band of the appropriate molecular weight indicated the expression of the desired protein. As a reference, a bacterial culture harboring an expression vector containing another gene was used. To determine whether the successfully expressed protein is soluble or not, the remaining cells of the expression culture were harvested by centrifugation, resuspended in buffer 0I (300

mM sodium chloride, 10 mM Tris-HCl pH 8.0 at 4°C), and lysed by sonication. Thereafter, the cytosol was clarified from insoluble material by centrifugation, and both the supernatant and the pellet were analyzed by SDS-PAGE for proteins as described above.

7.3.2. Isolation of inclusion bodies from *E. coli* cells

An appropriate amount of bacterial cells (usually 20 g) were resuspended in warm tab water and 30% LDAO in water was added to a final concentration of 0.6%. After 5 min at room temperature, lysozyme in buffer 0I (300 mM sodium chloride, 10 mM Tris-HCl pH 8.0 at 4°C) was added, and the cells were again left at room temperature for an additional 10 min. The cell suspension turned into a viscous paste that indicated cell lysis. Thereafter, chromosomal DNA was digested by adding DNaseI and the inclusion bodies were recovered by centrifugation at 10.000xg_{max} for 10 min. The pellet containing inclusion bodies and cellular debris was transferred to a Potter-Elvehjem homogeniser and resuspended with buffer 0I (300 mM sodium chloride, 10 mM Tris-HCl pH 8.0 at 4°C). Again, the inclusion bodies were collected by centrifugation at 10.000xg_{max} for 10 min and the homogenization/washing step was repeated twice with first buffer 0I supplemented with 20% glycerol followed by one washing step with water. The so obtained inclusion bodies were stored until further use at -32°C.

7.3.3. Heterologous expression of proteins in *E. coli*

Expression cultures in terrific broth were obtained as described under 7.3.1., and bacterial cells were grown at 24°C for 10 h. Thereafter,

protein expression was induced by the addition of IPTG (Gerbu) to a final concentration of 1 mM. In all cases where the proteins to be expressed were derived as inclusion bodies, expression was allowed to proceed for 6 to 8 h. In all other cases, bacterial cells were harvested 3 h after induction with IPTG by centrifugation and the recombinant protein was immediately purified from the cells.

7.3.4. Purification of overexpressed proteins from *E. coli*

All steps were carried out on ice or in a cold room at 4°C except purification steps involving buffers containing 8 M urea (room temperature). All equipment to purify proteins by fast performance liquid chromatography was from Amersham Pharmacia (Freiburg).

Purification of wild type and mutant *H. pylori* Che proteins CheV1, CheV2, CheV3, CheW, CheY and *E. coli* CheW and CheY. Inclusion bodies were purified from *E. coli* cells as described under 7.3.2. The inclusion bodies were solubilized in buffer FU (8 M urea, 10 mM Tris-HCl pH 8.0 at 20°C) and the solution was clarified by centrifugation at 75.000xg_{max} for 10 min. Thereafter, the supernatant was dialyzed overnight against buffer 0I (300 mM sodium chloride, 10 mM Tris-HCl pH 8.0 at 4°C) at 4°C. At the next day, precipitant was removed by centrifugation at 75.000xg_{max} for 10 min and the supernatant was applied to a Ni-NTA column (1.6x10 cm; Qiagen) equilibrated in buffer A. The column was washed with 20 column volumes of buffer A at a flow rate of 2 ml/min supplemented with 25 mM imidazole and developed with an imidazole gradient (1 ml/min) from 25 mM to 250 mM imidazole in buffer A. Eluent fractions were analyzed by SDS-PAGE for recombinant protein and fractions containing the protein of interest were pooled. To remove

the N-terminal His_6-tag when desired, thrombine protease (1 U/mg recombinant protein; Amersham Pharmacia Biotech) and calcium chloride (2.5 mM final concentration) were added and the solution was dialyzed overnight at 18°C against 5 liters of buffer A containing 2.5 mM calcium chloride. The dialyzed sample was again applied to a Ni-NTA column (usually 1.6x2 cm; Qiagen) to remove residual His_6-tagged proteins. In cases when necessary, bound protein was eluted from this column by a single step gradient of 5 mM imidazole in buffer A. Eluent fractions containing the protein were pooled, concentrated in a Centriprep K-10 device and applied at a flow rate of 0.43 ml/min to a HiLoad 26/60 Superdex 75 prep grade column (Amersham Pharmacia Biotech) which had been equilibrated in buffer A. The purified proteins were essentially pure (>95%) as judged from SDS-PAGE analysis.

Purification of CheF, CheF:H47G, CheF:D729K and CheF:K789R. The bacterial pellet was resuspended in buffer AG (buffer A supplemented with 20% (v/v) glycerol, 0.2 mM EDTA, 10 mM 2-mercaptoethanol and protease inhibitor cocktail for His_6-tagged proteins (Sigma) according to the manufacturers instructions) and cells were disrupted in a French pressure cell. After the addition of appropriate amounts of DNaseI, the solution was clarified by centrifugation and immediately applied to a Ni-NTA column (1.6x10 cm; Qiagen) equilibrated in buffer AG. The following purification steps followed the procedure described above except that Centriprep K 50 concentrators and a Sephacryl S300-HR column (2.6x95 cm) were used for concentration and size exclusion chromatography of recombinant CheF. All buffers were supplemented with 20% (v/v) glycerol. For the subsequent preparation of phosphorylated CheF the N-terminal His_6-tag was not removed.

Purification of full length and fragmented Car. After disruption of bacterial cells resuspended in buffer H (10 mM 2-mercaptoethanol, 2 mM EDTA, 20 mM Tris-HCl pH 8.0 at 4°C) containing 0.1 mM PMSF in a French press the cytosol was clarified as described above. Thereafter, the clear solution was incubated in a water bath at 52°C for 10 min, and precipitated *E. coli* proteins were removed by centrifugation. The resulting supernatant was again incubated in a water bath at 62°C for 10 min. Again, precipitated proteins were removed by centrifugation and the supernatant was applied at a flow rate of 1 ml/min to a DEAE cellulose column (2.6x10 cm; Whatman) equilibrated in buffer H. The column was washed with 20 column volumes of buffer H supplemented with 150 mM potassium chloride and developed with a linear potassium chloride gradient of 150 to 500 mM potassium chloride in buffer H. Eluent fractions were analyzed for protein by SDS-PAGE and fractions containing the desired protein were pooled and dialyzed overnight against buffer C (2.8 M potassium chloride, 10 mM 2-mercaptoethanol, 20 mM potassium phosphate pH 6.8 at 4°C). The dialyzed protein solution was then applied to a hydroxyapatite column (2.6x20 cm; BioRad) equilibrated in buffer C, the column washed with 5 column volumes of buffer C and subsequently developed with a linear potassium phosphate gradient to 500 mM in buffer C. Eluent fractions were again analyzed for protein by SDS-PAGE and fractions containing the desired protein were pooled and dialyzed overnight against buffer D (3 M potassium chloride, 2 mM EDTA, 1 mM 2-mercapto-ethanol, 20 mM potassium phosphate pH 8.0 at 4°C). Purified proteins were stored at 4°C.

Purification of Htr15. Htr15 inclusion bodies were purified from *E. coli* cells as described under 7.3.2. Htr15 inclusion bodies were solubilized in buffer FU (8 M urea, 10 mM Tris-HCl pH 8.0 at 20°C) and the solution was clarified by a centrifugation step of 75.000xg_{max} for 10 min. Protein was

dialyzed overnight against buffer H at 4°C. Precipitant was removed by centrifugation at 75.000xg_{max} for 10 min and the supernatant was applied to a DEAE-cellulose column as described above for Car. Eluent fractions were processed as described for Car, and Htr15 was further purified on a hydroxyapatite column. Eluent fractions were analyzed for protein by SDS-PAGE and fractions containing the desired protein were pooled and dialyzed overnight against buffer F (20 mM MES pH 6.0 at 4°C, 10 mM 2-mercaptoethanol, 2 mM EDTA). Thereafter, the protein was applied to a 10/10 HR MonoQ column (Amersham Pharmacia Biotech) previously equilibrated in buffer F. The column was washed with 5 column volumes of buffer F and subsequently developed with a linear potassium phosphate gradient to 400 mM in buffer F. Eluent fractions were again analyzed for protein by SDS-PAGE and fractions containing the desired protein were pooled and dialyzed overnight against buffer D (3 M potassium chloride, 2 mM EDTA, 1 mM 2-mercaptoethanol, 20 mM potassium phosphate pH 8.0 at 4°C). Purified protein was stored at 4°C.

Purification of wild type and chimeric FliM. Purification of FliM was as described by BREN & EISENBACH, 1998, with minor modifications. Subsequent steps were carried out at room temperature. FliM inclusion bodies were solubilized in buffer FU (8 M urea, 10 mM Tris-HCl pH 8.0 at 20°C) and the solution was clarified by a centrifugation step of 75.000xg_{max} for 10 min. The supernatant was applied to a Ni-NTA column (1.6x10 cm; Qiagen) previously equilibrated in buffer FU. The column was washed with 20 column volumes of buffer FU supplemented with 25 mM imidazole, the flow rate was adjusted to 2 ml/min and FliM bound to the resin was refolded by a linear gradient of buffer FU to buffer FG (1 M urea, 10% glycerol, 10 mM Tris-HCl pH 8.0 at 20°C) over a period of 60 min. The flow rate was adjusted to 1 ml/min and the column was developed

with a linear gradient of 25 to 400 mM imidazol in buffer FG. Eluent fractions were examined for protein by SDS-PAGE and fractions containing FliM were pooled and dialyzed overnight at 4°C against buffer FU.

Purification of MCP-like proteins Hp0599 and Cj0448. Initial purification of protein was as described above for the Che proteins. After the protein's His_6-tag was removed by digestion with thrombin, the protein was desalted on a HiPrep 26/60 desalting column (Amersham Pharmacia Biotech) equilibrated in buffer C (10 mM sodium chloride, 10 mM Tris-HCl pH 8.0 at 4°C) and applied to a MonoQ HR 10/10 column (Amersham Pharmacia Biotech) which had been equilibrated with the same buffer. The column was developed by a linear sodium chloride gradient from 10 to 200 mM in buffer C. The protein eluted between 50 and 100 mM sodium chloride and fractions containing the receptor were pooled, concentrated in a Centriprep K-30 device and applied to a HiLoad 26/60 Superdex 200 prep grade column (Amersham Pharmacia Biotech) which had been equilibrated in buffer A. The purified protein was stored on ice or was shock frozen in liquid nitrogen and stored at -80°C.

7.3.5. SDS-PAGE analysis of proteins

Complex protein mixtures or protein preparations were analyzed by SDS-PAGE following the method of LAEMMLI, 1970 as described by GALLAGHER, 1992. All minigels used throughout this work were composed of a 13% separating gel and a 7% stacking gel and were run at 130 V until the dye front reached the lower end of the gel. Size marker was Amersham Pharmacia's Low Molecular Weight Electrophoresis Calibration Kit and was used following the manufacturer's instructions. Proteins were either

visualized by Coomassie brilliant blue staining (7.3.6.), silver staining (7.3.7.) or were transferred to a PVDF membrane (Millipore) for immunodetection (7.3.8.).

7.3.6. Detection of proteins after SDS-PAGE by Coomassie brilliant blue

The polyacrylamide gel was submerged in staining solution (0.1% Coomassie brilliant blue in 10% glacial acetic acid, 20% methanol) and incubated after heating in a microwave oven on a platform shaker for 5 min. Thereafter, the gel was rinsed with destaining solution (10% glacial acetic acid, 20% methanol) followed by an incubation in destaining solution on a platform shaker for 5 min after heating in a microwave oven. The destaining solution was replaced by fresh destaining solution and again heated in a microwace oven. This destaining procedure was repeated until the gel was destained as desired and the blue protein bands were clearly visible against a light blue background.

7.3.7. Detection of proteins after SDS-PAGE by silver staining

The polyacrylamide gel was first incubated on a platform shaker in fixing solution 1 (10% glacial acetic acid, 30% methanol in water) for 15 min followed by one incubation in fixing solution 2 (5% glacial acetic acid, 10% ethanol in water) for 30 min and two subsequent incubations in fixing solution 3 (10% ethanol in water) for 15 min each. Thereafter, the gel was immersed in staining solution A (25 µl 37% formaldehyde, 21 µl 43% sodium thiosulfate in 50 ml water) for 60 s and was washed three

times with water. After incubation in staining solution B (25 µl 37% formaldehyde in 50 ml 0.2% silver nitrate) on the platform shaker for 6 min, the gel was again rinsed three times with water followed by an incubation in staining solution C (25 µl 37% formaldehyde, 5 µl 4.3% sodium thiosulfate in 50 ml 6% sodium carbonate) until the proteins appeared as visible bands of the desired intensity. The gel was immediately rinsed twice with water and then submerged in stop solution (3% glacial acetic acid, 5% glycerol in water).

7.3.8. Western transfer of proteins separated by SDS-PAGE to PVDF membrane

Protein samples were resolved by standard SDS-PAGE as described under 7.3.5. The gel was incubated in cathode buffer (25 mM Tris base, 40 mM glycine, 10% methanol; total buffer volume was 1 ml buffer per cm^2 of gel surface area) on a platform shaker for 15 min, whereas the membrane (Immobilon-P, Millipore) was first submerged in methanol for 15 sec followed by incubation in water for 2 min and incubation in anode buffer II (25 mM Tris base, 10% methanol) for 10 min. Thereafter, the transfer stack was assembled by placing two sheets of filter paper (Whatman 3MM) soaked in anode buffer I (0.3 M Tris base, 10% methanol) on top of the anode plate of the transfer system followed by one sheet of filter paper soaked in anode buffer II, the PVDF (Millipore) membrane, the gel and three filter papers soaked in cathode buffer. The transfer stack was covered by the cathode plate and protein transfer was initiated by applying an electrical current of 2.5 mA/cm^2 per cm^2 of gel surface area. After 30 min, the membrane was recovered from the transfer stack and rinsed carefully with water. If necessary, proteins transferred to the membrane were visualized by Ponceau S staining as follows: the

membrane was incubated in Ponceau S staining solution (0.4% Ponceau S in 6% trichloroacetic acid, 6% sulfosialic acid) on a platform shaker for 20 min. The membrane was destained in water until the protein bands became clearly visible against a pale rosy background. In all cases where proteins on the membrane were to be detected by immunological techniques, the membrane was destained completely in water and care was taken that the membrane did not get dry at any time.

7.3.9. Immunodetection of proteins immobilized on PVDF membanes

Subsequently, all quantities given refer to a membrane with no more than 100 cm^2 surface area. All incubation steps can either be performed at room temperature for one hour or overnight in a cold room at 4°C. All washing steps were performed with 50 ml of the appropriate solution at room temperature on a platform shaker for 10 min each. The membrane was blocked by incubation in 50 ml of 1x blocking solution (1% Western blocking reagent, Roche, in PBS). Thereafter, the membrane was incubated in 50 ml 0.5x blocking solution containing the first antibody in the desired dilution. The membrane was then washed twice with TPBS (0.05% Tween 20 in PBS) followed by two washing steps with 0.5x blocking solution. The alkaline phosphatase conjugated secondary antibody was diluted in 50 ml 0.5x blocking solution as recommended by the supplier's instructions and the membrane was incubated with the secondary antibody (alkaline phosphatase conjugated goat anti rabbit IgG, Jackson Immuno Research Inc.) solution. After four washing steps with TPBS, the secondary antibody was detected by incubating the membrane in NBT/BCIP solution (Sigma) at room temperature without agitating the membrane. The reaction was allowed to proceed until colored bands of

desired intensity were visible and stopped by washing the membrane with 20 mM EDTA.

7.3.10. Production of antisera against *H. pylori* chemotaxis proteins in rabbits

Antisera against CheF, CheV2, CheW, CheY and Hp0599 were raised in rabbits at the Institute's animal breeding facility. A solution of 400 µg/ml of the appropriate proteins in buffer 0I (300 mM sodium chloride, 10 mM Tris-HCl pH 8.0 at 4°C) was mixed with an equal amount of complete Freund's adjuvant to a stable emulsion. Two ml of this emulsion was injected subcutaneously in 500 µl portions into each animal. After 28 d, 1 ml of blood was taken from each rabbit. The blood was incubated at 37°C for 1 h followed by centrifugation for 10 min at 2000xg_{max}. Thereafter, the serum was carefully removed from the fluffy pellet by pipetting and the serum was stored in 100 µl aliquot parts at -80°C. At the same day, to each animal the antigen was applied again (400 µg protein per animal) in an emulsion of equal volumes of protein in buffer 0I (300 mM sodium chloride, 10 mM Tris-HCl pH 8.0 at 4°C) and incomplete Freund's adjuvant. Another 10 days later, 1 ml of blood was again taken from each animal, and serum was derived as described above. With these sera, it was attempted to detect the proteins that were used for animal immunizations on PVDF membranes as described under 7.3.9. Animals with sera positive to the desired epitopes were bled and serum was again obtained and stored as described above.

7.3.11. Protein concentration assay

Protein concentrations were determined following the method described by BRADFORD, 1976, using BioRad's Bradford reagent and BSA as standard. The concentration of solutions containing halophilic proteins was not determined since the BRADFORD method is not suited for highly acidic proteins.

7.4. Autophosphorylation and phosphotransfer reactions

7.4.1. Synthesis of [^{32}P] labeled dilithium acetyl phosphate

Acetyl phosphate was synthesized from acetic anhydride and orthophosphate as described by KORNBERG, 1956. Special care was taken to avoid exposure to radiation and spilling of radioactive chemicals. In short, 950 µl pyridine, 1.5 ml water and 500 µl 1 M K_2HPO_4 containing ^{32}P-labeled phosphate (typically 0.1 Ci orthophosphate) were mixed in a 30 ml Erlenmeyer flask, and the mixture was kept on ice on a magnetic stirrer. Acetic anhydride (110 µl) was added over a 3 min time period in 20 µl aliquots, and the mixture was stirred vigorously. Two minutes later, 4 M lithium hydroxide was added to adjust the pH to 7.5. Thereafter, chilled ethanol (23 ml, approx. -15°C) was added slowly to the reaction mixture. After one hour on ice, the precipitate was collected by centrifugation, washed twice with ice cold ethanol, and dried *in vacuo* over calcium chloride for 24 hours. The purity of the preparation was assayed by dissolving an appropriate amount of dried dilithium acetyl phosphate in water. The actual concentration of this solution was then assayed as described under 7.4.2. Typically, the concentration was as calculated from the weight of the synthesized substance and the preparation was

considered to be sufficiently pure and free of inorganic orthophosphate. The specific activity of the reaction product was usually 80 mCi/mmol at the day of synthesis as determined by liquid scintillation counting in a Tri-Carb 2100 TR Liquid Scintillation Analyzer (Packard) using rotiszint eco plus scintillation cocktail (Roth).

7.4.2. Acyl phosphate assay

Acetyl phosphate was assayed as described by LIPMANN & TUTTLE, 1945, for acyl phosphates. To determine the concentration of aqueous acetyl phosphate solutions, 2 ml test solution and 1 ml freshly prepared neutralized hydroxylamine reagent (mix of equal volumes 4 M hydroxylamine hydrochloride and 3.5 M sodium hydroxide) were added in a test tube and left at room temperature for 10 min. Thereafter, 3 ml ferric chloride reagent (prepared freshly by mixing equal volumes of 5% $FeCl_3$ in 0.1 M HCl and 12% trichloroacetic acid in 3 M HCl) was added and the OD of the solution at 540 nm was measured immediately. To determine the acetyl phosphate concentration in the test solution, a standard curve was calculated by measuring the OD at 540 nm of standard dilithium acetyl phosphate solutions prepared from commercially available non-radioactive dilithium acetyl phosphate. The assay is linear in an acetyl phosphate concentration range from 0.25 to 2.5 mM.

7.4.3. Preparation of phosphorylated CheF:D729K.

Purified CheF:D729K was incubated with 5 mM [γ^{32}P]-ATP (30 Ci/mmol), 5 mM magnesium chloride and 50 mM potassium phosphate buffer pH 7.5 at 30°C. After 30 min, the protein was applied to a HiTrap Chelating column

(Amersham Pharmacia Biotech) charged with Ni^{2+} and equilibrated in buffer A. The column was then washed with ten column volumes of buffer A followed by an equal amount of buffer C (50 mM potassium phosphate pH 7.5 at 20°C) and CheF:D729K-P_i was eluted with 150 mM imidazole in buffer C. Radioactive fractions were pooled and the specific activity of the protein preparation was determined by assaying the protein concentration (7.3.11.) and the activity of the sample in a liquid scintillation counter described under 7.3.6.

7.4.4. Phosphotransfer assay from phosphorylated CheF:D729K to response regulators

To assay the transfer of label from CheF:D729K phosphate, equal volumes of CheF:D729K phosphate in buffer P1 (50 mM potassium phosphate, 5 mM magnesium chloride) and response regulator in buffer P1 were thoroughly mixed in a microcentrifuge tube. Immediately and at the time points indicated, 20 µl samples were removed from the reaction mixture, mixed with an equal volume of 2x SDS-PAGE sample buffer (GALLAGHER, 1992) supplemented with 50 mM EDTA and samples were immediately shock frozen in liquid nitrogen. Thereafter, the protein samples were thawed and resolved by SDS-PAGE as described under 7.3.5. Transfer of label was either assayed by liquid scintillation counting of excised gel fragments (7.4.7.), or - after transfer of radiolabled proteins to PVDF membranes (7.3.8.) - by autoradiography (XAR-5, Kodak) or 'phosphoimaging' (7.4.8.).

7.4.5. Phosphotransfer assay from phosphorylated response regulator CheY:K106R to CheF:D729K

CheF:D729K was phosphorylated and allowed to bind to a 1 ml HiTrap Chelating column (Amersham Pharmacia Biotech) following the procedure described under 7.4.3. After washing the column with buffer C, 200 µl CheY:K106R (without His_6-tag) in buffer C were allowed to pass through the column at a flow rate of 1 ml/min. Eluent fractions of approximately 2 drops/microcentrifuge tubes were collected, assayed for radioactivity by a hand-held Beta-counter (Berthold LB 1210B) and immediately put on ice. From this CheY:K106R-P_i preparation, 20 µl were removed by pipetting, mixed with an equal volume of CheF:D729K (in 5 mM magnesium chloride, 300 mM sodium chloride, 50 mM potassium phosphate pH 7.5 at 20°C, 20% glycerol), incubated for 20 sec at room temperature. The reactions were quenched by the addition of an equal volume of 2x SDS-PAGE sample buffer (GALLAGHER, 1992) supplemented with 50 mM EDTA and samples were immediately shock frozen in liquid nitrogen. Thereafter, the protein samples were thawed and resolved by SDS-PAGE as described under 7.3.5. Transfer of label was assayed after the transfer of radiolabeled proteins to PVDF membranes (7.3.8.) by autoradiography (XAR-5, Kodak).

7.4.6. CheF autophosphorylation and transphosphorylation activities using [γ^{32}P]-ATP.

Proteins to be assayed were mixed in microcentrifuge tubes and 10x reaction buffer (50 mM magnesium chloride, 500 mM potassium phosphate pH 7.5 at 20°C) was added. After 5 min at 25°C, the reactions were initiated by the addition of [γ^{32}P]-ATP (5000 Ci/mmol) to a final

concentration of 200 µM. After 5 min, the reactions were terminated by the addition of an equal volume of 2x SDS-PAGE sample buffer (GALLAGHER, 1992) supplemented with 50 mM EDTA. Proteins were separated by SDS-PAGE (7.3.5), and radioactivity was quantitated as described under 7.4.4.

7.4.7. Response regulator autophosphorylation by acetyl phosphate.

Autophosphorylation of response regulator domain containing proteins was assayed following the method given above (7.4.5.) except that [^{32}P]-acetyl phosphate (80 mCi/mmol) in various concentrations was used as phosphodonor.

7.4.8. Quantitation of radiolabel on CheF after SDS-PAGE by liquid scintillation counting

After the protein mixture was separated by SDS-PAGE, the gel was recovered and protein bands corresponding to CheF were excised and transferred to microcentrifuge tubes containing 500 µl scintillation cocktail. The gel fragments were minced with a Teflon pestle and the slurry was transferred to scintillation tubes containing 10 ml scintillation cocktail. Radioactivity was quantified by liquid scintillation counting in a Tri-Carb 2100 TR Liquid Scintillation Analyzer (Packard) using rotiszint eco plus scintillation cocktail (Roth).

7.4.9. Quantitation of phosphotransfer reactions by 'phosphoimaging'

The protein mixture was separated by SDS-PAGE and proteins were subsequently transferred to a PVDF membrane as described under 7.3.8. The membranes were air dried at room temperature and exposed to a phosphoimager plate for 3 h. The plate was analyzed in a FujiFilm FLA-2000 phosphoimager using the AIDA 2.31 software package.

7.5. ATPase assay

The ATPase assays were conducted essentially as described by NINFA *et al.*, 1991. In short, proteins in buffer W (100 mM potassium phosphate pH 7.0 at 20°C) were mixed and 10x reaction buffer (1 mM dithiothreitol, 2 mM NADH, 50 mM magnesium chloride in 1M potassium phosphate pH 7.0 at 20°C), pyruvate kinase and lactate dehydrogenase (2 and 6 units, respectively; Sigma), NADH and phosphoenolpyruvate (0.2 and 1.0 mM final concentration, respectively; Sigma) were added. The volume was adjusted to 100 µl and the mixture was transferred to a disposable UVette UV-cuvette (1 cm path length; Eppendorf) thermostated to 30°C. Thereafter, the reaction was initiated by adding 2 µl ATP (150 mM), and NADH oxidation was monitored in a Perkin-Elmer Lambda 5 UV/VIS spectrophotometer. The rate of decay over a time period of 15-60 min was used to calculate ATP hydrolysis rates, using a value of 6220 $M^{-1}cm^{-1}$ for the extinction coefficient of NADH at 340 nm. In control experiments, expected decreases were rapidly generated by the addition of micromolar concentrations of ADP, indicating that the coupling reactions were not rate-limiting.

7.6. Circular dichroic measurements

CD spectroscopy was used to investigate the secondary structure content of proteins. Measurements were carried out in a Jobin Yvon Auto Dichrograph Mark IV CD spectrometer using a quartz cuvette (with thermostat; 0.1 mm optical path length, Hellma). Protein (250 µM) in buffer N (3 M potassium chloride, 25 mM Tris-HCl pH 8.0 at 4°C) was diluted in assay buffer to the desired concentration. For thermal stability assays, protein in the respective buffer was heated in the cuvette to the desired temperature and circular dichroism was measured every 10 sec at a constant wavelength of 222 nm over the time of the experiment. To assay different solute compositions in respect to their influence on secondary structure, protein in buffer K was diluted in the buffer to be assayed as described above, and CD spectra were recorded from 195 to 250 nm at 20°C.

7.7. ^{1}H-NMR spectroscopy with Car

Purified Car in buffer N (3 M potassium chloride, 25 mM Tris-HCl pH 8.0 at 4°C) was concentrated in a centrifuge at 4°C up to a protein concentration of 1 mM using centriprep K-30 devices. For ^{1}H-NMR measurements, 450 µl protein solution were mixed with 50 µl deuterium oxide and transferred to an NMR glass tube. NMR measurements were conducted by the Institute's NMR service group.

7.8. Protein crystallization

Crystallization of CheW. CheW was purified as described above (7.3.4.) to the step where the N-terminal His_6 tag was removed. After the second Ni-NTA column, the protein was dialyzed overnight against buffer 0I (300 mM sodium chloride, 10 mM Tris-HCl pH 8.0 at 4°C) containing 10% glycerol. The protein was concentrated in a centrifuge at 4°C using centriprep-10 devices to a final concentration of 500 µM. Thereafter, the protein solution was subjected to crystallization experiments using the hanging drop method as described in McPherson, 1999. Initial screening was performed at 18°C using Hampton Research's crystal screen kits I and II as well as the PEG/ion screen (Jancarik & Kim, 1991). After approximately 7 to 10 days, long hexagonal crystals grew in setups where 1.5 M lithium sulfate, 100 mM HEPES pH 7.5 was used as precipitant. From this initial condition, lithium sulfate concentration (1.0 to 1.8 M), buffer composition (Tris, potassium phosphate, 4-(2-hydroxyethyl)piperazine-1-ethanesulfonic acid, N-(2-acetamido)iminodiacetic acid, MES and dimethylarsinic acid) and pH (6.5 to 10.5) in steps of 0.25 pH unit, temperature (18°C and 4°C), protein concentrations and the precipitant to protein volume ratio in the drops were varied to improve conditions for crystal growth. To further increase crystal quality, Hampton Research's additive screen kits I, II and III were used to test the influence of small molecules on crystal growth.

Crystallization trial for halophilic proteins using the MPD-NaCl-water system. Crystallization trials for Car were essentially as described in Richard, 1995 using the hanging drop method with drops of a total volume of 7 µl. MPD was mixed on siliconized glass cover slides with 2, 3, 4 or 5 µl purified protein in buffer G (4 M sodium chloride, 100 mM Tris pH

8.0 at 20°C), and the drops were equilibrated at 18°C against a reservoir solution of buffer G containing MPD in the concentration range of 55 to 65% in steps of 2.5%. To assess pH influences, two different buffers (100 mM MES pH 5.3 at 20°C and 100 mM ADA pH 6.5 at 20°C) instead of buffer G were used in additional crystallization trials. Buffer G without protein served as a negative control in equivalent setups for protein crystal growth.

Crystallization trials for halophilic proteins using phosphate as precipitant by the hanging drop technique. Sodium potassium phosphate buffer at a concentration of 4 M in a pH range of 5.0 to 9.0 in steps of 0.5 pH units was used to assay the ability of phosphate salts to precipitate halophilic proteins. The protein (2 µl) in buffer G was mixed on siliconized glass cover slides with either an equal volume or with twice the volume of sodium potassium phosphate buffer and the cover slides were incubated upside down over sodium potassium phosphate buffer solutions in Q-plates (Hampton Research) at 18°C. Buffer G without protein served as a negative control in equivalent setups for protein crystal growth.

Crystallization trials for halophilic proteins using phosphate as precipitant by the microdialysis technique. Protein in buffer G was transferred to 10 µl microdialysis buttons, the buttons were sealed with a 10 kD cut-off dialysis membrane and submerged in 4 M potassium phosphate buffer in a pH range from 7.0 to 8.5 in steps of 0.5 pH units.

Crystallization of Hp0599 and Cj0448. Both proteins were crystallized and crystal quality was improved following the strategy outlined above for CheW.

8. References

Adler J. (1966) Chemotaxis in Bacteria. *Science* **153,** 708-716.

Aizawa S. I., Harwood C. S. & Kadner R. J. (2000) Signaling components in bacterial locomotion and sensory reception. *J. Bacteriol.* **182,** 1459-1471.

Alexandre G. & Zhulin I. B. (2001) More than one way to sense chemicals. *J. Bacteriol.* **183,** 4681-4686.

Alley M. R. (2001) The highly conserved domain of the *Caulobacter* McpA chemoreceptor is required for its polar localization. *Mol. Microbiol.* **40,** 1335-1343.

Alm R.A., Ling L.S., Moir D.T., King B.L., Brown E.D., Doig P.C., Smith D.R., Noonan B., Guild B.C., deJonge B.L., Carmel G., Tummino P.J., Caruso A., Uria-Nickelsen M., Mills D.M., Ives C., Gibson R., Merberg D., Mills S.D., Jiang Q., Taylor D.E., Vovis G.F., Trust T.J. (1999) Genomic-sequence comparison of two unrelated isolates of the human gastric pathogen *Helicobacter pylori*. *Nature* **397,** 176-80.

Arakawa T. & Timasheff S. N. (1982) Stabilization of protein structure by sugars. *Biochemistry* **21,** 6536-6544.

Armitage J. P. & Schmitt R. (1997) Bacterial chemotaxis: *Rhodobacter sphaeroides* and *Sinorhizobium meliloti* - variations on a theme? *Microbiology* **143,** 3671-3682.

Baracchini O. & Sherris J. C. (1959) The chemotactic effect of oxygen on bacteria. *J. Pathol. Bacteriol.* **77,** 565.

Barak R. & Eisenbach M. (1992) Correlation between phosphorylation of the chemotaxis protein CheY and its activity at the flagellar motor. *Biochemistry* **31,** 1821-1826.

Barnett M. J., Fisher R. F., Jones T., Komp C., Abola A. P., Barloy-Hubler F., Bowser L., Capela D., Galibert F., Gouzy J., Gurjal M., Hong A., Huizar L., Hyman R. W., Kahn D., Kahn M. L., Kalman S., Keating D. H., Palm C., Peck M. C., Surzycki R., Wells D. H., Yeh K. C., Davis R. W., Federspiel N. A. & Long S. R. (2001) Nucleotide sequence and predicted functions of the entire *Sinorhizobium meliloti* pSymA megaplasmid. *Proc. Natl. Acad. Sci. U.S.A.* **98,** 9883-8.

Beier D. & Frank R. (2000) Molecular characterization of two-component systems of *Helicobacter pylori*. *J. Bacteriol.* **182,** 2068-2076.

Bennett S. (1993) Development of the PID controller. *IEEE Control Sys.* **13,** 58-62.

Berendes A. (1998) Studien zur Struktur und Funktion der Basalplatte des Flagellenmotors von *Wolinella succinogenes*. Dissertation, Fakultät für Chemie, Biologie und Geowissenschaften, Technische Universität München.

Berg H. C. (2000) Constraints on models for the flagellar rotary motor. *Phil. Trans. R. Soc. Lond. B* **355,** 491-501.

Bhalla U. S. & Iyengar R. (1999) Emergent properties of networks of biological signaling pathways. *Science* **283,** 381-387.

Bibikov S. I., Brian R., Rudd K. E. & Parkinson J. S. (1997) A signal transducer for aerotaxis in *Escherichia coli*. *J. Bacteriol.* **179,** 4075-4079.

Bilwes A. M., Alex L. A., Crane B. R. & Simon M. I. (1999) Structure of CheA, a signal-transducing histidine kinase. *Cell* **96,** 131-141.

Bjorkholm B. M., Oh J. D., Falk P. G., Engstrand L. G. & Gordon J. I. (2001) Genomics and proteomics converge on *Helicobacter pylori*. *Curr. Opin. Microbiol.* **4,** 237-245.

Boos W. & Shuman H. (1998) Maltose/maltodextrin system of *Escherichia coli*: transport metabolism and regulation. *Microbiol. Mol. Biol. Rev.* **62,** 204-229.

Bornhorst J. A. & Falke J. J. (2000) Attractant regulation of the aspartate receptor-kinase complex: limited cooperative interactions between receptors and effects of the receptor modification state. *Biochemistry* **39,** 9486-9493.

Bourret R. B., Charon N. W., Stock A. M. & Wets A. H. (2002) Bright lights, abundant operons - Fluorescence and genomic technologies advance studies of bacterial locomotion and signal transduction: review of the BLAST meeting, Cuernavaca, Mexico, 14 to 19 January 2001. *J. Bacteriol.* **184,** 1-17.

Bradford M. M. (1976) A rapid and sensitive method for the quantitation of microgram quantities of protein utilizing the principle of protein-dye binding. *Anal. Biochem.* **72,** 248-254.

Bray D., Levin M. D. & Morton-Firth C. J. (1998) Receptor clustering as a cellular mechanism to control sensitivity. *Nature* **393,** 85-88.

Bren A. & Eisenbach M. (1998) The N terminus of the flagellar switch protein FliM is the binding domain for the chemotactic response regulator CheY. *J. Mol. Biol.* **278,** 507-514.

Bren A. & Eisenbach M. (2000) How signals are heard during bacterial chemotaxis: protein-protein interactions in sensory signal propagation. *J. Bacteriol.* **182,** 6865-6873.

Bren A., Welch M., Blat Y. & Eisenbach M. (1996) Signal termination in bacterial chemotaxis: CheZ mediates dephosphorylation of free rather than switch-bound CheY. *Proc. Natl. Acad. Sci. U.S.A.* **93,** 10090-10093.

Brooun A., Zhang W. & Alam M. (1997) Primary structure and functional analysis of the soluble transducer protein HtrXI in the archaeon *Halobacterium salinarium*. *J. Bacteriol.* **179,** 2963-2968.

Bullock W. O., Fernandez J. M. & Short J. M. (1987) XL1 blue - A high-efficiently plasmid transformigf recA$^-$ *Escherichia coli* strain with β-galactosidase selection. *Biotechniques* **5,** 376.

Capela D., Barloy-Hubler F., Gouzy J., Bothe G., Ampe F., Batut J., Boistard P., Becker A., Boutry M., Cadieu E., Dreano S., Gloux S., Godrie T., Goffeau A., Kahn D., Kiss E., Lelaure V., Masuy D., Pohl T., Portetelle D., Puhler A., Purnelle B., Ramsperger U., Renard C., Thebault P., Vandenbol M., Weidner S. & Galibert F. (2001) Analysis of the chromosome sequence of the legume symbiont *Sinorhizobium meliloti* strain 1021. *Proc. Natl. Acad. Sci. U.S.A.* **98,** 9877-9882.

Cluzel P., Surette M. & Leibler S. (2000) An ultrasensitive bacterial motor revealed by monitoring signaling proteins in single cells. *Science* **287,** 1652-1655.

Connaris H., Chaudhuri J. B., Danson M. J. & Hough D. W. (1999) Expression, reactivation and purification of enzymes *from Haloferax volcanii* in *Escherichia coli*. *Biotech. Bioeng.* **64,** 38-45.

Covacci A., Telford J. L., Del Giudice G., Parsonnet J. & Rappuoli R. (1999) *Helicobacter pylori* virulence and genetic geography. *Science* **284,** 1328-1333.

Danson M. J. & Hough D. W. (1997) The structural basis of protein halophilicity. *Comp. Biochem. Physiol.* **117A,** 307-312.

Doig P., de Jonge B. L., Alm R. A., Brown E. D., Uria-Nickelsen M., Noonan B., Mills S. D., Tummino P., Carmel G., Guild B. C., Moir D. T., Vovis G. F. & Trust T. J. (1999) *Helicobacter pylori* physiology predicted from genomic comparison of two strains. *Microbiol. Mol. Biol. Rev.* **63,** 675-707.

Donati M. (1586) *De Medica Historia Mirabili*. Mantua.

Duke T. A. & Bray D. (1999) Heightened sensitivity of a lattice of membrane receptors. *Proc. Natl. Acad. Sci. U.S.A.* **96,** 10104-10108.

Engelmann T. W. (1882) Zur Biologie der Schizomyceten. *Botanische Zeitung* **40,** 322.

Engelmann T. W. (1894) Die Erscheinungsweise der Sauerstoffausscheidung chlorophyllhaltiger Zellen im Licht bei Anwendung der Bacterienmethode. *Arch. Physiol.* **57,** 375.

Falk P. G., Hooper L. V., Midtvedt T. & Gordon J. I. (1998) Creating and maintaining the gastrointestinal ecosystem: what we know and need to know from gnotobiology. *Microbiol. Mol. Biol. Rev.* **62,** 1157-1170

Falke J. J., Bass R. B., Butler S. L., Chervitz S. A. & Danielson M. A. (1997) The two-component signaling pathway of bacterial chemotaxis: a molecular view of signal transduction by receptors kinases and adaptation enzymes. *Annu. Rev. Cell Dev. Biol.* **13,** 457-512.

Fasman G.D. (Ed.) Circular dichroism and the conformational analysis og biomolecules. Plenum press, New York, 1996.

Ferrando-May E., Brustmann B. & Oesterhelt D. (1993) A C-terminal truncation results in high-level expression of the functional photoreceptor sensory rhodopsin I in the archaeon *Halobacterium salinarium*. *Mol. Microbiol.* **9,** 943-953.

Finan T. M., Weidner S., Wong K., Buhrmester J., Chain P., Vorholter F. J., Hernandez-Lucas I., Becker A., Cowie A., Gouzy J., Golding B. & Puhler A. (2001) The complete sequence of the 1,683-kb pSymB megaplasmid from the N2-fixing endosymbiont *Sinorhizobium meliloti*. *Proc. Natl. Acad. Sci. U.S.A.* **98,** 9889-9894.

Forman D., Newell D. G., Fullerton F., Yarnell J. W., Stacey A. R., Wald N., & Sitas F. (1991) Association between infection with *Helicobacter pylori* and risk of gastric cancer: evidence from a prospective investigation. *Br. Med. J.* **302,** 1302-1305

Foster D. L., Mowbray S. L., Jap B. K. & Koshland D. E., Jr. (1985) Purification and characterization of the aspartate chemoreceptor. *J. Biol. Chem.* **260,** 11706-11710.

Foussard M., Cabantous S., Pedelacq J., Guillet V., Tranier S., Mourey L., Birck C. & Samama J. (2001) The molecular puzzle of two-component signaling cascades. *Microbes & Infection* **3,** 417-24.

Foynes S., Dorrell N., Ward S. J., Stabler R. A., McColm A. A., Rycroft A. N. & Wren B. W. (2000) *Helicobacter pylori* possesses two CheY response regulators and a histidine kinase sensor CheA which are essential for chemotaxis and colonization of the gastric mucosa. *Infection & Immunity* **68,** 2016-2023.

Frank H. S. (1958) Covalency in the hydrogen bond and the properties of water and ice. *Proc. R. Soc. (London) Series A* **247,** 481-492.

Frank H. S. & Wen W. Y. (1957) Structural aspects of ion-solvent interactions in aqueous solutions - a suggested picture of water structure. *Discuss. Faraday Soc.* **24,** 133-140.

Fraser C. M., Casjens S., Huang W. M., Sutton G. G., Clayton R., Lathigra R., White O., Ketchum K. A., Dodson R., Hickey E. K., Gwinn M., Dougherty B., Tomb J. F., Fleischmann R. D., Richardson D., Peterson J., Kerlavage A. R., Quackenbush J., Salzberg S., Hanson M., van Vugt R., Palmer N., Adams M. D., Gocayne J. & Venter J. C. (1997) Genomic sequence of a Lyme disease spirochaete *Borrelia burgdorferi*. *Nature* **390,** 580-586.

Fredrick K. L. & Helmann J. D. (1994) Dual chemotaxis signaling pathways in *Bacillus subtilis*: a sigma D-dependent gene encodes a novel protein with both CheW and CheY homologous domains. *J. Bacteriol.* **176,** 2727-2735.

Galibert F., Finan T. M., Long S. R., Puhler A., Abola P., Ampe F., Barloy-Hubler F., Barnett M. J., Becker A., Boistard P., Bothe G., Boutry M., Bowser L., Buhrmester J., Cadieu E., Capela D., Chain P., Cowie A., Davis R. W., Dreano S., Federspiel N. A., Fisher R. F., Gloux S., Godrie T., Goffeau A., Golding B., Gouzy J., Gurjal M., Hernandez-Lucas I., Hong A., Huizar L., Hyman R. W., Jones T., Kahn D., Kahn M. L., Kalman S., Keating D. H., Kiss E., Komp C., Lelaure V., Masuy D., Palm C., Peck M. C., Pohl T. M., Portetelle D., Purnelle B., Ramsperger U., Surzycki R., Thebault P., Vandenbol M., Vorholter F. J., Weidner S., Wells D. H., Wong K., Yeh K. C. & Batut J. (2001) The composite genome of the legume symbiont *Sinorhizobium meliloti*. *Science* **293,** 668-672.

Gallagher S. R. (1992) Current protocols in Molecular Biology, John Wiley and Sons, New York.

Galperin M. Y., Nikolskaya A. N. & Koonin E. V. (2001) Novel domains of the prokaryotic two-component signal transduction systems. *FEMS Microbiol. Lett.* **203,** 11-21.

Gegner J. A., Graham D. R., Roth A. F. & Dahlquist F. W. (1992) Assembly of an MCP receptor CheW and kinase CheA complex in the bacterial chemotaxis signal transduction pathway. *Cell* **70,** 975-982.

Gekko K. & Timasheff S. N. (1981) Thermodynamic and kinetic examination of protein stabilization by glycerol. *Biochemistry* **20,** 4677-4686.

Gestwicki J. E., Lamanna A. C., Harshey R. M., McCarter L. L., Kiessling L. L. & Adler J. (2000) Evolutionary conservation of methyl-accepting chemotaxis protein location in *Bacteria* and *Archaea*. *J. Bacteriol.* **182,** 6499-6502.

Graham D. Y., Lew G. M., Klein P. D., Evans D. G., Evans, D. J. J., Saeed Z.A. & Malaty H.M. (1992) Effect of treatment of *Helicobacter pylori* on the long-term recurrence of gastric or duodenal ulcer. A randomized, controlled study. *Ann. Intern. Med.* **116,** 705-708

Gribenko A., Lopez M. M., Richardson J. M., 3rd & Makhatadze G. I. (1998) Cloning overexpression purification and spectroscopic characterization of human S100P. *Protein Science* **7,** 211-215.

Halkides C. J., McEvoy M. M., Casper E., Matsumura P., Volz K. & Dahlquist F. W. (2000) The 1.9 Å resolution crystal structure of phosphono-CheY, an analogue of the active form of the response regulator, CheY. *Biochemistry* **39,** 5280-5286.

Halkides C. J., Zhu X., Phillion D. P., Matsumura P. & Dahlquist F. W. (1998) Synthesis and biochemical characterization of an analogue of CheY-phosphate, a signal transduction protein in bacterial chemotaxis. *Biochemistry* **37,** 13674-13680

Haupts U., Tittor J. & Oesterhelt D. (1999) Closing in on bacteriorhodopsin: progress in understanding the molecule. Ann. Rev. Biophys. Biomol. Struct. **28:**367-399.

Hayashi N., Matsubara M., Takasaki A., Titani K. & Taniguchi H. (1998) An expression system of rat calmodulin using T7 phage promoter in *Escherichia coli*. *Protein Expression & Purification* **12,** 25-28.

Hazelbauer G.L. (1992) Bacterial chemoreceptors. *Curr. Opin. Struct. Biol.* **2,** 505-510.

Hecht K. & Jaenicke R. (1989) Malate dehydrogenase from the extreme halophilic archaebacterium *Halobacterium marismortui*. Reconstitution of the enzyme after denaturation and dissociation in various denaturants. *Biochemistry* **28,** 4979-4985.

Heidelberg J. F., Eisen J. A., Nelson W. C., Clayton R. A., Gwinn M. L., Dodson R. J., Haft D. H., Hickey E. K., Peterson J. D., Umayam L., Gill S. R., Nelson K. E., Read T. D., Tettelin H., Richardson D., Ermolaeva M. D., Vamathevan J., Bass S., Qin H., Dragoi I., Sellers P., McDonald L., Utterback T., Fleishmann R. D., Nierman W. C. & White O. (2000) DNA sequence of both chromosomes of the cholera pathogen *Vibrio cholerae*. *Nature* **406,** 477-483.

Hess J. F., Bourret R. B. & Simon M. I. (1991) Phosphorylation assays for proteins of the two-component regulatory system controlling chemotaxis in *Escherichia coli*. *Methods in Enzymology* **200,** 188-204.

Hess J. F., Oosawa K., Kaplan N. & Simon M. I. (1988) Phosphorylation of three proteins in the chemotaxis signaling pathway of bacterial chemotaxis. *Cell* **53,** 79-87.

Hess J. F., Oosawa K., Matsumura P. & Simon M. I. (1987) Protein phosphorylation is involved in bacterial chemotaxis. *Proc. Natl. Acad. Sci. U.S.A.* **84,** 7609-7613.

Hou S., Larsen R. W., Boudko D., Riley C. W., Karatan E., Zimmer M., Ordal G. W. & Alam M. (2000) Myoglobin-like aerotaxis transducers in *Archaea* and *Bacteria*. *Nature* **403,** 540-544.

Isidori A. & Byrnes C. I. (1990) Output regulation of nonlinear systems. *IEEE Transactions on Automatic Control* **35,** 131-140.

Jancarik J. & Kim S.-H. (1991) Sparse matrix sampling: a screening method for crystallization of proteins. *Journal of Applied Crystallography* **24,** 409-411.

Jasuja R., Lin Y., Trentham D. R. & Khan S. (1999) Response tuning in bacterial chemotaxis. *Proc. Natl. Acad. Sci. U.S.A.* **96,** 11346-11351.

Josenhans C., Labigne A. & Suerbaum S. (1995) Comparative ultrastructural and functional studies of *Helicobacter pylori* and *Helicobacter mustelae* flagellin mutants: both flagellin subunits FlaA and FlaB are necessary for full motility in *Helicobacter* species. *J. Bacteriol.* **177,** 3010-3020.

Karatan E., Saulmon M. M., Bunn M. W. & Ordal G. W. (2001) Phosphorylation of the response regulator CheV is required for adaptation to attractants during *Bacillus subtilis* chemotaxis. *J. Biol. Chem*. **276,** 43618-43626.

Karlin S. & Mrazek J. (2000) Predicted highly expressed genes of diverse prokaryotic genomes. *J. Bacteriol.* **182,** 5238-5250.

Kelly D.J. (1998) The physiology and metabolism of the human gastric pathogen *Helicobacter pylori*. *Adv. Microb. Physiol.* **40,** 137-189.

Kim C., Jackson M., Lux R. & Khan S. (2001) Determinants of chemotactic signal amplification in *Escherichia coli*. *J. Mol. Biol.* **307,** 119-135.

Kim K. K, Yokota H. & Kim S. H. (1999) Four-helical-bundle structure of the cytoplasmic domain of a serine chemotaxis receptor. *Nature* **400,** 787-792.

Kim S. H. (1994) 'Frozen' dynamic dimer model for transmembrane signaling in bacterial chemotaxis receptors. *Protein Science* **3,** 159-165.

Kimura Y., Nakano H., Terasaka H. & Takegawa K. (2001) *Myxococcus xanthus* mokA encodes a histidine kinase-response regulator hybrid sensor required for development and osmotic tolerance. *J. Bacteriol.* **183,** 1140-1146.

Kirby J. R., Kristlich C. J., Saulmon M. M., Zimmer M. A., Garrity L. F., Zhulin I. B. & Ordal G. W. (2001) CheC is related to the family of flagellar proteins and acts independently from CheD to control chemotaxis in *Bacillus subtilis*. *Mol. Microbiol.* **42,** 572-585.

Kornberg A., Kornberg S. A. & Simms E. S. (1956) Metaphosphate synthesis by an enzyme from *Escherichia coli*. *Biochimica and Biophysica Acta* **20,** 215-227.

Kumar R., Hunziker W., Gross M., Naylor S., Londowski J. M. & Schaefer J. (1994) The highly efficient production of full-length and mutant rat brain calcium-binding proteins (calbindins-D28K) in a bacterial expression system. *Arch. Biochem. Biophys.* **308,** 311-317.

Kushner D. J. (1988) What is the 'true' internal environment of halophilic and other bacteria. *Can. J. Microbiol.* **34,** 482-486.

Kyte J. & Doolittle R. F. (1982) A simple model for displaying the hydropathic character of a protein. *J. Mol. Biol.* **157,** 105-132.

Laemmli U. K. (1970) Cleavage of structural proteins during the assembly of the head of bacteriophage T4. *Nature* **227,** 680-685.

Lakshmikanth G. S., Sridevi K., Krishnamoorthy G., Udgaonkar J. B. (2001) Structure is lost incrementally during the unfolding of barstar*. Nat. Struct. Biol.* **8,** 799-804.

Landegren U., Kaiser R., Sanders J. & Hood L. (1988) A ligase-mediated gene detection technique. *Science* **241,** 1077-1080.

Lee A. (1996) The nature of *Helicobacter pylori*. *Scand. J. Gastroenterol. - Suppl.* **214,** 5-8; discussion 9-12.

Lee B. C., Croonquist P. A., Sosnick T. R. & Hoff W. D. (2001) PAS domain receptor photoactive yellow protein is converted to a molten globule state upon activation. *J. Biol. Chem.* **276,** 20821-20823.

Lee S. Y., Cho H. S., Pelton J. G., Yan D., Henderson R. K., King D. S., Huang L., Kustu S., Berry E. A. & Wemmer D.E. (2001) Crystal structure of an activated response regulator bound to its target. *Nat. Struct. Biol.* **8,** 52-56.

Le Moual H. & Koshland D. E. Jr. (1996) Molecular evolution of the C-terminal cytoplasmic domain of a superfamily of bacterial receptors involved in taxis. *J. Mol. Biol.* **261,** 568-585.

Letunic I., Goodstadt L., Dickens N. J., Doerks T., Schultz J., Mott R., Ciccarelli F., Copley R. R., Ponting C. P. & Bork P. (2002) Recent improvements to the SMART domain-based sequence annotation resource. *Nucleic Acids Res.* **30,** 242-4.

Levit M. N., Liu Y. & Stock J. B. (1998) Stimulus response coupling in bacterial chemotaxis: receptor dimers in signalling arrays. *Mol. Microbiol.* **30,** 459-466.

Lipmann F. & Tuttle L. C. (1945) A specific micromethod for the determination of acyl phosphates. *J. Biol. Chem.* **159,** 21-28.

Lukat G. S., McCleary W. R., Stock A. M. & Stock J. B. (1992) Phosphorylation of bacterial response regulator proteins by low molecular weight phospho-donors. *Proc. Natl. Acad. Sci. U.S.A.* **89,** 718-722.

Luo Y, Baldwin RL. (1999) The 28-111 disulfide bond constrains the alpha-lactalbumin molten globule and weakens its cooperativity of folding. *Pro.c Natl. Acad. Sci. U.S.A.* **96,** 11283-11287.

Lybarger S. R. & Maddock J. R. (2000) Differences in the polar clustering of the high- and low-abundance chemoreceptors of *Escherichia coli*. *Proc. Natl. Acad. Sci. U.S.A.* **97,** 8057-8062.

Lybarger S. R. & Maddock J. R. (2001) Polarity in action: asymmetric protein localization in bacteria. *J. Bacteriol.* **183,** 3261-3267.

Madern D. & Zaccai G. (1997) Stabilisation of halophilic malate dehydrogenase from *Haloarcula marismortui* by divalent cations. Effects of temperature, water isotope, cofactor and pH. *Eur. J. Biochem.* **249,** 607-611.

Marg B. et al. (2002) In preparation.

Martin A. C., Wadhams G. H. & Armitage J. P. (2001) The roles of the multiple CheW and CheA homologues in chemotaxis and in chemoreceptor localization in *Rhodobacter sphaeroides*. *Mol. Microbiol.* **40,** 1261-1272.

Marwan W., Bibikov S. I., Montrone M. & Oesterhelt D. (1995) Mechanism of photosensory adaptation in *Halobacterium salinarium*. *J. Mol. Biol.* **246,** 493-499.

Mayover T. L., Halkides C. J. & Stewart R. C. (1999) Kinetic characterization of CheY phosphorylation reactions: comparison of P-CheA and small-molecule phosphodonors. *Biochemistry* **38,** 2259-2271.

McCleary W. R. & Zusman D. R. (1990) FrzE of *Myxococcus xanthus* is homologous to both CheA and CheY of *Salmonella typhimurium*. *Proc. Nat. Acad. Sci. U.S.A.* **87,** 5898-5902.

McDonell M. W., Simon M. N. & Studier F. W. (1977) Analysis of restriction fragments of T7 DNA and determination of molecular weights by electrophoresis in neutral and alkaline gels. *J. Mol. Biol.* **110,** 119-146.

McPherson A. (1999) The mechanisms and kinetics of macromolecular crystal growth, Cold Spring Harbor Laboratory Press Cold Spring Harbor.

Mizote T., Yoshiyama H. & Nakazawa T. (1997) Urease-independent chemotactic responses of *Helicobacter pylori* to urea, urease inhibitors, and sodium bicarbonate. *Infect. Immun.* **65,** 1519-1521.

Montecucco C. & Rappuoli R. (2001) Living dangerously: how *Helicobacter pylori* survives in the human stomach. *Nat. Rev. Mol. Cell Biol.* **2,** 457-466.

Némethy G. & Scheraga H. A. (1964) Structure of water and hydrophobic bonding in proteins. IV. The thermodynamic properties of liquid deuterium oxide. *J. Chem. Phys.* **41,** 680-689.

Ng W. V., Kennedy S. P., Mahairas G. G., Berquist B., Pan M., Shukla H. D., Lasky S. R., Baliga N. S., Thorsson V., Sbrogna J., Swartzell S., Weir D., Hall J., Dahl T. A., Welti R., Goo Y. A., Leithauser B., Keller K., Cruz R., Danson M. J., Hough D. W., Maddocks D. G., Jablonski P. E., Krebs M. P., Angevine C. M., Dale H., Isenbarger T. A., Peck R. F., Pohlschroder M., Spudich J. L., Jung K. W., Alam M., Freitas T., Hou S., Daniels C. J., Dennis P. P., Omer A. D., Ebhardt H., Lowe T. M.,

Liang P., Riley M., Hood L. & DasSarma S. (2000) Genome sequence of *Halobacterium* species NRC-1. *Proc. Natl. Acad. Sci. U.S.A.* **97,** 12176-12181.

Nierman W. C., Feldblyum T. V., Laub M. T., Paulsen I. T., Nelson K. E., Eisen J., Heidelberg J. F., Alley M. R., Ohta N., Maddock J. R., Potocka I., Nelson W. C., Newton A., Stephens C., Phadke N. D., Ely B., DeBoy R. T., Dodson R. J., Durkin A. S., Gwinn M. L., Haft D. H., Kolonay J. F., Smit J., Craven M. B., Khouri H., Shetty J., Berry K., Utterback T., Tran K., Wolf A., Vamathevan J., Ermolaeva M., White O., Salzberg S. L., Venter J. C., Shapiro L. & Fraser C. M. (2001) Complete genome sequence of *Caulobacter crescentus*. *Proc. Natl. Acad. Sci. U.S.A.* **98,** 4136-4141.

Ninfa E. G., Stock A., Mowbray S. & Stock J. (1991) Reconstitution of the bacterial chemotaxis signal transduction system from purified components. *J. Biol. Chem.* **266,** 9764-9770.

Nomura A., Stemmermann G. N., Chyou P. H., Kato I., Perez P. G. & Blaser M. J. (1991) *Helicobacter pylori* infection and gastric carcinoma among Japanese Americans in Hawaii. *N. Engl. J. Med.* **32,** 1132-1136

Oren A. (1994) The ecology of the extremely halophilic archaea. *FEMS Microbiol. Rev.* **13,** 415-439.

Ota H. & Katsuyama T. (1992) Alternating laminated array of two types of mucin in the human gastric surface mucous layer. *Histochem. J.* **24,** 86-92.

Packer H. L. & Armitage J. P. (2000) Behavioral responses of *Rhodobacter sphaeroides* to linear gradients of the nutrients succinate and acetate. *Appl. Environm. Microbiol.* **66,** 5186-5191.

Parkhill J., Wren B. W., Mungall K., Ketley J. M., Churcher C., Basham D., Chillingworth T., Davies R. M., Feltwell T., Holroyd S., Jagels K., Karlyshev A. V., Moule S., Pallen M. J., Penn C. W., Quail M. A., Rajandream M. A., Rutherford K. M., van Vliet A. H., Whitehead S. & Barrell B. G. (2000) The genome sequence of the food-borne pathogen *Campylobacter jejuni* reveals hypervariable sequences. *Nature* **403,** 665-668.

Parsonnet J. (1995) The incidence of *Helicobacter pylori* infection. *Aliment. Pharmacol. Ther.* **9,** suppl. 2, 45-51.

Parsonnet J., Friedman G. D., Vandersteen D. P., Chang Y., Vogelman J. H., Orentreich N. & Sibley R. K. (1991) *Helicobacter pylori* infection and the risk of gastric carcinoma. *N. Engl. J. Med.* **325,** 1127-1131

Pearson W. R. & Lipman D. J. (1988) Improved tools for biological sequence comparison. *Proc. Natl. Acad. Sci. U.S.A.* **85,** 2444-2448.

Pellequer J. L., Wager-Smith K. A., Kay S. A. & Getzoff E. D. (1998) Photoactive yellow protein: a structural prototype for the three-dimensional fold of the PAS domain superfamily. *Proc. Natl. Acad. Sci. U.S.A.* **95,** 5884-5890.

Pfeffer W. (1883) Locomotorische Richtungsbewegungen durch chemische Reize, G. Fischer Verlag, Stuttgart.

Pfeffer W. (1887) Über chemotaktische Bewegungen von Bacterien, Flagellaten und Volvocineen, Verlag Engelmann, Leipzig.

Pittman M. S., Goodwin M. & Kelly D. J. (2001) Chemotaxis in the human gastric pathogen *Helicobacter pylori*: different roles for CheW and the three CheV paralogues and evidence for CheV2 phosphorylation. *Microbiology* **147,** 2493-2504.

Pittman M. S., Jackson C. L., Kelly D. J. & Clayton C. L. (1997) Novel chemotaxis like genes in *Helicobacter pylori*: Characterisation of CheY and CheY a homologue of the myxobacterial FrzE protein. *Gut* **41** Suppl., A15.

Pontius B. W. (1993) Close encounters: why unstructured polymeric domains can increase rates of specific macromolecular association. *Trends Biochem. Sci.* **18,** 181-186.

Rebbapragada A., Johnson M. S., Harding G. P., Zuccarelli A. J., Fletcher H. M., Zhulin I. B. & Taylor B. L. (1997) The Aer protein and the serine chemoreceptor Tsr independently sense intracellular energy levels and transduce oxygen redox and energy signals for *Escherichia coli* behavior. *Proc. Natl. Acad. Sci. U.S.A.* **94,** 10541-1056.

Richard S., Bonneté F., Dym O. & Zaccai G. (1995) The MPD-NaCl-water system for the crystallization of halophilic proteins. In: Halophiles, Cold Spring Harbor Laboratory Press, Plainview, New York.

Richard S. B., Madern D., Garcin E. & Zaccai G. (2000) Halophilic adaptation: novel solvent protein interactions observed in the 2.9 and 2.6 Å resolution structures of the wild type and a mutant of malate dehydrogenase from Haloarcula marismortui. *Biochemistry* **39,** 992-1000.

Rosario M.M., Fredrick K.L., Ordal G.W. & Helmann J.D. (1994) Chemotaxis in *Bacillus subtilis* requires either of two functionally redundant CheW homologs. *J. Bacteriol.* **176,** 2736-2739.

Rosenberg A. H., Lade B. N., Chui D. S., Lin S. W., Dunn J. J. & Studier F. W. (1987) Vectors for selective expression of cloned DNAs by T7 RNA polymerase. *Gene* **56,** 125-135.

Rubinstenn G., Vuister G. W., Mulder F. A., Dux P. E., Boelens R., Hellingwerf K. J. & Kaptein R. (1998) Structural and dynamic changes of photoactive yellow protein during its photocycle in solution. *Nat. Struct. Biol.* **5,** 568-570.

Rudolph J., Nordmann B., Storch K. F., Gruenberg H., Rodewald K. & Oesterhelt D. (1996) A family of halobacterial transducer proteins. *FEMS Microbiol. Lett.* **139,** 161-168.

Rudolph J. & Oesterhelt D. (1996) Deletion analysis of the che operon in the archaeon *Halobacterium salinarium*. *J. Mol. Biol.* **258,** 548-54.

Rudolph J. & Oesterhelt D. (1995) Chemotaxis and phototaxis require CheA histidine kinase activity in the archaeon *Halobacterium salinarium*. *EMBO J.* **14,** 667-673.

Rudolph J., Tolliday N., Schmitt C., Schuster S. C. & Oesterhelt D. (1995) Phosphorylation in halobacterial signal transduction. *EMBO J.* **14,** 4249-4257.

Sanders D. A. & Koshland D. E. Jr. (1988) Receptor interactions through phosphorylation and methylation pathways in bacterial chemotaxis. *Proc. Natl. Acad. Sci U.S.A.* **85,** 8425-8429.

Sanger F., Nicklen S. & Coulson A. R. (1977) DNA sequencing with chain-terminating inhibitors. *Proc. Natl. Acad. Sci. U.S.A.* **74,** 5463-5467.

Sasaki J. & Spudich J. L. (2000) Proton transport by sensory rhodopsins and its modulation by transducer-binding. *Biochim. Biophys. Acta* **1460,** 230-239.

Scharf B. E., Fahrner K. A. & Berg H. C. (1998) CheZ has no effect on flagellar motors activated by CheY13DK106YW. *J. Bacteriol.* **180,** 5123-5128.

Seeley S. K., Weis R. M. & Thompson L. K. (1996) The cytoplasmic fragment of the aspartate receptor displays globally dynamic behavior. *Biochemistry* **35,** 5199-5206.

Segall J. E., Ishihara A. & Berg H. C. (1985) Chemotactic signaling in filamentous cells of *Escherichia coli*. *J. Bacteriol.* **161,** 51-59.

Shah D. S., Porter S. L., Harris D. C., Wadhams G. H., Hamblin P. A. & Armitage J. P. (2000) Identification of a fourth cheY gene in *Rhodobacter sphaeroides* and interspecies interaction within the bacterial chemotaxis signal transduction pathway. *Mol. Microbiol.* **35,** 101-112.

Sherris J. C., Preston N. W. & Shoesmith J. G. (1957) The influence of oxygen and arginine on the motility of a strain of *Pseudomonas* sp. *J. Gen. Microbiol.* **16,** 86-96.

Shimizu T., Akamatsu T., Ota H. & Katsuyama T. (1996) Immunohistochemical detection of *Helicobacter pylori* in the surface mucous gel layer and its clinicopathological significance. *Helicobacter* **1,** 197-206.

Shimizu T. S., Le Novere N., Levin M. D., Beavil A. J., Sutton B. J. & Bray D. (2000) Molecular model of a lattice of signalling proteins involved in bacterial chemotaxis. *Nat. Cell Biol.* **2,** 792-796.

Silversmith R. E., Appleby J. L. & Bourret R. B. (1997) Catalytic mechanism of phosphorylation and dephosphorylation of CheY: kinetic characterization of imidazole phosphates as phosphodonors and the role of acid catalysis. *Biochemistry* **36,** 14965-14974.

Slomiany B. L., Sarosiek J. & Slomiany A. (1987) Gastric mucus and the mucosal barrier. *Dig. Dis.* **5,** 125-145.

Sohlemann P., Soppa J., Oesterhelt D. & Lohse M. J. (1997) Expression of β 2-adrenoceptors in halobacteria. *Naunyn Schmiedebergs Arch. Pharmacol.* **355,** 150-160.

Somero G. N. (1986) Protons, osmolytes , and fittness of internal milieu for protein function. *Am. J. Physiol.* **251,** R197-R213.

Sourjik V. & Berg H. C. (2000) Localization of components of the chemotaxis machinery of *Escherichia coli* using fluorescent protein fusions. *Mol. Microbiol.* **37,** 740-751.

Sourjik V. & Schmitt R. (1996) Different roles of CheY1 and CheY2 in the chemotaxis of *Rhizobium meliloti*. *Mol. Microbiol.* **22,** 427-436.

Sourjik V. & Schmitt R. (1998) Phosphotransfer between CheA CheY1, and CheY2 in the chemotaxis signal transduction chain of *Rhizobium meliloti*. *Biochemistry* **37,** 2327-2335.

Southern E. M. (1979) Measurement of DNA length by gel electrophoresis. *Anal. Biochem.* **100,** 319-323.

Spudich J.L., Yang C.S., Jung K.H. & Spudich E.N. (2000) Retinylidene proteins: structures and functions from archaea to humans. *Annu. Rev. Cell Dev. Biol.* **16,** 365-392.

Spudich J. L. (1994) Protein-protein interaction converts a proton pump into a sensory receptor. *Cell* **79,** 747-750.

Srivastava R. C., Madamwar D. B. & Singh V. (1987) Equation for the growth of *Halobacterium halobium*. *Indian J. Exp. Biol.* **25,** 497-498.

Stewart R. C. (1997) Kinetic characterization of phosphotransfer between CheA and CheY in the bacterial chemotaxis signal transduction pathway. *Biochemistry* **25,** 2030-2040.

Stock M. A., Robinson V. L. & Goudreau P. N. (2000) Two-component signal transduction. *Annu. Rev. Biochem.* **69**, 183-215.

Stock J. (1999) Sensitivity cooperativity and gain in chemotaxis signal transduction. *Trends Microbiol.* **7,** 1-4.

Stock J. B., Surette M. G., Levit M. & Park P. (1995) Two-component signal transduction, (Hoch J. A. & Silhavy T. J., Eds.) pp 25-562, ASM Press, Washington, D.C.

Storch K. F., Rudolph J. & Oesterhelt D. (1999) Car: a cytoplasmic sensor responsible for arginine chemotaxis in the archaeon *Halobacterium salinarum*. *EMBO J.* **18,** 1146-1158.

Stover C. K., Pham X. Q., Erwin A. L., Mizoguchi S. D., Warrener P., Hickey M. J., Brinkman F. S., Hufnagle W. O., Kowalik D. J., Lagrou M., Garber R. L., Goltry L., Tolentino E., Westbrock-Wadman S., Yuan Y., Brody L. L., Coulter S. N., Folger K. R., Kas A., Larbig K., Lim R., Smith K., Spencer D., Wong G. K., Wu Z. & Paulsen I. T. (2000) Complete genome sequence of *Pseudomonas aeruginosa* PA01, an opportunistic pathogen. *Nature* **406,** 959-964.

Strogatz S. H. (2001) Exploring complex networks. *Nature* **410,** 268-276.

Studier F. W. & Moffatt B. A. (1986) Use of bacteriophage T7 RNA polymerase to direct selective high-level expression of cloned genes. *J. Mol. Biol.* **189,** 113-130.

Studier F. W., Rosenberg A. H., Dunn J. J. & Dubendorff J. W. (1990) Use of T7 RNA polymerase to direct expression of cloned genes. *Methods Enzymol.* **185,** 60-89.

Suerbaum S. (1995) The complex flagella of gastric *Helicobacter* species. *Trends Microbiol.* **3,** 168-70; discussion 170-171.

Suerbaum S., Josenhans C. & Labigne A. (1993) Cloning and genetic characterization of the *Helicobacter pylori* and *Helicobacter mustelae* flaB flagellin genes and construction of *H. pylori* flaA- and flaB-negative mutants by electroporation-mediated allelic exchange. *J. Bacteriol.* **175,** 3278-3288.

Sundberg S. A., Alam M., Lebert M., Spudich J. L., Oesterhelt D. & Hazelbauer G. L. (1990) Characterization of *Halobacterium halobium* mutants defective in taxis. *J. Bacteriol.* **12,** 2328-2335.

Surette M. G., Levit M., Liu Y., Lukat G., Ninfa E. G., Ninfa A. & Stock J. B. (1996) Dimerization is required for the activity of the protein histidine kinase CheA that mediates signal transduction in bacterial chemotaxis. *J. Biol. Chem.* **271,** 939-945.

Surette M. G. & Stock J. B. (1996) Role of alpha-helical coiled-coil interactions in receptor dimerization signaling and adaptation during bacterial chemotaxis. *J. Biol. Chem.* **271,** 17966-17973.

Tabor S. & Richardson C. C. (1987) DNA sequence analysis with a modified bacteriophage T7 DNA polymerase. *Proc. Natl. Acad. Sci. U.S.A.* **84,** 4767-4771.

Takami H., Nakasone K., Takaki Y., Maeno G., Sasaki R., Masui N., Fuji F., Hirama C., Nakamura Y., Ogasawara N., Kuhara S. & Horikoshi K. (2000) Complete genome sequence of the alkaliphilic bacterium *Bacillus halodurans* and genomic sequence comparison with *Bacillus subtilis*. *Nucleic Acids Res.* **28,** 4317-4331.

Taylor B. L. & Zhulin I. B. (1998) In search of higher energy: metabolism-dependent behaviour in bacteria. *Mol. Microbiol.* **28,** 683-690

Timasheff S. N. (1992) Solvent effects on protein stability. *Curr. Opin. Struct. Biol.* **2,** 35-39.

Timasheff S.N. (1991) Stabilization of protein structure by solvent additives. In *Pharmaceutical Biotechnology, Vol. 2* edited by Borchavdt R. T. Plenum press, New York.

Tittor J., Paula S., Subramaniam S., Heberle J., Henderson R. & Oesterhelt D. (2002) Proton translocation by bacteriorhodopsin in the absence of substantial conformational changes. *J. Mol. Biol.* **319,** 555-565.

Tomb J. F., White O., Kerlavage A. R., Clayton R. A., Sutton G. G., Fleischmann R. D., Ketchum K. A., Klenk H. P., Gill S., Dougherty B. A., Nelson K., Quackenbush J., Zhou L., Kirkness E. F., Peterson S., Loftus B., Richardson D., Dodson R., Khalak H. G., Glodek A., McKenney K., Fitzegerald L. M., Lee N., Adams M. D. & Venter J. C. (1997) The complete genome sequence of the gastric pathogen *Helicobacter pylori*. *Nature* **388,** 539-547.

Venyaminov S. Y. & Vassilenko K. S. (1994) Determination of protein tertiary structure class from circular dichroism spectra. *Anal. Biochem.* **222,** 176-84.

Wadhams G. H., Martin A. C. & Armitage J. P. (2000) Identification and localization of a methyl-accepting chemotaxis protein in *Rhodobacter sphaeroides*. *Mol. Microbiol.* **36,** 1222-1233.

Weibull C. (1960) The Bacteria, Academic Press, New York.

Welch M, Oosawa K., Aizawa S.I. and Eisenbach M. (1993) Phosphorylation-dependent binding of a signal molecule to the flagellar switch of bacteria. *Proc. Natl. Acad. Sci. U.S.A.* **90**, 8787-8791

Woese C. R., Kandler O. & Wheelis M. L. (1990) Towards a natural system of organisms: proposal for the domains Archaea, Bacteria, and Eucarya. *Proc. Natl. Acad. Sci. U.S.A.* **87,** 4576-4579.

Worbs M. & Wahl M. C. (2000) Expression purification crystallization and preliminary X-ray diffraction studies of bacterial and archaeal L4 ribosomal proteins. *Acta Crystallog. D* **56,** 645-647.

Wright P. E. & Dyson H. J. (1999) Intrinsically unstructured proteins: re-assessing the protein structure-function paradigm. *J. Mol. Biol.* **293,** 321-331.

Wüthrich K. (1986) NMR of Proteins and Nucleic Acids, Wiley Interscience, New York.

Wylie D., Stock A., Wong C. Y. & Stock J. (1988) Sensory transduction in bacterial chemotaxis involves phosphotransfer between Che proteins. *Biochem. Biophys. Res. Commun.* **151**, 891-896

Yi T. M., Huang Y., Simon M. I. & Doyle J. (2000) Robust perfect adaptation in bacterial chemotaxis through integral feedback control. *Proc. Natl. Acad. Sci. U.S.A.* **97,** 4649-4653.

Yoshiyama H., Nakamura H., Kimoto M., Okita K. & Nakazawa T. (1999) Chemotaxis and motility of *Helicobacter pylori* in a viscous environment. *J. Gastroenterol.* **34,** 18-23.

Zhang W., Brooun A., McCandless J., Banda P. & Alam M. (1996) Signal transduction in the archaeon *Halobacterium salinarium* is processed through three subfamilies of 13 soluble and membrane-bound transducer proteins. *Proc. Natl. Acad. Sci. U.S.A.* **93,** 4649-4654.

Zhulin I. B., Taylor B. L. & Dixon R. (1997) PAS domain S-boxes in Archaea, Bacteria and sensors for oxygen and redox. *Trends Biochem. Sci.* **22,** 331-333.

Equipment

Beta-counter	Berthold LB 1210B Berthold Technologies GmbH & Co. KG, Bad Wildbad
Chromatography media	Dimethyl ethyl cellulose DE52, Whatman, Faifield, NJ, USA; Ni-NTA, Qiagen, Hilden; Hydroxyapatite BioRad, Richmond, CA, USA; all other media were purchased from Amersham Pharmacia Biotech, Freiburg
CD spectrometer	Auto Dichrograph Mark IV, Jobin Yvon GmbH, Grassbrunn
DNA sequencer	ABI Prism 377, Applied Biosystems, Foster City, CA, USA
FPLC System and Accessories	Amersham Pharmacia Biotech, Freiburg
French Press	Aminco 20K French Pressure Cell, Polytec GmbH, Waldbronn
Incubator	Multitron AJ120, Infors AG, Bottmingen, Switzerland
PCR machine	GeneAmp PCR System 9700, Applied Biosystems, Foster City, CA, USA
Phosphoimager	FujiFilm FLA-2000, Fuji Photo Film Co., Ltd., Tokyo, Japan
Scintillator	Tri-Carb 2100 TR Liquid Scintillation Analyzer, Packard BioScience, Dreieich
Sonifier	Sonifier Cell Disruptor B-30, Branson Sonic Power Co. Danbury, CT, USA
Transfection apparatus	Gene Pulser, BioRad, Richmond, CA, USA

Consumables

Centriprep	Centriprep K, Millipore, Eschbronn
Crystallization consumables	Hampton Research, Laguna Niguel, CA, USA
Cuvette for CD spectroscopy	Hellma GmbH & Co KG, Müllheim
Dialysis Tubing	10.000 Da exclusion limit, Sigma-Aldrich Chemie, Deisenhofen
Electroporation cuvettes	0.2 mm gap, BioRad, Richmond, CA, USA
Filter paper	Whatman 3MM, Whatman, Fairfield, NJ, USA
Microfuge Tubes	0.5 and 1.5 ml, Eppendorf AG, Hamburg
PVDF Membrane	Immobilon P, Millipore
Spin colums	AutoSeq G-50, Amersham Pharmacia Biotech, Freiburg and MultiScrenn-HV 96, Millipore, Eschbronn
X-ray film	XAR-5, Eastman Kodak GmbH, Stuttgart-Wangen

Kits

DNA purification kit	QIAquick, Qiagen, Hilden
DNA sequencing kit	ABI Prism BigDye Terminator Cycle Sequencing Ready Reaction Kit, Perking Elmer, Wellesley, MA, USA

Plasmid isolation kit	QIAprep, Qiagen, Hilden
Quick change site directed mutagenesis kit	Stratagene, La Jolla, CA, USA

Enzymes

DNA Ligase	T4 DNA Ligase, Gibco BRL, Invitrogen GmbH, Karlsruhe
DNaseI	Roche Diagnostics GmbH, Mannheim
DNA polymerase	TaKaRa LA Taq, Takara shuzo Co., Ltd., Shiga, Japan
Lactate dehydrogenase	Boehringer Mannheim, Mannheim
Lysozyme	Roche Diagnostics GmbH, Mannheim
Pfu DNA Ligase	Stratagene, La Jolla, CA, USA
Polynucleotide kinase	USB, Cleveland, OH, USA
Pyruvate kinase	Boehringer Mannheim, Mannheim
Restriction endonucleases	New England Biolabs GmbH, Schwalbach/ Taunus
Shrimp alkaline phosphatase	USB, Cleveland, OH, USA
Thrombine	Amersham Pharmacia Biotech, Freiburg

Fine Chemicals

Agarose	Seakem, Teknova, Half Moon Bay, CA, USA
Coomasie Brilliant Blue	Serva, Heidelberg
DNA size standard	One kb DNA size marker, Gibco BRL, Invitrogen GmbH, Karlsruhe
dNTPs	PCR nucleotide mix, Amersham Pharmacia Biotech, Freiburg
FREUND's Adjuvant (complete and incomplete)	Sigma-Aldrich Chemie, Deisenhofen
Gel filtration size standard	Gel filtration LMW and HMW Calibration kits, Amersham Pharmacia Biotech, Freiburg
IPTG	Gerbu Biotechnik GmbH, Gaiberg
NADH, grade II, 98%	Boehringer Mannheim, Mannheim
NBT/BCIP	NBT/BCIP solution, Sigma-Aldrich Chemie, Deisenhofen
Phosphoenolpyruvate	Sigma-Aldrich Chemie, Deisenhofen
PMSF	Sigma-Aldrich Chemie, Deisenhofen
Protease inhibitor cocktail	Protease inhibitor cocktail for His_6-tagged proteins, Sigma-Aldrich Chemie, Deisenhofen
Protein molecular weight marker for SDS-PAGE	LMW, Amersham Pharmacia Biotech, Freiburg
Pyruvate	Sigma-Aldrich Chemie, Deisenhofen

Scintillation cocktail	rotiszint eco plus scintillation cocktail, Roth, Karlsruhe
SDS, 99%	Roth, Karlsruhe
Western Blocking Reagent	Hoffmann-La Roche Ltd., Basel, Switzerland

Antibodies

Secondary antibodies	Alkaline phosphatase conjugated goat anti rabbit IgG, Jackson Immuno Research LaboratoriesInc., West Grove, PA, USA, purchased from Dianova, Hamburg

Laboratory Animals

Rabbits	Charles River, Sulzfeld

Radiochemicals

[γ^{32}P]-ATP	[γ^{32}P]-ATP triethylammonium salt, >5000 Ci/mmol, Amersham Pharmacia Biotech, Freiburg
[γ^{32}P]-orthophosphoric acid	216 mCi/ml, Hartmann Analytic GmbH, Braunschweig

Computer Programs

AIDA	AIDA 2.31 Software package, Fuji Photo Film Co., Ltd., Tokyo, Japan
DNASIS	Hitachi Software engineering Europe S&A, Berlin
OLIGO	Primer Analysis Software Version 4.04, National Biosciences Inc., Plymouth, MN, USA

Oligonucleotides to amplify genes by PCR used in this work.

I. Genes expressed from pFS4000.

The expression plasmid pFS4000 containing the *car* gene cloned into pT7-7 (using the NdeI and HindIII restriction sites of the vector) was a kind gift of F. STORCH (STORCH, 1999). This vector was used to express the genes listed below by ligating the respective PCR products in pFS4000 digested with NdeI and HindIII. The expressed proteins do not contain additional amino acids compared to the wild type proteins.

HtpIII

HtpIII.for.1: 5'-GATCTACCATATGTCTAAAAACAAACATGAAC-3'
HtpIII.rev.1: 5'-CGTCCCAAGCTTACTGGTCGTGGAGCTC-3'

HtB

HtB.for.1: 5'-GATCTACCATATGAGCAACGATAATGACAC-3'
HtB.rev.1: 5'-GCTCCCAAGCTTAGCTGAGCTTGCCGAC-3'

Htr15

HtY.for.1: 5'-GATCTACCATATGCTGCGCATCTTTCG-3'
HtY.rev.1: 5'-GCTCCCAAGCTTATTGGCTATCCGTGGTCAG-3'

Car domain 1

HxL1: 5'-AATAAGAAACATATGGATCCAGCATCG-3'
Htc7.Dom1.rev: 5'-GCTCCCAAGCTTAGGTCTCGTGGAGGT-3'

Car domain 2

HxL1: 5'-AATAAGAAACATATGGATCCAGCATCG-3'
Htc7.Dom2.rev: 5'-GCTCCCAAGCTTACTCGTCGGCGACGCCC-3'

Car domain 3

HxL1: 5'-AATAAGAAACATATGGATCCAGCATCG-3'
Htc7.Dom3.rev: 5'-GCTCCCAAGCTTACCGCTCGGCCGACTCC-3'

Car domain 4

Htc7.Dom4.for: 5'-GATCTACCATCTGGAGAAAGTCAAAAACCAGC-3'
HxR1: 5'-AGCAACGACGAAGCTTTAGCGGCG-3'

Car domain 5

Htc7.Dom5.for: 5'-GATCTACCATCTGGGCGAACATCTCTCGGA-3'
HxR1: 5'-AGCAACGACGAAGCTTTAGCGGCG-3'

Car domain 6

Htc7.Dom6.for: 5'-GATCTACCATCTGGCGACCATCGAGGAAATC-3'
HxR1: 5'-AGCAACGACGAAGCTTTAGCGGCG-3'

II. Genes expressed from pFS4004 and pFS4005.

The car gene cloned into pT7-7 with an N-terminal and C-terminal His_6-tag was a kind gift of F. STORCH (STORCH, 1999). The tag is directly fused to the respective recombinant proteins without additional amino acids as linker.

III. Genes expressed from pET36b(+).

The expressed proteins do not contain additional amino acids as compared to the wild type proteins.

H. salinarum CheR

CheR.1.II.for: 5'-GATCTACCATATGCGACGCAGGGGAGTCGAGGAATACGCAGGCTACCTGACGCTG CTC-3'
CheR.688.3.II.rev: 5'-GCACTAATCTCGAGCCTACTAGTTGTCAGCGACCCGACT-3'

The resulting PCR product was digested with NdeI and XhoI and cloned into pET36b(+)digested with the same restriction endonucleases.

H. salinarum CheB

CheB.1.for: 5'-GAACTACTCTAGAAATAATTTTCTTTAACTTTAAGAAGGAGATATACATATGACAGA GGCACTGGTGG-3'
CheB.1.rev: 5'-ACTATGCAAGCTTACGTCGTCCTCCGTATC-3'

The resulting PCR product was digested with XbaI and HindIII and cloned into pET36b(+) digested with the same restriction endonucleases.

IV. Expression of Hp0599

The expressed protein contains an N-terminal His_6-tag followed by a thrombine recognition sequence (MGSSHHHHHHSSGLVPRGSH)

H. pylori Hp0599

Hpyl.ORF.1.for: 5'-GATCTACCATATGGGCAGCAGCCATCATCATCATCATCACAGCAGCGGCCTGGTGCCG CGCGGCAGCGGGATGTTTGGGAATAAGCAGTTG-3'
Hpyl.ORF.637118.rev: 5'-GCACTATGCCCTAGGCTACTATTCGGCCTTTTTGAATTTTTTC-3'

The resulting PCR product was digested with NdeI and AvrII and cloned into pET36b(+) digested with the same restriction endonucleases.

V. Genes expressed from pET28a(+).

The expressed proteins all contain an N-terminal His_6-tag followed by a thrombine recognition sequence (MGSSHHHHHHSSGLVPRGSH)

E. coli CheY

EcCheY.for: 5'-GGGAATCTCCATATGGCGGATAAAGAACTTAAATTTTTGGTTGTG-3'
EcCheY.rev: 5'-GATCAGTCCTCGAGCATGCCCAGTTTCTCAAAGATTTTGTTGAG-3'

E. coli FliM

Ec.FliM.for: 5'-GGGAATCTCCATATGGGCGATAGTATTCTTTCTCAAGCTGAAATT-3'

Ec.FliM.rev: 5'-GATCAGTCCTCGAGTTTGGGCTGTTCCTCGTTCAGAGAATTTAA-3'

H. pylori CheV1

Hp0019.for: 5'-GGGAATCTCCATATGGCTGATAGTTTAGCGGGCATTGATCAAGTT-3'
Hp0019.reV: 5'-GATCAGTCCTCGAGTGCTAATTCCAAAAATTGCTTAACCACTCG-3'

H. pylori CheW

Hp0391.for: 5'-GGGAATCTCCATATGAGCAACCAATTAAAAGATTTATTTGAAAGA-3'
Hp0391.rev: 5'-GATCAGTCCTCGAGGAAGTCTTTTTTTAAGATTTCTTCCACTCT-3'

H. pylori CheF

Hp0392.for: 5'-GGGAATCTCCATATGGATGATTTGCAAGAAATAATGGAAGACTTC-3'
Hp0392.rev: 5'-GATCAGTCCTCGAGCGATTGGTCTCCTTCTAATTTAATGCTGCG-3'

H. pylori CheV2

Hp0393.for: 5'-GGGAATCTCCATATGGCAGAAAAAACAGCTAACGATTTAAAACTA-3'
Hp0393.rev: 5'-GATCAGTCCTCGAGCGCATTCTTGTCTAAAATCTTAGAAATTTC-3'

H. pylori CheY

Hp1067.for: 5'-GGGAATCTCCATATGTTGAAACTACTGGTAGTAGATGATAGCTCA-3'
Hp1067.rev: 5'-GATCAGTCCTCGAGATCGTTTGTCCCTAAAACAACCTCTAATTT-3'

H. pylori FliM

Hp1031.for: 5'-GGGAATCTCCATATGGCTGATATTTTAAGCCAAGAAGAAATTGAT-3'
Hp1031.rev: 5'-GATCAGTCCTCGAGCTCTTCTTCTATTTTCATAATATCGCCCAC-3'

H. pylori CheV3

Hp0616.for: 5'-GGGAATCTCCATATGGTGGTAAGAGATATTGACAAAACGACTTCG-3'
Hp0616.rev: 5'-GATCAGTCCTCGAGTGAAAGCGTTTTTTTAAGCATTTCATGGAT-3'

C. jejuni Cj0448

Cj0448.for: 5'-GGGAATCTCCATATGTTTGGAAGTAAAATAAACCATTCTGATCTT-3'
Cj0448.rev: 5'-GATCAGTCCTCGAGATGATCTGACTCATCAAGCATTTCTTTAAA-3'

The resulting PCR products were all digested with NdeI and XhoI and cloned into pET28a(+) digested with the same restriction endonucleases.

For details of the pET vector DNA sequence see http://www.novagen.com. All enzymes were purchased from New England Biolabs.

Nucleotide sequence of synthetic CheB gene:

```
1    ATGACTGAAGCTTTAGTTGTTGATGATTCTCAT 33
34   TTTATGCGTACTGTTATTTCTGATATTTTAGAA 66
67   GATGGTGGTGTTGATGTTGTTGGTACTGCTGAA 99
100  AATGGTGCTCGTGCTTTAGATGCTGTTACTGAT 132
133  GTTCAACCGGATGTTATTACTATGGATGTTGAA 165
166  ATGCCTGAAATGGATGGTATTGAAGCTACTGCT 198
199  GAAATTATGCGTGAACAACCGACTCCGATTTTA 231
232  ATGGTTTCTGCTTTAACTACTGAAGATGCTGAT 264
265  GCTACTTTAGAAGCTATGGAAAAAGGTGCTATT 297
298  GATACTTTTGCTAAACCGGGTGGTACTATTTCT 330
331  ACTGAATTATCTGGTCATTCTGAAGAATTAGTT 363
364  GCTGCTGTTGAACGTGTTGCTTCTGCTGATCCG 396
397  ACTGCTGGTCATGATGTTGAAATGGAACCGGCT 429
430  TCTCCGCCGGATGCTACTACTTCTGAATATGCT 462
463  GATAATCCGACTTTATTAATTGGTGCTTCTACT 495
496  GGTGGTCCGAATGTTGTTGAATCTATTTTAGCT 528
529  TCTTTACCGGCTGAAGCTGATTTTCGTGTTTTA 561
562  ATTGTTCAACATATGCCGGATCAATTTACTTCT 594
595  CGTTTTGCTGATCGTTTAGATGCTGCTTCTCAA 627
628  TATGATATTACTGAAGCTGAAGATGGTTCTCGT 660
661  ATTGGTGGTGGTGAAGGTTTAGTTGCTCGTGGT 693
694  GATTATCATATGCGTGTTTCTGGTTATTCTAAT 726
727  GGTCGTTTACGTGTTCGTTTAGATCAATCTGAA 759
760  CGTTTACATTCTGTTCGTCCGGCTATTGATGTT 792
793  ACTTTTAAATCTGCTGCTGAACGTGTTACTGAT 825
826  CCGTTAGTTTCTGTTGTTTTAACTGGTATGGGT 858
859  TCTGATGGTGCTGATGGTGTTCGTGCTGTTAAA 891
892  GATGCTGGTGGTGCTACTTTAGCTCAAAATGAA 924
925  GCTACTTCTGCTGTTTTTGGTATTCCGGAACGT 957
958  GCTATTGAAACTGGTTGTGTTGATGATGTTTTA 990
991  CCGGTTGATCAATTAACTGAAGCTATTGCTGAT 1023
1024 TCTATTCGTCGTACTACT 1041
```

Nucleotide sequence of synthetic CheR gene:

```
1   ATGCGTCGTCGTGGTGTTGAAGAATATGCTGGT 33
34  TATTTAACTTTATTAGAAGAAGATGATGATGAT 66
67  GAACGTGCTGAATTATTAGATACTTTATCTGTT 99
100 AATGTTACTGAATTTTTTTCGTGATGAAAAAGTT 132
133 TGGACTGCTTTACGTGATGTTTTATTAGAATTA 165
166 GCTGATACTGTTCGTTCTATTGATATTTGGTCT 198
199 GCTGCTTGTGCTGATGGTCGTGAACCTTATTCT 231
232 TTAGCTATGTTAGCTTTAGATGCTGGTTTAGAT 264
265 CCTCGTAATGTTTCTATTTTAGCTACTGATATT 297
298 GATGAAGATGCTTTAGCTCGTGCTCGTGCTGGT 330
331 CGTTATGAATCTACTCGTACTGCTGATATTTCT 363
364 GATCAATTAGGTTTTTTTAGATAATCCTCAAGAA 396
397 TATGTTGATCGTGAAGGTGATCGTGCTTTTGTT 429
430 GTTAATGATCGTGTTAAAGATTTAGTTACTTTT 462
463 GAACGTCATGATTTAATTACTGGTGATCCTAAA 495
496 TCTGGTTTTGATTTAGTTGCTTGTCGTAATGTT 528
529 TGTATTTATATTGATAAACAATATAAATTACCT 561
562 ATTTTAGATACTGTTTCTAAATCTTTACGTGAA 594
595 GGTGGTCATTTAGTTTTAGGTCAAACTGAAACT 627
628 TTACCTGGTGAAGTTAAAGAACGTTTTGAAGCT 660
661 GAAGATCCTCGTATTCGTATTTATTCTCGTGTT 693
694 GCTGATACT 702
```

9. Summary

In the present study, the protein network components that enable chemotaxis in *Halobacterium salinarum* and *Helicobacter pylori* were examined to characterize their function in the respective organisms. The main results of this work are:

- The soluble transducer proteins Car, Htr15, Hp0599 and Cj0448 are highly homologous to membrane-bound chemoreceptors from enteric bacteria.

- The soluble transducer proteins Car and Htr15 from *H. salinarum* were overexpressed in *E. coli* BL21(DE3) cells and purified therefrom using standart chromatographic techniques. Car was found to be a mainly α-helical protein of molten globule-like structure as determined by CD-spectroscopy and ^{1}H-NMR.

- The soluble transducer proteins Hp0599 from *H. pylori* and its ortholog, Cj0448 from *Campylobacter jejuni*, were overexpressed in *E. coli*, purified to homogeneity and crystallized. Both proteins gave thin platelets that were not suited for structure determination by X-ray crystallography.

- The only very recently structurally characterized coupling protein CheW was crystallized and the best protein crystals diffracted to a resolution of 4.6 Å.

- Hp0599 is tetrameric in solution, an oligomerization state that is in accordance with its presumed aggregation in cytosolic signalling arrays.

- The CheF protein from *H. pylori* is an autophosphorylating hybrid histidine kinase with a response regulator domain fused to its C-terminus. The protein autophosphorylates at a conserved histidine residue with an apparent first order rate constant of 0.2/min.

- The autophosphorylation activity of CheF is highly modulated by the soluble receptor protein Hp0599. This modulation of CheF activity is dependent on the presence of the coupling protein CheW.

- The hybrid response regulators CheV can be phosphorylated by the CheF protein kinase. The response regulator CheY also serves as a substrate for CheF-mediated phosphorylation.

- The phosphotransfer reaction from CheF to CheY is very fast and below the detection limit of the assays employed in this study (< 5 sec), whereas the transfer of phosphate groups to CheV2 proceeds considerably slower (> 180 sec).

- The half-life of CheY-phosphate is 14 sec, whereas the half-life of CheV2 is much higher (> 1 min).

- CheY and CheF (in its response regulator domain) exhibit an autophosphorylation activity with acetyl phosphate as phosphor donor, whereas CheV2 and CheV3 autophosphorylate only very weak.

- The response regulator CheY was purified in its phosphorylated state and shown to reverse-phosphorylate the CheF kinase.

Lebenslauf

Name:	Andreas Schaer
Geburtstag:	15. April 1971
Geburtsort:	Freiburg im Breisgau
Familienstand:	ledig

Ausbildung:

1998-2002	Promotion am Max-Planck-Institut für Biochemie in Martinsried in der Arbeitsgruppe von Prof. Dr. D. Oesterhelt. Doktorarbeit: "Studies on chemotaxis in *Halobacterium salinarum* and *Helicobacter pylori*".
1994-1995	Auslandsaufenthalt an der University of California, Berkeley, und am Lawrence Berkeley National Lab.
1991-1998	Studium der Biochemie an der Universität Tübingen. Diplom: 3. Februar 1998. Diplomarbeit: "Über den Metabolismus des Valins in neuralen Zellen".
1990-1991	Zivildienst im Alten- und Pflegeheim St. Antonius, Freiburg i. Br.
1990	Abitur am Technischen Gymnasium Freiburg i. Br.